

DYNAMIC SIMULATION OF A FLEXIBLE ROBOT ARM AND CONTROLLER

Nabil G. Chalhoub
A. Galip Ulsoy
Department of Mechanical Engineering
and
Applied Mechanics

September 1983

THE UNIVERSITY OF MICHIGAN
ENGINEERING LIBRARY

Robot Systems Division

COLLEGE OF ENGINEERING
UNIVERSITY OF MICHIGAN
ANN ARBOR, MICHIGAN 48109

en 8m

UMR1113

TABLE OF CONTENTS

ABSTRACT	3
INTRODUCTION	4
MODELING	5
CONTROL	19
SIMULATION	23
DISCUSSION	29
SUMMARY	30
REFERENCES	37
APPENDIX I - Static Equilibrium and Reaction Forces	40
APPENDIX II - Equations of Motion	41
APPENDIX III - Equations of Rigid Body Motion Only	48
APPENDIX IV - Derivation of the Controller Design	54
APPENDIX V - Listing of the Computer Program	59
FIGURES	74
TABLES	99

NOTATION

- The underbar beneath any variable ($\underline{\quad}$) indicates an n dimensional vector.
- The symbol $\delta(\quad)$ in front of any variable denotes either virtual displacement or virtual force.
- A star superscript indicates a value related to the center of mass. Other values are related to the rotating coordinates ($\underline{i}, \underline{j}, \underline{k}$).
- A dot or a double dot over any symbol, ($\dot{\quad}$) or ($\ddot{\quad}$), indicates first or second derivative with respect to time.
- The symbol $\frac{\delta(\underline{\quad})}{\delta t}$ denotes the derivative with respect to time of the vector components only (i.e derivatives with respect to time of the basis vectors $\underline{i}, \underline{j}, \underline{k}$ are excluded).

ABSTRACT

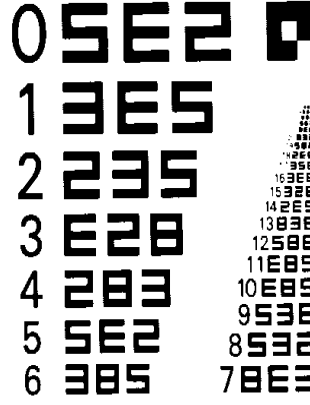
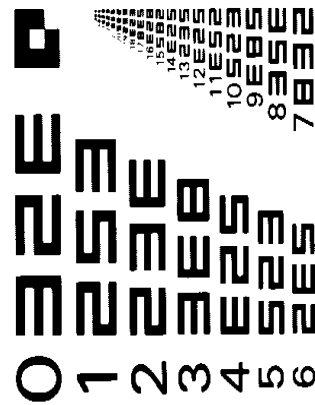
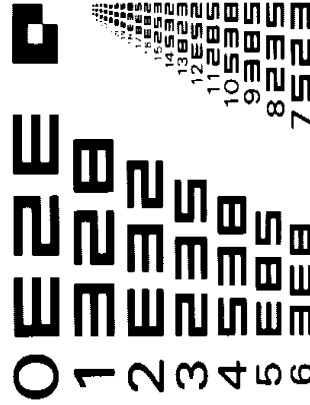
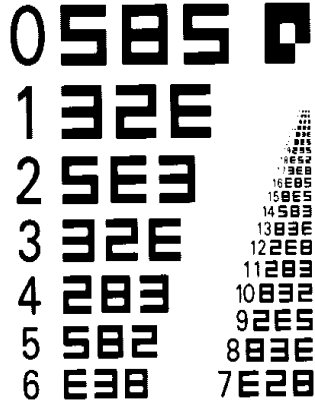
High performance requirements in robotics have led to the consideration of structural flexibility in robot arms. This paper employs an assumed modes method to model both the rigid body and flexible motion of a spherical coordinate robot arm. This model is used to investigate relationships between the arm structural flexibility and a linear controller for the rigid body motion. This simple controller is used to simulate the controllers currently used in industrial robots. The simulation results illustrate the differences between leadscrew driven and unconstrained axes of the robot; they indicate the trade-off between speed and accuracy; and show potential instability mechanisms due to the interaction between the controller and the robot structural flexibility.

RIT ALPHANUMERIC RESOLUTION TEST OBJECT, RT-171

MEMORIAL DRIVE, ROCHESTER, NEW YORK 14623

PRODUCED BY GRAPHIC ARTS RESEARCH CENTER

ROCHESTER INSTITUTE OF TECHNOLOGY, ONE LOMB



The first step in improving the performance of robots is to obtain a reasonably accurate dynamic model. Usual techniques solve for the gross body motion and the flexible motion separately. Since the elastic motion is small then its effect on the gross body motion is neglected. Therefore, only the effect of the rigid body motion on the flexible motion is considered. This is done by solving the gross body equations for inertial forces which in turn are introduced as excitation source to the elastic problem. Recent techniques use coupled reference position and elastic deformation models. Some researchers used finite element techniques to describe the elastic deformation [3], [4]. Others used the assumed modes method [5]. The latter approach is employed in this study. This approximate technique can be used to yield a set of equations which represent the combined rigid and flexible motion.

The next step is to design a controller which insures the desired performance of the manipulator. The conventional linear control techniques have led to poor performance when robots are operated over a wide range of tasks. Therefore, a sophisticated controller design is needed to control the complex, nonlinear and nonstationary dynamic system. Adaptive controller techniques [6], [7] seem to be a promising solution to this problem.

In this study, a simple integral plus state feedback controller is used to control the rigid body motion only. This simple, linear controller is used to simulate the controller used in present manipulators. The illustration of the inter-relationships between the robot structural flexibility and the controller design is discussed in this report. This should serve as a basis for the design of advanced controllers aimed at solving the arm flexibility problem.

2. MODELING

The physical system is a spherical coordinate robot, which has two revolute and one prismatic joints. It consists of an arm connected to a rotating base.

The arm is made of two beams such that the second beam can move axially into the first beam. The entire arm is free to rotate around the horizontal axis passing through the pivot point A and parallel to \underline{K} . This is schematically illustrated in Figure 1.

The robot arm is modeled by two Euler-Bernoulli beams of length L_1 and L_2 respectively as shown in Figure 2. A reference inertial frame $(\underline{I}, \underline{J}, \underline{K})$ fixed at point O , is chosen along with a non-inertial, body fixed, rotating reference frame $(\underline{i}, \underline{j}, \underline{k})$. The equations are derived in terms of the latter to keep the mass moment of inertia constant throughout the rigid body motion of the robot.

The first beam can rotate around point O with angular velocity $\dot{\phi}$ around the vertical axis passing through \underline{J} , and $\dot{\psi}$ around the horizontal axis along \underline{K} . The second beam is fitted into the first one and has one additional degree of freedom τ which allows it to move axially into the first beam. The load at the end-of arm is modeled with a concentrated mass at the end of the second beam.

The stiffness of the beam is much higher in the \underline{i} direction than in either \underline{j} or \underline{k} directions. Therefore, the longitudinal vibrations of the two beams are neglected and transverse vibrations only are considered in addition to the rigid body motion. Variations of the mass moment of inertia due to the flexible motion is assumed to be negligible.

Expressions for the total kinetic energy and the total potential energy are derived. The generalized forces corresponding to the generalized coordinates are determined by the virtual work principle. These results are used in applying Lagrange's equations to obtain the dynamic equations of the system.

Two separate cases are considered in this report to model the flexible motion in the dynamic equations:

- (1) Both beams of the robot arm are considered to be flexible

- (2) Only the portion of the second beam protruding from the first beam is considered to be flexible.

For the first case, only the kinetic and potential energies are derived. The position vector of any point on the first beam is:

$$\underline{R}_1 = r_1 \underline{i} + V \underline{j} + W \underline{k} \quad (1)$$

where r_1 is time invariant, since flexible motion along \underline{i} is neglected (i.e. no longitudinal vibrations). V and W represent the flexible motion of the beam in the \underline{j} and \underline{k} directions respectively. The rotation vector of the noninertial frame $(\underline{i}, \underline{j}, \underline{k})$ is defined as follows:

$$\underline{\Omega} = \dot{\varphi} \underline{j} + \dot{\vartheta} \underline{k} = \dot{\varphi} \sin \vartheta \underline{i} + \dot{\varphi} \cos \vartheta \underline{j} + \dot{\vartheta} \underline{k} \quad (2)$$

the time rate of change of \underline{R}_1 is given by:

$$\begin{aligned} \dot{\underline{R}}_1 = \frac{\delta \underline{R}_1}{\delta t} + \underline{\Omega} \times \underline{R}_1 = & (W \dot{\varphi} \cos \vartheta - \dot{\vartheta} V) \underline{i} + (V \dot{\varphi} + \dot{\vartheta} r_1 - W \dot{\varphi} \sin \vartheta) \underline{j} \\ & + (W \dot{\varphi} + V \dot{\varphi} \sin \vartheta - r_1 \dot{\varphi} \cos \vartheta) \underline{k} \end{aligned} \quad (3)$$

The position vector of any point along the portion of the second beam located inside the first beam is

$$\underline{R}_2 = x' \underline{i} + V \underline{j} + W \underline{k} \quad (4)$$

where $x' = L_1 + \tau - L_2 + x$ and must satisfy the following condition,

$$L_1 - L_2 + \tau \leq x' \leq L_1 \quad (4a)$$

L_1 is the length of the first beam, L_2 is the length of the second beam, τ is the length of the part of the second beam protruding from the first beam and x is the distance from the lower end of the second beam to the desired point within the range defined for x' (see figure 3). Note that $\dot{x}' = \dot{x}$, since longitudinal vibration along the second beam is neglected. This portion of the second beam and the first beam are assumed to have the same mode shapes. Therefore, V and W defined in equation (4) are the same functions used for \underline{R}_1 . The time rate of change of \underline{R}_2 is:

$$\begin{aligned} \dot{\underline{R}}_2 = \frac{\delta R_2}{\delta t} + \underline{\Omega} \times \underline{R}_2 = (\dot{r} + W\dot{\varphi}\cos\vartheta - V\dot{\vartheta})\underline{i} + (\dot{V} + \dot{x}' - W\dot{\varphi}\sin\vartheta)\underline{j} \\ + (\dot{W} + V\dot{\varphi}\sin\vartheta - x'\dot{\varphi}\cos\vartheta)\underline{k} \end{aligned} \quad (5)$$

Similarly, the position vector of any point on the protruding part of the second beam is:

$$\underline{R}_3 = y'\underline{i} + V'\underline{j} + W'\underline{k} \quad (6)$$

where $y' = L_1 + y$ and $\dot{y}' = \dot{r} = \dot{y}$. The time rate of change of \underline{R}_3 is

$$\begin{aligned} \dot{\underline{R}}_3 = \frac{\delta R_3}{\delta t} + \underline{\Omega} \times \underline{R}_3 = (\dot{r} + \dot{\varphi}W'\cos\vartheta - \dot{\vartheta}V')\underline{i} \\ + (\dot{V}' - \dot{\varphi}W'\sin\vartheta + \dot{y}')\underline{j} + (\dot{W}' + V'\dot{\varphi}\sin\vartheta - y'\dot{\varphi}\cos\vartheta)\underline{k} \end{aligned} \quad (7)$$

The assumed modes method [8] is used to obtain the expressions for the transverse vibrations V , W , V' and W' . They are written as a linear combination of admissible functions (Φ_i) which are functions of spatial coordinates, multiplied by time dependent generalized coordinates $q_i(t)$.

$$V = \sum_{i=1}^n \Phi_i q_i(t) \quad (8)$$

Treating the continuous beam as a two degree of freedom system, then n should be set to 2. The admissible functions are chosen to be the first two eigenfunctions of a clamped-free beam in order to satisfy the boundary conditions of the two beams. The eigen-functions are given in reference [9]. The final expression for V , W , V' and W' depend on the mode shape selected for each beam.

These results are then used to develop the kinetic energy for each part of the robot-arm including the payload. The total kinetic energy will be

$$T_t = \sum_{i=1}^m T_i + T_p = \sum_{i=1}^m \frac{1}{2} \int_{m_i} (\dot{\underline{R}}_i \cdot \dot{\underline{R}}_i) dm_i + \frac{1}{2} m_p (\dot{\underline{R}}_p \cdot \dot{\underline{R}}_p) \quad (9)$$

where m is the number of links in the robot arm, T_i is the kinetic energy of each link and T_p is the kinetic energy of the payload. The total potential energy of

the robot arm consists of the strain energy of the two beams [10] plus the potential energy due to gravity.

$$\begin{aligned}
 V_i = & \left\{ m_1 \frac{L_1}{2} + m_2 \left[L_1 + r - \frac{L_2}{2} \right] + m_p (L_1 + r) \right\} g \sin \vartheta \quad (10) \\
 & + \left\{ m_1 V \Big|_{\frac{L_1}{2}} + m'_2 V \Big|_{L_1 - \frac{L_2}{2} + \frac{r}{2}} + m''_2 V \Big|_{L_1 + \frac{r}{2}} + m_p V \Big|_{L_1 + r} \right\} g \cos \vartheta \\
 & + \sum_{i=1}^m \left\{ \frac{1}{2} \int_0^{L_i} EI_i(\xi) \left(\frac{\partial^2 V_i(\xi, t)}{\partial \xi^2} \right)^2 d\xi + \frac{1}{2} \int_0^{L_i} EI_i(\xi) \left(\frac{\partial^2 W_i(\xi, t)}{\partial \xi^2} \right)^2 d\xi \right\} \\
 & + \sum_{i=1}^m \left\{ \frac{1}{2} \int_0^{L_i} P_i(\xi, t) \left(\frac{\partial V_i(\xi, t)}{\partial \xi} \right)^2 d\xi + \frac{1}{2} \int_0^{L_i} P_i(\xi, t) \left(\frac{\partial W_i(\xi, t)}{\partial \xi} \right)^2 d\xi \right\}
 \end{aligned}$$

Where ξ is a dummy spatial coordinate used for integration. m_1 is the mass of the first beam, m'_2 is the mass of the part of the second beam located inside the first beam, m''_2 is the mass of the part of the second beam protruding from the first beam. $P_i(\xi, t)$ is the tension force in the i^{th} beam. The first term is the potential energy due to gravity. The second term is the potential energy associated with the flexible motion. The integral terms represent the strain energy of the two beams. Equations (9) and (10) are then substituted in Lagrange's equation [8] to write the unconstrained equations of motion:

$$\frac{d}{dt} \left(\frac{\partial T_i}{\partial \dot{q}_i} \right) - \frac{\partial T_i}{\partial q_i} + \frac{\partial V_i}{\partial q_i} = Q_i \quad (11)$$

where Q_i is the generalized force associated with the generalized coordinate $q_i(t)$.

For the second case, a complete derivation of the equations of motion is presented. Note that this case can be obtained from the previous one by dropping out the flexibility terms associated with the first beam and the part of the second beam located inside the first beam. Since the latter undergo rigid body motion only, then the position vector of their mass center would be of

great importance. For the first beam, we have

$$\underline{\tilde{R}}_1^* = \frac{L_1}{2} \underline{\tilde{i}} \quad (12)$$

The velocity term is

$$\dot{\underline{\tilde{R}}}_1^* = \frac{\delta R_1^*}{\delta t} + \underline{\tilde{\Omega}} \times \underline{\tilde{R}}_1^* = \frac{L_1}{2} \dot{\underline{\tilde{y}}} - \frac{L_1}{2} \dot{\varphi} \cos \vartheta \underline{\tilde{k}} \quad (13)$$

The position vector of the mass center of the part of the second beam located inside the first beam is

$$\underline{\tilde{R}}_2^* = \underline{x}'^* \underline{\tilde{i}} \quad (14)$$

where \underline{x}'^* remains in the range defined in (4a). The time rate of change of $\underline{\tilde{R}}_2^*$ is given by

$$\dot{\underline{\tilde{R}}}_2^* = \frac{\delta R_2^*}{\delta t} + \underline{\tilde{\Omega}} \times \underline{\tilde{R}}_2^* = \dot{r} \underline{\tilde{i}} + \dot{\vartheta} \underline{x}'^* \underline{\tilde{j}} - \dot{\varphi} \underline{x}'^* \cos \vartheta \underline{\tilde{k}} \quad (15)$$

Position and velocity terms for the part of the second beam protruding from the first beam are the same as their counterparts in the first case. They are defined in equations (6) and (7). Since the flexibility effect is restricted to a portion of the second beam only, then the prime sign (') on V and W is dropped in equations (6) and (7) for the rest of the report. Note that r cannot approach zero since it would violate one of the major assumptions set for the Euler-Bernoulli beam. That is r must always be much greater than the cross sectional dimensions. Following the same reasoning as before, the assumed modes method is implemented to obtain the expressions for V and W . Selecting the first two eigen-functions of a clamped-free beam [9] for the admissible functions, V and W become:

$$\begin{aligned} V &= \sum_{i=1}^2 \Phi_i q_{1i}(t) = \Phi_1 q_{11}(t) + \Phi_2 q_{12}(t) \\ W &= \sum_{j=1}^2 \Phi_j q_{2j}(t) = \Phi_1 q_{21}(t) + \Phi_2 q_{22}(t) \end{aligned} \quad (16)$$

where Φ_1 and Φ_2 have the general forms

$$\Phi_i = \cosh\left(\frac{\varepsilon_i y}{r}\right) - \cos\left(\frac{\varepsilon_i y}{r}\right) - \alpha_i \left[\sin h\left(\frac{\varepsilon_i y}{r}\right) - \sin\left(\frac{\varepsilon_i y}{r}\right) \right] \quad (17)$$

The values of ε_i and α_i for each mode are given in Table 1 [9]. Substitute (16) and (17) into (7) to get the complete form for \tilde{R}_3 . These results are then used to develop the kinetic energy for each link.

Since the first beam undergoes a fixed point rotation, then its kinetic energy can be simply defined by:

$$T_1 = \frac{1}{2} \Omega \cdot \tilde{H}_0 \quad (18)$$

Where \tilde{H}_0 is the angular momentum of momentum around point 0. It has the following form:

$$\tilde{H}_0 = A\Omega_x \tilde{i} + B\Omega_y \tilde{j} + C\Omega_z \tilde{k} \quad (19)$$

Assuming properties of a thin rod (i.e, dimensions of the cross section is \ll then the length of the rod), gives $A = 0$ and $B = C = \frac{m_1 L_1^2}{3}$. Therefore, \tilde{H}_0 becomes:

$$\tilde{H}_0 = \frac{m_1 L_1^2}{3} \cos\vartheta \varphi \tilde{j} + \frac{m_1 L_1^2}{3} \varphi \tilde{k} \quad (20)$$

Using (20) in (18), T_1 will be:

$$T_1 = \frac{m_1 L_1^2}{6} \left\{ \varphi^2 \cos^2\vartheta + \varphi^2 \right\} \quad (21)$$

The kinetic energy of the portion of the second beam inside the first beam has rotational and translational parts:

$$T_2 = \frac{1}{2} m_2 \left(\dot{\tilde{R}}_2^* \cdot \dot{\tilde{R}}_2^* \right) + \frac{1}{2} \Omega \cdot \tilde{H}^* \quad (22)$$

where \tilde{H}^* is the angular momentum of momentum around the mass center located by \tilde{R}_2^* . It has the following form:

$$\tilde{H}^* = A_1 \Omega_x \tilde{i} + A_2 \Omega_y \tilde{j} + A_3 \Omega_z \tilde{k} \quad (23)$$

where A_i 's $i=1,2,3$ are the mass moment of inertia around the mass center.

$A_1 = 0$ and $A_2 = A_3 = \frac{m'_2(L_2 - r)^2}{12}$. \tilde{H}^* becomes:

$$\tilde{H}^* = \frac{m'_2(L_2 - r)^2}{12} \left\{ \dot{\varphi} \cos \vartheta \underline{j} + \dot{\vartheta} \underline{k} \right\} \quad (24)$$

Using (24) into (22), T_2 will be

$$T_2 = \frac{1}{2} m'_2 \left\{ \dot{r}^2 + \dot{\vartheta}^2 \left[L_1 + \frac{r}{2} - \frac{L_2}{2} \right]^2 + \dot{\varphi}^2 \left[L_1 + \frac{r}{2} - \frac{L_2}{2} \right]^2 \cos^2 \vartheta \right\} \quad (25)$$

$$+ \frac{m'_2(L_2 - r)^2}{24} \left\{ \dot{\varphi}^2 \cos^2 \vartheta + \dot{\vartheta}^2 \right\}$$

The kinetic energy of the part of the second beam protruding from the first beam is:

$$T_3 = \frac{1}{2} \int_{m''_2} (\dot{\underline{R}}_3 \cdot \dot{\underline{R}}_3) dm''_2 = \frac{1}{2} \int_{m''_2} \left\{ (\dot{r} + \dot{\varphi} W \cos \vartheta - \dot{\vartheta} V)^2 \right. \quad (26)$$

$$\left. + (\dot{V} + \dot{\vartheta} y' - W \dot{\varphi} \sin \vartheta)^2 + (\dot{W} + V \dot{\varphi} \sin \vartheta - y' \dot{\varphi} \cos \vartheta)^2 \right\} dm''_2$$

Position and velocity vectors of the payload have the same form as \underline{R}_3 and $\dot{\underline{R}}_3$ but evaluated at a distance $(L_1 + r)$. The payload is considered to be a point mass, does not include rotation around its own mass center, then its kinetic energy will be:

$$T_p = \frac{1}{2} m_p (\dot{\underline{R}}_p \cdot \dot{\underline{R}}_p) \quad (27)$$

$$= \frac{1}{2} m_p \left\{ (\dot{r} + \dot{\varphi} W \cos \vartheta - \dot{\vartheta} V)^2 + [\dot{V} + \dot{\vartheta} (L_1 + r) - W \dot{\varphi} \sin \vartheta]^2 \right.$$

$$\left. + (\dot{W} + V \dot{\varphi} \sin \vartheta - (L_1 + r) \dot{\varphi} \cos \vartheta)^2 \right\}_{L_1 + r}$$

The total kinetic energy is:

$$T_t = \sum_{i=1}^3 T_i + T_p \quad (28)$$

The total potential energy consists of the strain energy of the two beams [10] and the potential energy associated with the rigid body motion. The strain energy terms include the effect of the bending moment and the axial force. The bending moment effect is represented as follows:

$$\frac{1}{2} \int_0^r EI_2(y) \left(\frac{\partial^2 V(y,t)}{\partial y^2} \right)^2 dy + \frac{1}{2} \int_0^r EI_2(y) \left(\frac{\partial^2 W(y,t)}{\partial y^2} \right)^2 dy \quad (29)$$

while the axial force effect is:

$$\frac{1}{2} \int_0^r T(y,t) \left(\frac{\partial V(y,t)}{\partial y} \right)^2 dy + \frac{1}{2} \int_0^r T(y,t) \left(\frac{\partial W(y,t)}{\partial y} \right)^2 dy \quad (30)$$

where $T(y,t)$ is the axial force (tension) in the second beam. It consists of two parts:

1. The axial force due to centripetal acceleration is [10]:

$$\begin{aligned} T_1(y,t) &= \int_y^r (\dot{\varphi}^2 \cos^2 \vartheta + \dot{\varphi}^2) \rho A_2 (L_1 + \xi) d\xi + [\dot{\varphi}^2 \cos^2 \vartheta + \dot{\varphi}^2] m_p (L_1 + r) \\ &= \rho A_2 (\dot{\varphi}^2 \cos^2 \vartheta + \dot{\varphi}^2) \left(L_1 r + \frac{r^2}{2} \right) \left[1 - \frac{L_1 y + \frac{y^2}{2}}{L_1 r + \frac{r^2}{2}} \right] + m_p (L_1 + r) [\dot{\varphi}^2 \cos^2 \vartheta + \dot{\varphi}^2] \end{aligned}$$

This term represents the effect of the rigid body motion on the flexible motion.

2. The axial force due to gravity effect:

$$T_2(y,t) = \left\{ m_p + \rho A_2 \int_y^r d\xi \right\} g \sin \vartheta = [m_p + \rho A_2 (r - y)] g \sin \vartheta$$

Combining the two components, we get

$$\begin{aligned} T(y,t) &= \rho A_2 (\dot{\varphi}^2 \cos^2 \vartheta + \dot{\varphi}^2) \left(L_1 r + \frac{r^2}{2} \right) \left[1 - \frac{L_1 y + \frac{y^2}{2}}{L_1 r + \frac{r^2}{2}} \right] \\ &+ m_p (L_1 + r) [\dot{\varphi}^2 \cos^2 \vartheta + \dot{\varphi}^2] + [m_p + \rho A_2 (r - y)] g \sin \vartheta \end{aligned} \quad (31)$$

The axial force $T(y, t)$ has a tendency to increase the stiffness of the second beam. The total potential energy will be:

$$\begin{aligned}
 V_t = & \left\{ m_1 \frac{L_1}{2} + m_2 \left[L_1 + r - \frac{L_2}{2} \right] + m_p (L_1 + r) \right\} g \sin \vartheta \quad (32) \\
 & + \left\{ m_2'' V|_{L_1 + \frac{r}{2}} + m_p V|_{L_1 + r} \right\} g \cos \vartheta \\
 & + \frac{1}{2} \int_0^r EI_2(y) \left(\frac{\partial^2 V(y, t)}{\partial y^2} \right)^2 dy + \frac{1}{2} \int_0^r EI_2(y) \left(\frac{\partial^2 W(y, t)}{\partial y^2} \right)^2 dy \\
 & + \frac{1}{2} \int_0^r T(y, t) \left(\frac{\partial V(y, t)}{\partial y} \right)^2 dy + \frac{1}{2} \int_0^r T(y, t) \left(\frac{\partial W(y, t)}{\partial y} \right)^2 dy
 \end{aligned}$$

where the first term represents the potential energy due to gravity. The second, third and fourth terms represent the potential energy associated with the flexible motion. The rest are strain energy terms associated with rigid body motion. Before we derive the virtual work of the system, we need to evaluate all internal and reaction forces.

Both beams of the robot arm are connected to their driving motors by leadscrews. When all controlling forces and torques are not applied, the system will maintain its configuration due to the constraint forces exerted by the leadscrews which balance the weight of the system. Expressions for the constraint forces are obtained from the detailed analysis of the static equilibrium of the two beams. This analysis is included in APPENDIX I

The virtual work principle is implemented to obtain an expression for the generalized forces. The virtual work of the first beam is (see Figure 4)

$$\begin{aligned}
 \delta W_{B1} = & (R'_1 \underline{i} + R'_2 \underline{j}) \cdot \delta \underline{R}_1 - m_1 g (\sin \vartheta \underline{i} + \cos \vartheta \underline{j}) \cdot \delta \underline{R}_1 \quad (33) \\
 & - [(F_s + R_1) \underline{i} + R_2 \underline{j}] \cdot \delta \underline{R}_1|_{L_1} + (T_{c\vartheta} + T'_1 - T_1) \underline{k} \cdot \delta X_1 \\
 & + T_{c\varphi} (\sin \vartheta \underline{i} + \cos \vartheta \underline{j}) \cdot \delta X_1
 \end{aligned}$$

where R'_1 , R'_2 , F_s , R_1 , R_2 , T'_1 , and T_1 are all defined in APPENDIX I. $\delta \underline{R}_1$ is the virtual displacement of the displacement vector \underline{R}_1 , $T_{c\vartheta}$ and $T_{c\varphi}$ are the

controller torque in ϑ and φ directions respectively. $\delta\tilde{X}_1$ is the virtual rotation vector of the first beam.

$$\delta\tilde{X}_1 = \sin\vartheta\delta\varphi\tilde{i} + \cos\vartheta\delta\varphi\tilde{j} + \delta\vartheta\tilde{k} \quad (34)$$

after simplification we obtain,

$$\delta W_{B1} = (T_{c\vartheta} + aF_s)\delta\vartheta + T_{c\varphi}\delta\varphi \quad (35)$$

The virtual work of the second beam is,

$$\begin{aligned} \delta W_{B2} = & F_c\tilde{i} \cdot \delta\tilde{R}_2|_{(L_1+r-L_2)} + (R_1\tilde{i} + R_2\tilde{j}) \cdot \delta\tilde{R}_2|_{L_1} + F_s\tilde{i} \cdot \delta\tilde{R}_2|_{L_1} \\ & + T_1\tilde{K} \cdot \delta\tilde{X}_2 - m_2'g(\sin\vartheta\tilde{i} + \cos\vartheta\tilde{j}) \cdot \delta\tilde{R}_2|_{(L_1+\frac{r}{2}-\frac{L_2}{2})} \\ & - m_2''g(\sin\vartheta\tilde{i} + \cos\vartheta\tilde{j}) \cdot \delta\tilde{R}_3|_{(L_1+\frac{r}{2})} \\ & - m_p g(\sin\vartheta\tilde{i} + \cos\vartheta\tilde{j}) \cdot \delta\tilde{R}_3|_{(L_1+r)} + \int_0^r p(y,t)V(y,t)dy \end{aligned} \quad (36)$$

where F_c is the controller force, $\delta\tilde{R}_2$ and $\delta\tilde{R}_3$ are the virtual displacements of \tilde{R}_2 and \tilde{R}_3 , $\delta\tilde{X}_2$ is the virtual rotation vector of the second beam. Note that in this case $\delta\tilde{X}_1 = \delta\tilde{X}_2$. The last term in equation (36) represent the virtual work done by the transverse distributed force $p(y,t)$. The latter arises from the tangential component of the acceleration vector.

$$\begin{aligned} p(y,t) = & \int_0^y \left\{ 2\rho A_2\dot{\vartheta}r + \rho A_2\dot{\varphi}^2 \cos\vartheta \sin\vartheta (L_1 + \xi) \right\} d\xi \\ = & 2\rho A_2\dot{\vartheta}ry + \rho A_2\dot{\varphi}^2 \cos\vartheta \sin\vartheta (L_1y + \frac{y^2}{2}) \end{aligned} \quad (37)$$

Substituting these terms in equation (36) we get,

$$\begin{aligned} \delta W_{B2} = & \left\{ F_c - m_2''g \cos\vartheta \left[\frac{0.7035}{r} q_{11}(t) + \frac{2.0314}{r} q_{12}(t) \right] \right\} \delta r \\ & + \left\{ -aF_s + m_2''g \sin\vartheta \left[0.68q_{11}(t) + 1.43q_{12}(t) \right] + 2m_p g \sin\vartheta (q_{11}(t) - q_{12}(t)) \right\} \delta\vartheta \\ & + \left\{ -0.68m_2''g \cos\vartheta - 2m_p g \cos\vartheta + 1.14\rho A_2\dot{\vartheta}r^2 \right\} \delta\vartheta \end{aligned}$$

$$\begin{aligned}
& + \rho A_2 \dot{\varphi}^2 \cos\vartheta \sin\vartheta (0.57r^2 L_1 + 0.225r^3) \delta q_{11}(t) \\
& + \left\{ -1.43m_2''g \cos\vartheta + 2m_p g \cos\vartheta + 0.182\rho A_2 \dot{\varphi} r^2 \right. \\
& \left. + \rho A_2 \dot{\varphi}^2 \cos\vartheta \sin\vartheta (0.091r^2 L_1 - 0.02r^3) \right\} \delta q_{12}(t)
\end{aligned}$$

The numerical values, that appear in these equations, are due to the integration of the product of spatial terms, φ_i 's and their derivatives, over the length, r , of the flexible part of the second beam. The integration is done numerically using Gaussian quadrature of high order (40 points) [11]. Therefore, the total virtual work will be:

$$\begin{aligned}
\delta W_t = \delta W_{B1} + \delta W_{B2} = & \left\{ F_c - m_2''g \cos\vartheta \left(\frac{0.7035}{r} q_{11}(t) + \frac{2.0314}{r} q_{12}(t) \right) \right\} \delta r \\
& + \left\{ T_{c\vartheta} + m_2''g \sin\vartheta (0.68q_{11}(t) + 1.43q_{12}(t)) + 2m_p g \sin\vartheta (q_{11}(t) - q_{12}(t)) \right\} \delta\vartheta \\
& + \left\{ T_{c\varphi} \right\} \delta\varphi + \left\{ -0.68m_2''g \cos\vartheta - 2m_p g \cos\vartheta + 1.14\rho A_2 \dot{\varphi} r^2 \right. \\
& \left. + \rho A_2 \dot{\varphi}^2 \cos\vartheta \sin\vartheta (0.57r^2 L_1 + 0.225r^3) \right\} \delta q_{11}(t) \\
& + \left\{ -1.43m_2''g \cos\vartheta + 2m_p g \cos\vartheta + 0.182\rho A_2 \dot{\varphi} r^2 \right. \\
& \left. + \rho A_2 \dot{\varphi}^2 \cos\vartheta \sin\vartheta (0.091r^2 L_1 - 0.02r^3) \right\} \delta q_{12}(t)
\end{aligned} \tag{38}$$

and the generalized forces are:

$$Q_r = F_c - m_2''g \cos\vartheta \left(\frac{0.7035}{r} q_{11}(t) + \frac{2.0314}{r} q_{12}(t) \right) \tag{38a}$$

$$\begin{aligned}
Q_\vartheta = & T_{c\vartheta} + m_2''g \sin\vartheta (0.68q_{11}(t) + 1.43q_{12}(t)) \\
& + 2m_p g \sin\vartheta (q_{11}(t) - q_{12}(t))
\end{aligned} \tag{38b}$$

$$Q_\varphi = T_{c\varphi} \tag{38c}$$

$$Q_{q_{11}}(t) = -0.68m''_2g \cos\vartheta - 2m_p g \cos\vartheta + 1.14\rho A_2 \dot{\vartheta} \dot{r}^2 + \rho A_2 \dot{\varphi}^2 \cos\vartheta \sin\vartheta (0.57r^2 L_1 + 0.225r^3) \quad (38d)$$

$$Q_{q_{12}} = -1.43m''_2g \cos\vartheta + 2m_p g \cos\vartheta + 0.182\rho A_2 \dot{\vartheta} \dot{r}^2 + \rho A_2 \dot{\varphi}^2 \cos\vartheta \sin\vartheta (0.091r^2 L_1 - 0.02r^3) \quad (38e)$$

$$Q_{q_{21}} = Q_{q_{22}} = 0 \quad (38f)$$

The unconstrained equations of motion can now be derived by substituting the results obtained in equations 18-38 in Lagrange's equation which is defined earlier in equation 11. The resulting equations of motion are seven highly nonlinear, coupled, second order ordinary differential equations of motion. These equations can be greatly simplified once the role played by the leadscrews and the effect of the gross body motion on the flexible motion and vice versa are understood.

The rigid body motion in r and ϑ directions is completely controlled by the leadscrews. A self-locking condition is assumed [12], that is the leadscrew cannot rotate unless the control torque is applied. This means, that inertial forces (due to coriolis and centripetal acceleration), gravity and flexibility terms would not affect the rigid body motion in the r and ϑ directions. Thus, rendering the behavior of the robot in these two directions to be similar to the simple system depicted in Figure 6. In other words, the leadscrews cancel the effect of flexible motion on r and ϑ as well as the effect of inertial forces. Therefore, the constraint equations in the r direction could be stated as follows:

1. If the control force is not applied (i.e. $F_c = 0$), then r will no longer change and the constraint equation will be

$$\dot{r} = 0 \quad (39)$$

2. If the control force is applied (i.e. $F_c \neq 0$), then the leadscrew, which causes the translational motion of the second beam, exerts a dynamic reaction force to cancel the effect of both the rigid and flexible inertial terms. Thus, making the equation of motion for r independent of the other coordinates. It is simply

written as:

$$(m_2 + m_p)\ddot{r} = F_c \quad (40)$$

which is a linear, second order ordinary differential equation. Similarly, the constraint equations in the ϑ direction could be written in the following way:

1. If the control torque is not applied, $T_{c\vartheta} = 0$, then ϑ will no longer change. The constraint equation is:

$$\ddot{\vartheta} = 0 \quad (41)$$

2. If the control torque is applied, $T_{c\vartheta} \neq 0$, then due to the leadscrew constraint which cancels the centrifugal, coriolis and flexible motion terms; the equation of motion for ϑ will only be dependent on r .

$$\left\{ \frac{m_1 L_1^2}{3} + \frac{m_2 L_2^2}{12} + m_2 \left[L_1 + r - \frac{L_2}{2} \right]^2 + m_p (L_1 + r)^2 \right\} \ddot{\vartheta} = T_{c\vartheta} \quad (42)$$

Note that ϑ depends on r in the inertia term only. The physical system does not impose any constraint on φ . Therefore, it is expected that the elastic motion would affect the gross body motion in that direction. Moving to the second phase of the problem, which is the effect of the rigid body motion on the flexible motion, we note that the inertial forces generated from the gross body motion are serving as external driving forces into the elastic problem. This occurs twice in this study:

1. In the strain energy derivation, where inertial forces are introduced in equation (31) and are shown to increase the stiffness of the system.
2. In the virtual work principle where inertial forces are introduced in equation (37) and are shown to excite the motion in the $q_{11}(t)$ and $q_{12}(t)$ directions. The reader is referred to APPENDIX II for the listing of the constrained equations of motion. APPENDIX III shows that the constrained equations for the rigid body motion can be derived as a special case of the general equations of motion presented in APPENDIX II. This provides a

partial confirmation of the validity of the modeling procedure.

3. CONTROL

The dynamic model of the robot has a total of seven degrees of freedom, three for the rigid body motion (r, ϑ, φ) and four for the flexible motion ($q_{11}(t), q_{12}(t), q_{21}(t), q_{22}(t)$). This results in a set of seven coupled, highly nonlinear, second order ordinary differential equations of motion. These equations reveal the nonlinearity and nonstationarity characteristics inherent in manipulators. The dependence of inertia characteristics of robots on their geometric configuration and the payload causes the system parameters to be time dependent. Therefore, in order for the robot to have good performance over a wide range of motions and payloads, a sophisticated controller design is needed. This design has to take into consideration the following:

- (1) The nonlinearity and the nonstationarity characteristics.
- (2) The flexible motion which is included in the equations of motion.

Adaptive control method seems to be a promising technique to handle the first feature [3]. Since, its main task is to adjust the feedback gains of the manipulator so that its closed loop performance characteristics would closely match the desire ones. The second feature is very intricate. It involves the controllability and observability problems that arise due to the distributed nature of the beam. The protruding part of the second beam is assumed to have continuously distributed mass and elasticity. An infinite number of degrees of freedom are necessary to specify the position of every particle on the beam. Consequently, the beam possess an infinite number of elastic modes. Since, our interest is up to the second elastic mode only, then the sensors should be sensitive to the first two modes and insensitive to the remaining neglected ones. This is known as the observation spillover problem.

A certain mode can be made unobservable to a sensing element if this latter is located at the node of this particular mode. Therefore, the locations of the sensing elements should be carefully chosen. Prior knowledge of the shape of the modes of the system will be of great help in the selection of the best locations for sensor elements to reduce the observation spillover [13] from the unwanted modes. However, this technique cannot be used to address the controllability problem since in our system, the forcing elements are restricted to the joints.

Unfortunately, relocation of the sensing element can improve the observability problem but does not solve it completely. A search for special sensing systems which are able to filter out the unwanted signal or, in other words, could be insensitive for some modes showed that the comb filter is a good candidate for such tasks [13].

Should the flexible motion be included in the control action, then accurate measurements of the actual displacement and velocity of the flexible part are needed to be fed back into the controller. This requires an additional sensor for end-of-arm motion (i.e., accelerometer, strain gauge, etc.) since the flexible motion is not observable from the joint sensors alone. In the case where the complete state vector cannot be evaluated by measuring devices, then the state observer method [14] may be applied.

Experimental work is needed to determine the shape of the first few modes. These experiments will be conducted on a stationary robot. The equipment to be used in the testing are a spectrum analyzer in conjunction with a Hewlett-Packard 85 micro-computer. A hammer, with an accelerometer attached to it, is used as the excitation source and the vibration is measured with an accelerometer mounted on the arm.

In light of the problems that need to be tackled by the controller to maintain good performance of the manipulator over a wide range of motion and payload, a brief description of the robot controllers presently in use will be given. These are designed to control the rigid body motion only. In most controller designs, the nonlinear terms in the equations of motion have been neglected. This design practice is valid as long as the robot is restricted to slow motion. However, when manipulators are operated at high speed, the neglected nonlinear terms become significant and the omission of the flexible motion in the control action can lead to undesirable vibrations. For accurate performance of the robot, a great portion of the production time has to be wasted waiting for these vibrations to damp out. Therefore, in general, a linear control system is expected to perform poorly over a wide range of tasks. In an attempt to show the deficiency of the controller existing in current robots, a simple linear control system is designed to control the general motion described by the set of equations listed in APPENDIX II.

To relax the controller requirements, the operating ranges for τ , ϑ , and φ will be restricted to the vicinity of an equilibrium point. The payload is kept constant throughout this study. In an attempt to reduce link deformations [2], a common practice is to choose the ratio of the weight of the payload to that of the robot arm to be 10:1. Under these conditions, it would be possible to design a linear controller for this model. Since, the flexible motion is not intended to be included in the control action, then the linear controller should be designed based on the equations listed in APPENDIX III (i.e. equations of motion which describe the rigid body motion only). This linear controller would then be applied on the general equations of motion.

The first step in building the controller is to write the rigid body equations of motion in terms of state variables which are defined as follows:

$$\begin{aligned} y_1 &= r & y_3 &= \varphi & y_5 &= \dot{\vartheta} \\ y_2 &= \dot{r} & y_4 &= \dot{\varphi} & y_6 &= \ddot{\vartheta} \end{aligned} \quad (43)$$

The nonlinear state equations whose general form is

$$\dot{\underline{y}} = f(\underline{y}, \underline{u}, t) \quad (44)$$

are linearized around the equilibrium point (1, 0, 0). The resulting equation can be written as:

$$\dot{\underline{y}} = A\underline{y} + B\underline{u} \quad (45)$$

where $A_{6 \times 6}$ is the plant matrix, $\underline{u}_{3 \times 1}$ is the control vector. In general, equation (45) does not lead to the desired poles. Hence, a state feedback controller technique [15] is implemented to replace the system poles by the desired ones (see Figure 7). The latter are a compromise between the desired transient response and the physical limitations of the system. The detailed derivation of the state feedback gain matrix K_s is included in APPENDIX IV. Only its final form is presented in this section:

$$K_s = \begin{bmatrix} (m_2 + m_p) W_{nr}^2 & 0 & 0 & 2(m_2 + m_p)\xi W_{nr} & 0 & 0 \\ 0 & \alpha W_{n\vartheta}^2 & 0 & 0 & 2\xi\alpha W_{n\vartheta} & 0 \\ 0 & 0 & \alpha W_{n\varphi}^2 & 0 & 0 & 2\xi\alpha W_{n\varphi} \end{bmatrix} \quad (46)$$

An integral action is added to the state feedback controller to eliminate the steady state error or any disturbances in the system. This is illustrated in Figure 8. The integral gains, K_{ii}^I , are determined from the root locus diagrams for r , ϑ and φ respectively. The chosen values of the K_{ii}^I 's were found to lie in the vicinity of the breakaway point.

When the rigid body controller is applied to the general equations of motion, listed in APPENDIX II, the following features are anticipated:

- (1) Since r and ϑ equations of motion don't include any flexibility terms and are independent of the φ coordinate, then their motions are expected to closely follow the desired ones.

- (2) Equation of motion for φ contains flexibility terms which act as a disturbance source to the rigid body motion in the φ direction. However, the integral action in the rigid body controller will enable the system to overcome the disturbances and follow the desired response with zero steady state error.
- (3) The rigid body motion would excite the flexible motion. Instability might occur if at least one of the servo loop frequencies approaches the natural frequencies of the flexible part.

4. SIMULATION

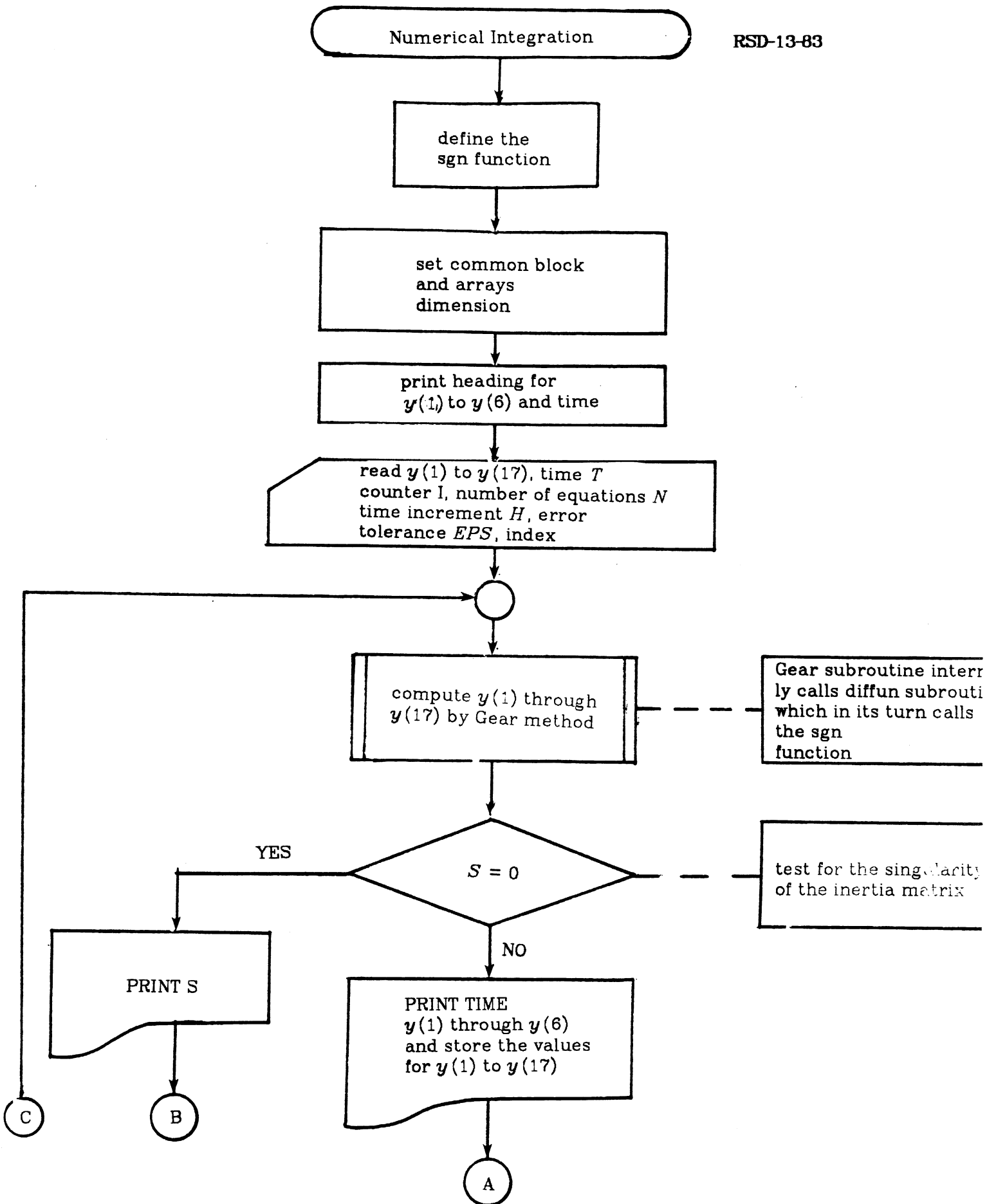
The simulation of the robot arm is very important tool in studying the system's behavior. Written in a form of a computer program, it gives the opportunity to conduct tests that were considered to be hazardous or physically unrealizable. These tests are of great importance especially when dealing with systems that are at their early stages of development.

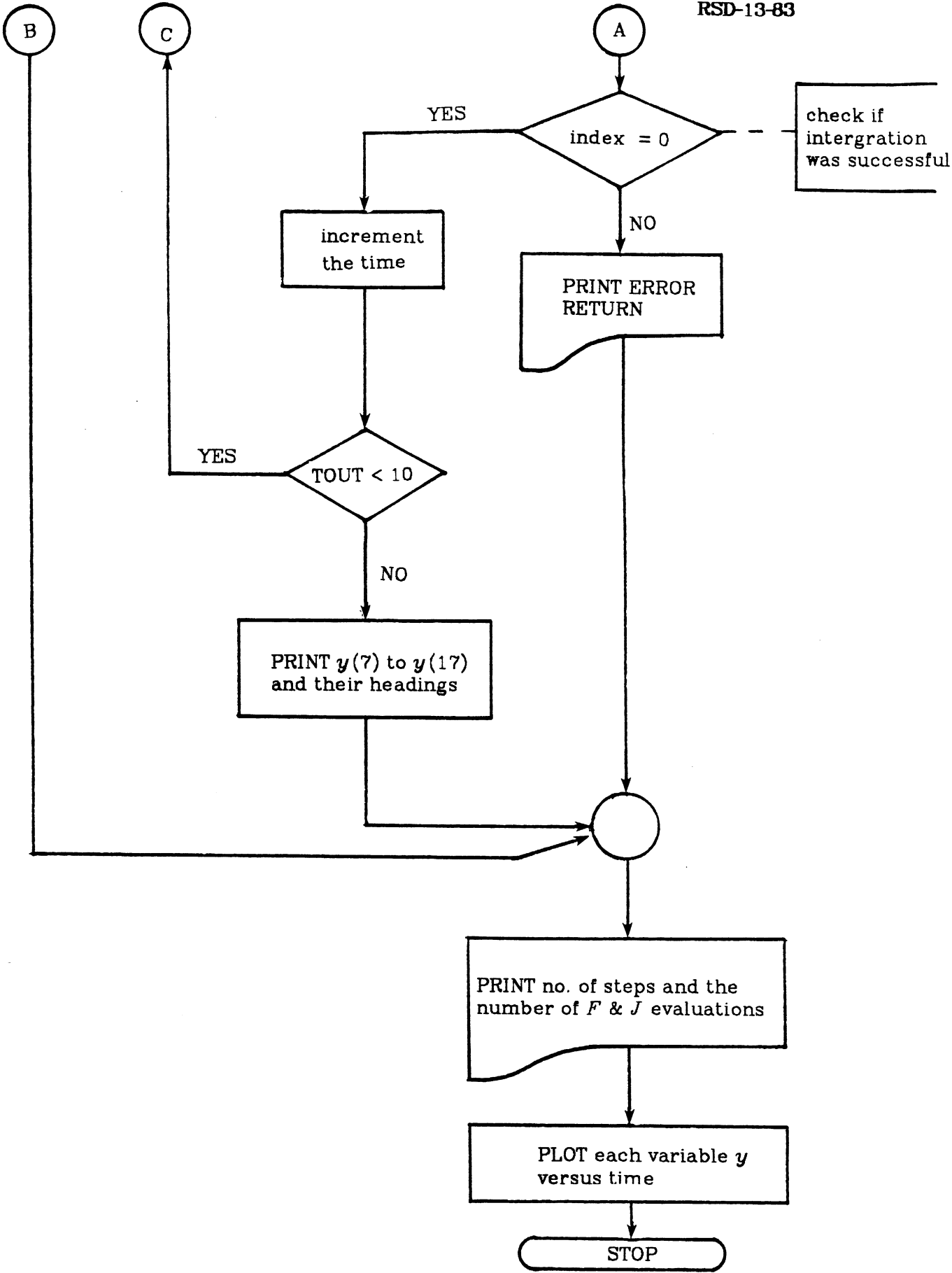
The mathematical description of the model along with the equations obtained from the controller lead to a set of complex, coupled, highly nonlinear equations. No closed form solutions exist for these equations. Instead, they are solved numerically on a digital computer.

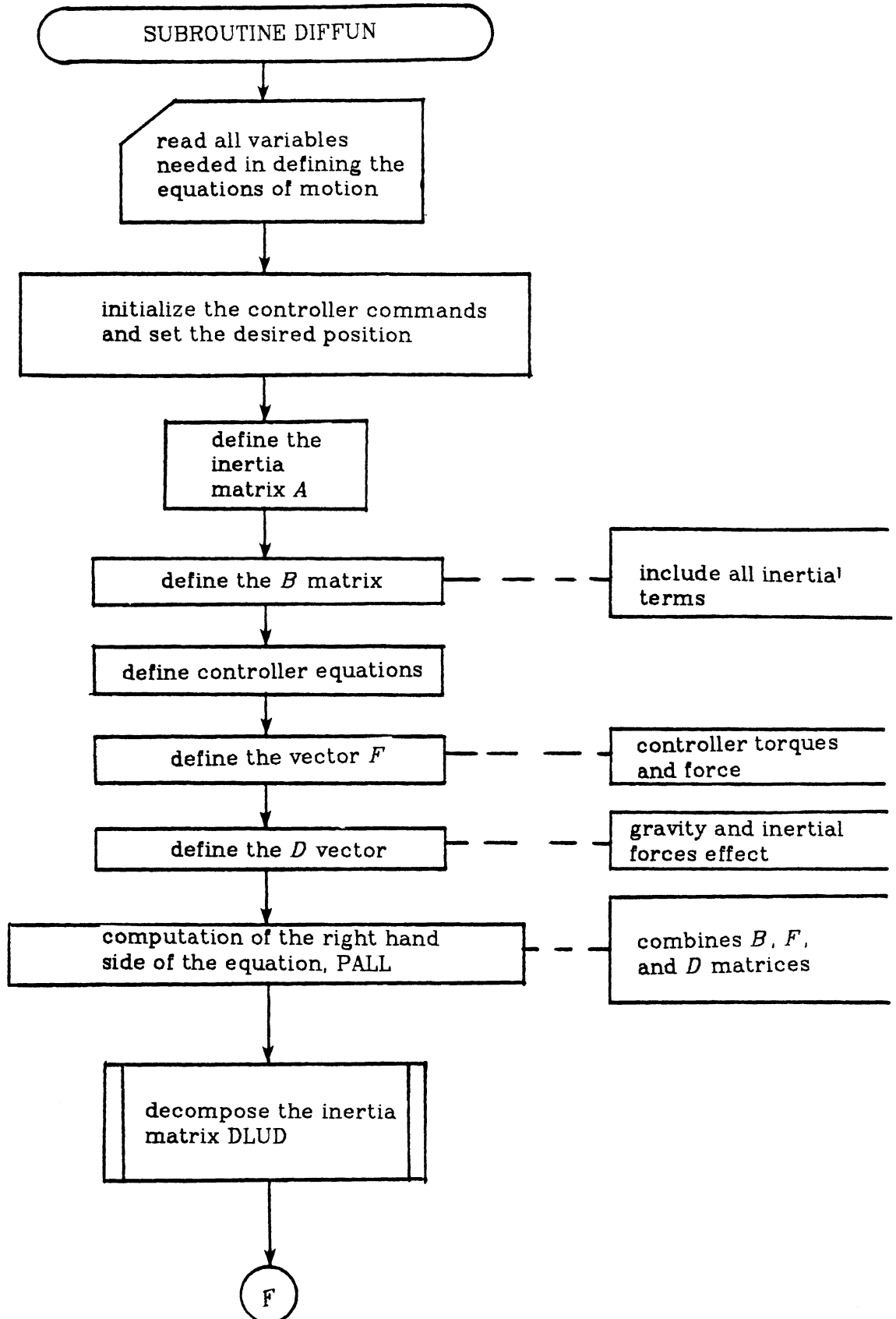
This set of equations involves both very rapidly and very slowly changing terms, all of a decaying nature. Systems possessing this feature are classified as stiff systems. In this work, Gear's method is implemented in the solution of these equations [16]. It is a numerical method well suited for stiff systems. A FORTRAN subroutine package, based on a program written by C. W. Gear, is available through the Michigan Terminal System under the code NAAS:NAL. It has the ability of solving the initial value problem for systems of ordinary differential equations. Such a system has to have the following form:

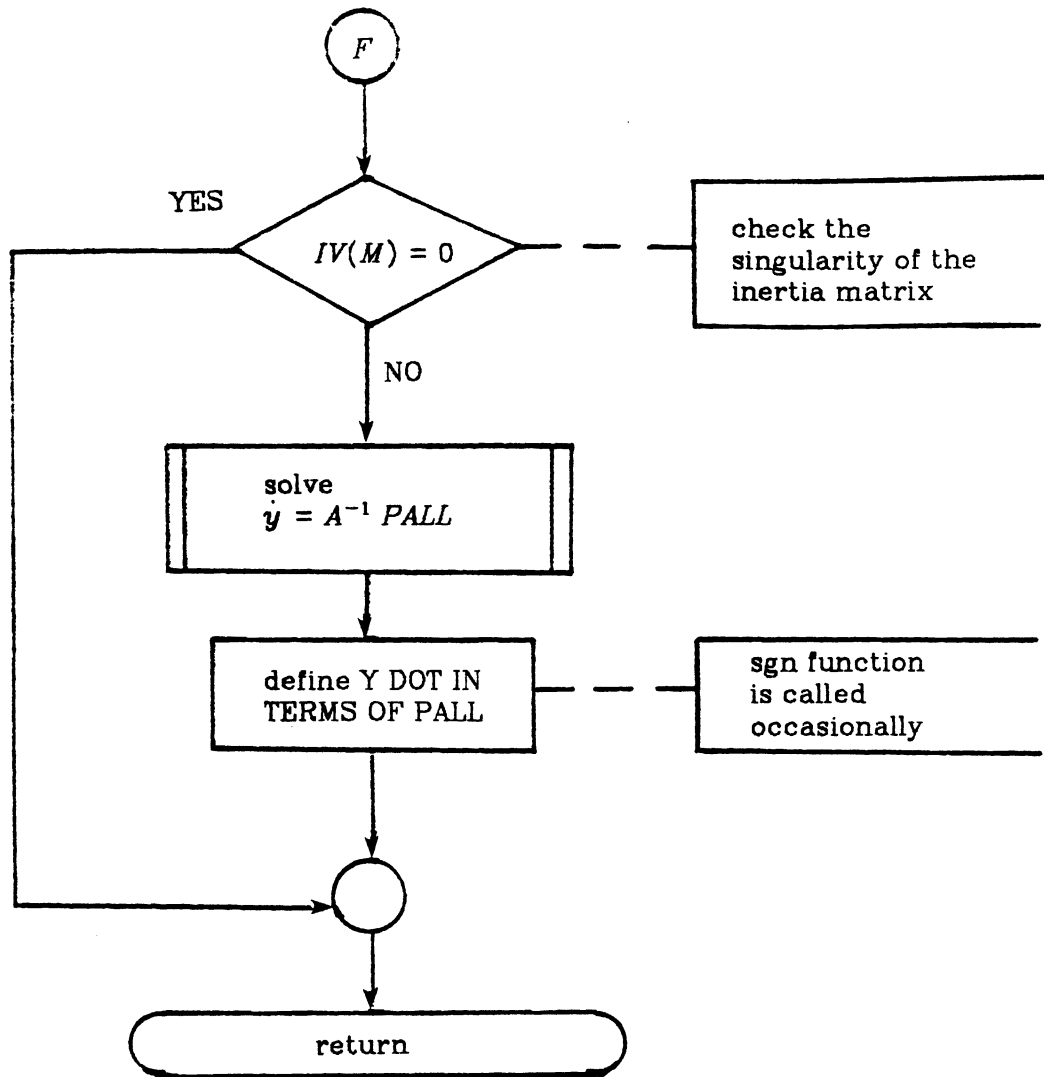
$$\dot{y} = f(y, t)$$

where y , \dot{y} and f are vectors of length $N \geq 1$. \dot{y} is the first derivative of y with respect to time. t denotes the time variable. Hence, our system of equations has to be reduced to first order form. Thus, leading to seventeen first order ordinary differential equations (three equations are obtained from the controller) which form the bulk of the DIFFUN subroutine. The latter is called internally by the DGEAR subroutine. Flowcharts of the main computer program and the DIFFUN subroutine are included in this section. The reader is referred to APPENDIX V for the listing of the computer program.









5. DISCUSSION

The computer program written to simulate the dynamic model of the robot arm is now used to investigate the inter-relationships between the robot structural flexibility and the controller design. These include the effect of constraints due to transmission mechanisms, resonance, forced excitation due to inertial forces, instability mechanisms and parametric excitation.

The standard set of physical system parameters used in the computer program are:

mass of the first beam (m_1) = 0.465 Kg

mass of the second beam (m_2) = 0.9366 Kg

mass of the payload (m_p) = 0.07 Kg

cross sectional area of the second beam (A_2) = 0.000173 m^2

length of the first beam (L_1) = 0.361 m

length of the second beam (L_2) = 2 m

gravitational acceleration (g) = 9.81 m/sec^2

aluminum density (ρ) = 2707 Kg/m^3

flexural rigidity (EI) = 1121.9 Pa

reference position for τ is 1m

reference position for ϑ is 0 rad

reference position for φ is 0 rad

desired reference position for τ is 2m

desired reference position for ϑ is 0.5 rad

desired reference position of φ is 0.5 rad

integral action gains are:

for τ : $K_{11}^I = 8.8$

for ϑ : $K_{22}^I = 5.8$

for φ : $K_{33}^I = 44.2$

The servo natural frequencies are

for r : $W_{nr} = 4 \text{ rad/sec}$

for ϑ : $W_{n\vartheta} = 4 \text{ rad/sec}$

for φ : $W_{n\varphi} = 8 \text{ rad/sec}$

In an attempt to make the integration of the equations of motion less costly, the difference between the servo loop and the flexible motion frequencies is reduced. This is done by giving the second beam a length $L_2 = 2\text{m}$ which is six times greater than the actual length. This has resulted in a decrease in the stiffness of the second beam and helped to exaggerate its vibratory motion.

Given these values, the equations of motion listed in appendices II and III are integrated separately. The results for the rigid body motion only are shown in Figures 9-11 while the results obtained for the rigid and flexible motion are shown in Figures 12-18. Comparison of the results obtained from these two runs, show that there is no obvious difference between the results for r , ϑ , φ for the two cases. This can be explained as follows:

- (1) The plots for r and ϑ are expected to be the same due to the leadscrew constraints which made them insensitive to gravity, inertial forces and flexible motion effects.
- (2) Since there is no constraint in the φ direction, the plots in the two runs corresponding to the φ motion are expected to be slightly different. This difference is mainly expected to be from the flexible motion, since in both cases, φ is subjected to inertial forces and is not affected by gravity. Numerical values obtained from the computer runs show that the difference is roughly in the order of 10^{-6}m . The small effect of the flexible motion on the rigid body motion explains the reason for getting similar φ plots.

Figure 15 represents the motion of the flexible coordinate $q_{11}(t)$. Its transient response shows the whip effect that the rigid body motion has on the flexible motion. Note that in modeling the robot arm, the gravity effect on the flexible motion is included, and the general equations of motion represents a conservative system since no damping is considered in the derivation. Therefore, it is expected that the steady state response would be a sustained oscillation around a negative value. The latter represents the static deflection caused by gravity.

The motion of $q_{12}(t)$ is illustrated in Figure 16. This plot has two additional features:

- (1) The magnitude of the vibratory motion is on the order of 10^{-3} while the one for $q_{11}(t)$ was on the order of 10^{-1} . This is due to the larger amount of energy required to excite the higher modes.
- (2) After 4 seconds, the natural frequency of the second flexible mode is decreased due to the vanishing effect of inertial forces which tend to increase the stiffness of the flexible part.

Figures 17 and 18, which illustrate the flexible motion of $q_{21}(t)$ and $q_{22}(t)$, represent a very important aspect of this particular robot design. Their transient responses show the whip effect, due to the rigid body motion, and then die out with time. These interesting results can be interpreted as follows:

- (1) Gravity doesn't affect the flexible motion in the $q_{21}(t)$ and $q_{22}(t)$ directions. Therefore, their motions are expected to either die out to zero with time or oscillate around zero (i.e. no static deflection).
- (2) Since there is no constraint on the rigid body motion in the φ direction, then the flexible part would not be able to conserve the strain energy in the $q_{21}(t)$ and $q_{22}(t)$ directions. The motion of the latter would act as a disturbance source on the rigid body motion in the φ direction. These

disturbances are compensated for in the rigid body controller.

To better explain the second feature, a model, which simulates the rigid body motion in the φ direction as well as the flexible motions of $q_{21}(t)$ and $q_{22}(t)$ is shown in Figure 19. $x_1(t)$ and $x_2(t)$ represent the rigid body motion and the flexible motion coordinates respectively. Note that only one flexible mode is considered in this model. $F_1(t)$ is the rigid body control force. $F_2(t)$ is the flexible motion control force. However, in our system, the controller is designed for the rigid body motion only, then $F_2(t)$ will remain zero at all times. Only the resulting equations of motion are listed here.

$$\ddot{x}_1 + \omega_{n1}^2(x_1 - x_2) = \frac{F_1}{m_1}$$

$$\ddot{x}_2 + \omega_{n2}^2(x_2 - x_1) = \frac{F_2}{m_2}$$

In an attempt to prove that the flexible motion cannot store the strain energy, an initial condition is given to the flexible motion coordinate, $x_2(t)$, while the rigid body coordinate, $x_1(t)$, is set to zero. The results of this simulation (see Figures 20-21) prove that the flexible motion, $x_2(t)$, could be driven to zero while exciting the rigid body motion, $x_1(t)$. The rigid body controller is then reactivated to bring $x_1(t)$ to its initial position.

Additional runs are made with modifications to the standard set of parameters to study the behavior of the system in the following areas:

1. Effect of gravity
2. Instability mechanisms
3. Speed - accuracy trade off.

The first study is done by simply eliminating the effect of gravity. Set $g = 0$ in the base program. Since gravity affects the flexible motion in the $q_{11}(t)$ and $q_{12}(t)$ directions only, then similar results are obtained to those as in the base run for the rigid body motion (i.e. plots for τ , ϑ and φ) and the flexible motion in

the $q_{21}(t)$ and $q_{22}(t)$ directions. The steady state response of the $q_{11}(t)$ and $q_{12}(t)$ oscillate around zero instead of the static deformation position. This is illustrated in Figures 22-23.

Instability can occur if one of the servo loop frequencies coincides with the flexible motion frequencies. There are two ways in which this can occur:

- (1) The servo loop frequency is increased to match the flexible motion frequency (i.e. a sharp increase in the speed of the rigid body motion).
- (2) The flexible motion frequency is decreased to approach the servo loop frequency (i.e. making the system more flexible).

The first case should be ruled out since increasing the speed of the rigid body motion would drastically increase the effect of the inertial forces. The latter have a tendency to increase the stiffness of the system. Consequently, the flexible motion frequencies would become hard to predict. Hence, the second way is adopted in this study. In the base program, EI is reduced to 17.04 Pa to make the system more flexible and $g = 0$ simply to reduce the cost of this run. The results are shown in Figures 24-28. The plots for τ and ϑ are the same as in the base run results (see Figures 12-13) since they are insensitive to either EI or g . Comparing Figures 24-28 with their counterparts in the base run (Figures 14, 17, 18, 22 and 23), we note the following:

- (1) φ becomes more oscillatory (compare Figure 24 with Figure 14). Thus, for a "soft" system, the flexible motion has a very significant effect on the rigid body motion.
- (2) Figure 25 reflects the reduction in the flexible motion frequency and shows the increase in the magnitude of the oscillatory motion of $q_{11}(t)$.
- (3) Figure 26 shows the instability in the system.

- (4) The response of $q_{21}(t)$ and $q_{22}(t)$ are more oscillatory (compare Figures 27-28 with Figures 17-18).

The speed accuracy trade off case is done by raising the servo loop natural frequencies for r , ϑ and φ , in the base run, from 4, 4 and 8 rad/sec to 20, 20 and 40 rad/sec. The integral gains have to be changed accordingly to $K_{11}^I = 1192$, $K_{22}^I = 692$ and $K_{33}^I = 5537$. Similarly, g has been set to zero in an attempt to reduce the cost of this run. Comparing the results obtained (see Figures 29-35) with those of the base run with $g = 0$ (see Figures 17,18,22, and 23), a general comment can be drawn. The overall oscillatory flexible motion has increased in magnitude. This increase is in the order of 10^{-2} to 10^{-1} for $q_{11}(t)$ and $q_{21}(t)$. Therefore, leading to the conclusion that high-speed operation would deteriorate the accuracy of the system.

6. SUMMARY

The purpose of this study is to investigate the inter-relationships between the robot structural flexibility and the controller design. These relationships will be used as the basis for designing and evaluating controllers for the flexible as well as rigid body motion of the robot arm.

A spherical coordinate laboratory robot is used as the focus for this study. The dynamic model for the robot includes the flexibility effects of the flexible link. The assumed modes method is used to approximate the dynamics of the infinite dimensional link. This approximation incorporates the first two flexible modes only. The latter is considered to adequately describe the flexible motion, since higher modes are unlikely to be excited. The generalized forces are obtained from the virtual work principle, and Lagrange's equation is implemented to derive the equations of motion. An integral plus state feedback controller is used to control the rigid body motion only. This simple controller design is adopted to simulate the robot controllers currently in use. The

dynamic model and the controller design are used as the basis for the simulation studies. The latter demonstrates the potential mechanisms by which structural dynamics and controller design can interact.

The effects of constraints, due to transmission mechanisms such as lead screws, have given the robot arm a cantilever beam-like behavior in the r and ϑ directions. This leads to the conservation of the strain energy which is manifested by the sustained vibratory motion of $q_{11}(t)$ and $q_{12}(t)$. The absence of the constraint in the φ direction caused the strain energy to dissipate since it acts as a disturbance on the rigid body motion. Consequently, the rigid body controller was able to damp out the vibration in the $q_{21}(t)$ and $q_{22}(t)$ directions. The possibility of resonance, parametric excitation, and forced excitation due to inertial forces are covered in this report.

The simple controller design employed here, can be improved significantly by including the effect of the flexible motion in the control action. This can be done in three different ways:

- (1) Design a controller based on a detailed dynamic model of the manipulator which includes the effect of flexibility. This approach has many drawbacks. The dynamic model would be very complex even for low order beam models. Any discrepancy in the dynamic model or disturbances in the system would considerably affect the overall performance of the robot, since no actual measurements are being fed back to the controller. In other words, the robot would behave as an open loop system.
- (2) A full kinematic state measurement at the end point of the robot arm is fed back to the controller. The latter activates the actuators at the joints to correct for the malpositioning of the end effector. This approach compensates for the inaccuracy of the dynamic model as well as for any disturbances in the system. It does not require any additional actuators.

The major drawback of this method is the difficulty of getting accurate measurements of the position and orientation of the end effector over a large operation volume.

- (3) Acknowledging the fact that large deflections in manipulators are due to bending, one approach calls for sensing and correcting the bending of each link separately by using a "straightness servo" [17]. This technique requires as many additional hydraulic actuators as links. Its main advantage is that each link is controlled by a simple independent control loop. This approach, in effect, requires both additional sensors and actuators to compensate for the flexible motion.

7. REFERENCES

- [1] Asada, H., Kanade, T., Takeyama, I., "Control of a Direct Drive Arm," in *Robotics Research and Advanced Applications*, edited by Wayne J. Book, ASME Booklet, Nov. 1982, pp 63-72.
- [2] Thompson, B.S., Sung, C.K., "A Variational Formulation For The Dynamic Viscoelastic Finite Element Analysis Of Robotic Manipulators Constructed From Composite Materials," *ASME Design and Production Engineering Conf.* Dearborn, MI, Sept. 1983.
- [3] Sunada, W.H., Dubowsky, S., "On The Dynamic Analysis And Behavior Of Industrial Robotic Manipulators With Elastic Members," *ASME Paper No. 82-Det-45*.
- [4] Shabana, A., Wehage, R.A., "Variable Degree Of Freedom Component Mode Analysis Of Inertia Variant Flexible Mechanical Systems," *ASME Paper No. 82-Det-93*.
- [5] Book, W.J., Maizza-Neto, O., Whitney, D.E., "Feedback Control Of Two Beams, Two Joint Systems With Distributed Flexibility," *ASME Journal of Dynamic Systems, Measurements and Control*, Vol. 97, No. 4, Dec. 1975, pp 424-431.
- [6] Dubowsky, S., Desforges, D.T., "The Application Of Model-Referenced Adaptive Control To Robotic Manipulators," *ASME Journal of Dynamic Systems, Measurement and Control*, Vol. 101, No. 3, Sept. 1979, pp 193-200.
- [7] Horowitz, R., Tomizuka, M., "An Adaptive Control Scheme For Mechanical Manipulators-Compensation Of Nonlinearity And Decoupling Control," *ASME Paper No. 80-WA/DSC-6*.
- [8] Meirovitch, Leonard, *Elements Of Vibration Analysis*, McGraw Hill, New York, 1975.

- [9] Young, D., "Vibration Of Rectangular Plates By The Ritz Method," *Journal of Applied Mechanics*, Vol. 72, Dec. 1950, pp 448-453.
- [10] Meirovitch, L., *Analytical Methods In Vibrations*, McGraw Hill, New York, 1967, pp 440-445.
- [11] Desai, C., Abel, J., *Introduction To The Finite Element Method, A Numerical Method For Engineering Analysis*, Van Nostrand Reinhold, 1972.
- [12] Joseph E. Shigley, *Mechanical Engineering Design*, McGraw Hill, New York, 1977.
- [13] Balas, M., "Feedback Control Of Flexible Systems," *IEEE Trans. on Automatic Control*, Vol. AC-23, No. 4, Aug. 1978.
- [14] Landau, *Adaptive Control Systems*, Marcel Dekker, 1979.
- [15] D'Azzo, and Houpis, *Linear Control System Analysis And Design*, McGraw-Hill, New York, 1981.
- [16] Gear, C.W., "Ordinary Differential Equation System Solver," *Univ. of Michigan Computing Center*, Dec. 1974.
- [17] Zalucky, A., Hardt, D.E., "Active Control Of Robot Structure Deflections," *ASME Robotics Research and Advanced Applications*, Nov. 1982, pp 83-100.
- [18] Takahashi, Y., Rabins, M., Auslander D. , *Control And Dynamic Systems*, Addison-Wesley, Nov. 1972.

ACKNOWLEDGEMENTS

The authors are pleased to acknowledge the financial support of the Center for Robotics and Integrated Manufacturing at The University of Michigan, and the United States Air Force under AFOSR contract number F49620-82-C-0089. They are also grateful to Mary Ann Pruder for assistance with the preparation of this manuscript.

8. APPENDIX I - Static Equilibrium and Reaction Forces

Free body diagrams of the two beams are shown in Figures 4 and 5. The constraint torque exerted by the first leadscrew to prevent the rotation of the first beam around the pivot point O is denoted by T'_1 . The constraint forces and torque exerted by the second leadscrew on the second beam are R_1 , R_2 and T_1 . F_s is the friction force at the point of contact of the two beams. R'_1 and R'_2 are the reaction forces at the pivot point O . The constraint variables and the reaction forces are computed from the conditions of static equilibrium. Only the results are listed in this appendix:

$$R_1 = (m_2 + m_p)g \sin\vartheta - F_s$$

$$R_2 = (m_2 + m_p)g \cos\vartheta$$

$$T_1 = \left[r m_p + m_2 \left(r - \frac{L_2}{2} \right) \right] g \cos\vartheta - a F_s$$

$$R'_1 = (m_1 + m_2 + m_p)g \sin\vartheta$$

$$R'_2 = (m_1 + m_2 + m_p)g \cos\vartheta$$

$$T'_1 = \left[m_2 \left(L_1 + r - \frac{L_2}{2} \right) + m_p (L_1 + r) + m_1 \frac{L_1}{2} \right] g \cos\vartheta$$

9. APPENDIX II - Equations of Motion

Only, the resulting seven highly nonlinear, coupled, second order ordinary differential equations of motion are listed in this appendix. The equation of motion for r is,

$$\begin{aligned} (m_2 + m_p)\ddot{r} &= F_c & \text{for } F_c \neq 0 \\ \dot{r} &= 0 & \text{for } F_c = 0 \end{aligned}$$

The equation of motion for ϑ is,

$$\begin{aligned} \left\{ \frac{m_1 L_1^2}{3} + \frac{m_2 L_2^2}{12} + m_p (L_1 + r)^2 + m_2 \left(L_1 + r - \frac{L_2}{2} \right)^2 \right\} \ddot{\vartheta} &= T_{c\vartheta} & \text{for } T_{c\vartheta} \neq 0 \\ \dot{\vartheta} &= 0 & \text{for } T_{c\vartheta} = 0 \end{aligned}$$

The equation of motion for φ is,

$$\begin{aligned} & \frac{m_1 L_1^2}{3} \left[\ddot{\varphi} \cos^2 \vartheta - 2\dot{\varphi} \dot{\vartheta} \cos \vartheta \sin \vartheta \right] - \rho A_2 \dot{r} \dot{\varphi} \cos^2 \vartheta \left[L_1 - \frac{L_2}{2} + \frac{r}{2} \right]^2 \\ & + \rho A_2 \dot{\varphi} \cos^2 \vartheta (L_2 - r) \left[L_1 - \frac{L_2}{2} + \frac{r}{2} \right]^2 + \rho A_2 \dot{\varphi} \dot{r} \cos^2 \vartheta (L_2 - r) \left[L_1 - \frac{L_2}{2} + \frac{r}{2} \right] \\ & - 2\rho A_2 \dot{\varphi} \dot{\vartheta} \sin \vartheta \cos \vartheta (L_2 - r) \left[L_1 - \frac{L_2}{2} + \frac{r}{2} \right]^2 - \frac{\rho A_2}{4} \dot{r} \dot{\varphi} \cos^2 \vartheta (L_2 - r)^2 \\ & + \frac{\rho A_2}{12} \ddot{\varphi} \cos^2 \vartheta (L_2 - r)^3 - \frac{\rho A_2}{6} \dot{\varphi} \dot{\vartheta} \sin \vartheta \cos \vartheta (L_2 - r)^3 \\ & + \rho A_2 \left\{ \left[\dot{\varphi} r \cos^2 \vartheta + \dot{\varphi} \dot{r} \cos^2 \vartheta - 2\dot{\varphi} \dot{\vartheta} r \cos \vartheta \sin \vartheta \right] (q_{21}^2 + q_{22}^2) + \dot{\varphi} r \cos^2 \vartheta (2q_{21}\dot{q}_{21} + 2q_{22}\dot{q}_{22}) \right. \\ & + \left[\dot{r} r \cos \vartheta + \dot{r}^2 \cos \vartheta - r \dot{r} \dot{\vartheta} \sin \vartheta \right] (0.78q_{21} + 0.43q_{22}) + r \dot{r} \cos \vartheta (0.78\dot{q}_{21} + 0.43\dot{q}_{22}) \\ & - \left[\dot{\vartheta} r \cos \vartheta + \dot{\vartheta} \dot{r} \cos \vartheta - \dot{\vartheta}^2 r \sin \vartheta \right] (q_{11}q_{21} + q_{12}q_{22}) - r \dot{\vartheta} \cos \vartheta \left[\dot{q}_{11}q_{21} + q_{11}\dot{q}_{21} + q_{12}q_{22} + q_{12}\dot{q}_{22} \right] \\ & - \left[\dot{r}^2 \sin \vartheta + \dot{r} \dot{r} \sin \vartheta + r \dot{r} \dot{\vartheta} \cos \vartheta \right] (0.5q_{11}q_{21} + 0.65q_{11}q_{22} - 0.65q_{12}q_{21} + 0.5q_{12}q_{22}) \\ & \left. - r \dot{r} \sin \vartheta \left[0.5(\dot{q}_{11}q_{21} + q_{11}\dot{q}_{21}) + 0.65(\dot{q}_{11}q_{22} + q_{11}\dot{q}_{22}) \right. \right. \\ & \left. \left. - 0.65(\dot{q}_{12}q_{21} + q_{12}\dot{q}_{21}) + 0.5(\dot{q}_{12}q_{22} + q_{12}\dot{q}_{22}) \right] \right\} \end{aligned}$$

$$\begin{aligned}
& - (\dot{r} \sin \vartheta + r \dot{\vartheta} \cos \vartheta) [\dot{q}_{11} q_{21} + \dot{q}_{12} q_{22}] - r \sin \vartheta [\ddot{q}_{11} q_{21} + \dot{q}_{11} \dot{q}_{21} + \ddot{q}_{12} q_{22} + \dot{q}_{12} \dot{q}_{22}] \\
& - L_1 [\dot{\vartheta} r \sin \vartheta + \ddot{\vartheta} r \sin \vartheta + r \ddot{\vartheta} \cos \vartheta] (0.78 q_{21} + 0.43 q_{22}) - \ddot{\vartheta} L_1 \sin \vartheta (0.78 \dot{q}_{21} + 0.43 \dot{q}_{22}) \\
& - (\ddot{\vartheta} r^2 \sin \vartheta + 2 r \dot{r} \dot{\vartheta} \sin \vartheta + r^2 \ddot{\vartheta} \cos \vartheta) [0.57 q_{21} + 0.09 q_{22}] - r^2 \ddot{\vartheta} \sin \vartheta (0.57 \dot{q}_{21} + 0.09 \dot{q}_{22}) \\
& + [\dot{\varphi} r \sin^2 \vartheta + \ddot{\varphi} r \sin^2 \vartheta + 2 \dot{\varphi} \dot{\vartheta} r \sin \vartheta \cos \vartheta] (q_{21}^2 + q_{22}^2) + \dot{\varphi} r \sin^2 \vartheta (2 q_{21} \dot{q}_{21} + 2 q_{22} \dot{q}_{22}) \\
& + [r^2 \sin \vartheta + r \dot{r} \sin \vartheta + r \dot{\vartheta} r \cos \vartheta] (0.5 q_{21} q_{11} + 0.65 q_{21} q_{12} - 0.65 q_{22} q_{11} + 0.5 q_{22} q_{12}) \\
& + r \dot{r} \sin \vartheta [0.5 (\dot{q}_{21} q_{11} + q_{21} \dot{q}_{11}) + 0.65 (\dot{q}_{21} q_{12} + q_{21} \dot{q}_{12}) - 0.65 (\dot{q}_{22} q_{11} + q_{22} \dot{q}_{11}) \\
& \quad + 0.5 (\dot{q}_{22} q_{12} + q_{22} \dot{q}_{12})] + r \sin \vartheta (\ddot{q}_{21} q_{11} + \dot{q}_{21} \dot{q}_{11} + \ddot{q}_{22} q_{12} + \dot{q}_{22} \dot{q}_{12}) \\
& + [\dot{r} \sin \vartheta + r \dot{\vartheta} \cos \vartheta] (\dot{q}_{21} q_{11} + \dot{q}_{22} q_{12}) + L_1 \ddot{\vartheta} \sin \vartheta (0.78 r \dot{q}_{21} + 0.43 r \dot{q}_{22} + 0.78 r \ddot{q}_{21} + 0.43 r \ddot{q}_{22}) \\
& - L_1 \cos \vartheta [0.78 (r \ddot{q}_{21} + \dot{r} \dot{q}_{21}) + 0.43 (r \ddot{q}_{22} + \dot{r} \dot{q}_{22}) + 0.78 (\ddot{r} \dot{q}_{21} + r \ddot{q}_{21}) + 0.43 (\ddot{r} \dot{q}_{22} + r \ddot{q}_{22})] \\
& - [r^2 \cos \vartheta + r \dot{r} \cos \vartheta - r \dot{\vartheta} r \sin \vartheta] (0.35 q_{21} - 0.25 q_{22}) - r \dot{r} \cos \vartheta (0.35 \dot{q}_{21} - 0.25 \dot{q}_{22}) \\
& \quad - [2 r \dot{r} \cos \vartheta - r^2 \ddot{\vartheta} \sin \vartheta] (0.57 \dot{q}_{21} + 0.09 \dot{q}_{22}) - r^2 \cos \vartheta (0.57 \ddot{q}_{21} + 0.09 \ddot{q}_{22}) \\
& + (\ddot{\varphi} r \sin^2 \vartheta + \ddot{\varphi} r \sin^2 \vartheta + 2 \dot{\varphi} \dot{\vartheta} r \sin \vartheta \cos \vartheta) (q_{11}^2 + q_{12}^2) + 2 \dot{\varphi} r \sin^2 \vartheta (q_{11} \dot{q}_{11} + q_{12} \dot{q}_{12}) \\
& - 2 L_1 [\dot{\varphi} \sin \vartheta \cos \vartheta r + \dot{\varphi} \ddot{\vartheta} \cos^2 \vartheta - \dot{\varphi} \dot{\vartheta} r \sin^2 \vartheta + \dot{\varphi} r \sin \vartheta \cos \vartheta] (0.78 q_{11} + 0.43 q_{12}) \\
& \quad - 2 \dot{\varphi} r L_1 \sin \vartheta \cos \vartheta (0.78 \dot{q}_{11} + 0.43 \dot{q}_{12}) \\
& - 2 [\dot{\varphi} r^2 \sin \vartheta \cos \vartheta + 2 r \dot{r} \dot{\varphi} \sin \vartheta \cos \vartheta + \dot{\varphi} r^2 \ddot{\vartheta} \cos^2 \vartheta - \dot{\varphi} r^2 \ddot{\vartheta} \sin^2 \vartheta] (0.57 q_{11} + 0.09 q_{12}) \\
& \quad - 2 \dot{\varphi} r^2 \sin \vartheta \cos \vartheta (0.57 \dot{q}_{11} + 0.09 \dot{q}_{12}) + (L_1^2 \ddot{r} + 2 L_1 r \dot{r} + r^2 \ddot{r}) \dot{\varphi} \cos^2 \vartheta \\
& + \left[L_1^2 \ddot{r} + L_1 r^2 + \frac{r^3}{3} \right] (\dot{\varphi} \cos^2 \vartheta - 2 \dot{\varphi} \dot{\vartheta} \sin \vartheta \cos \vartheta) + m_p \left\{ 4 [\dot{\varphi} \cos^2 \vartheta - 2 \dot{\varphi} \dot{\vartheta} \cos \vartheta \sin \vartheta] (q_{21}^2 + q_{22}^2 - 2 q_{21} q_{22}) \right. \\
& + 4 \dot{\varphi} \cos^2 \vartheta (2 q_{21} \dot{q}_{21} + 2 q_{22} \dot{q}_{22} - 2 \dot{q}_{21} q_{22} - 2 q_{21} \dot{q}_{22}) + 2 [\dot{r} \cos \vartheta - r \dot{\vartheta} \sin \vartheta] (q_{21} - q_{22}) \\
& \quad + 2 r \cos \vartheta (\dot{q}_{21} - \dot{q}_{22}) - 4 [\dot{\vartheta} \cos \vartheta - \ddot{\vartheta} \sin \vartheta] (q_{11} q_{21} - q_{11} q_{22} - q_{12} q_{21} + q_{12} q_{22}) \\
& - 4 \dot{\vartheta} \cos \vartheta (q_{11} q_{21} + q_{11} q_{22} - q_{11} q_{22} - q_{11} q_{22} - q_{12} q_{21} - q_{12} q_{21} + q_{12} q_{22} + q_{12} q_{22}) \\
& \quad - 4 \dot{\vartheta} \cos \vartheta (q_{11} q_{21} - q_{11} q_{22} - q_{12} q_{21} + q_{12} q_{22}) \\
& - 4 \sin \vartheta (\ddot{q}_{11} q_{21} + \dot{q}_{11} \dot{q}_{21} - \ddot{q}_{11} q_{22} - \dot{q}_{11} \dot{q}_{22} - \ddot{q}_{12} q_{21} - \dot{q}_{12} \dot{q}_{21} + \ddot{q}_{12} q_{22} + \dot{q}_{12} \dot{q}_{22}) \\
& \left. - 2 [\dot{\vartheta} \sin \vartheta (L_1 + r) + \ddot{\vartheta} r \sin \vartheta + \ddot{\vartheta} \cos \vartheta (L_1 + r)] (q_{21} - q_{22}) - 2 \dot{\vartheta} \sin \vartheta (L_1 + r) (\dot{q}_{21} - \dot{q}_{22}) \right\} \\
& + 4 (\dot{\varphi} \sin^2 \vartheta + 2 \dot{\varphi} \dot{\vartheta} \sin \vartheta \cos \vartheta) [q_{21}^2 + q_{22}^2 - 2 q_{21} q_{22}] + 8 \dot{\varphi} \sin^2 \vartheta (q_{21} \dot{q}_{21} + q_{22} \dot{q}_{22} - \dot{q}_{21} q_{22} - q_{21} \dot{q}_{22}) \\
& \quad + 4 \dot{\vartheta} \cos \vartheta (\dot{q}_{21} q_{11} - \dot{q}_{21} q_{12} - \dot{q}_{22} q_{11} + \dot{q}_{22} q_{12})
\end{aligned}$$

$$\begin{aligned}
& + 4\sin\vartheta(\ddot{q}_{21}q_{11} + \dot{q}_{21}\dot{q}_{11} - \ddot{q}_{21}q_{12} - \dot{q}_{21}\dot{q}_{12} - \ddot{q}_{22}q_{11} - \dot{q}_{22}\dot{q}_{11} + \ddot{q}_{22}q_{12} + \dot{q}_{22}\dot{q}_{12}) \\
& \quad - 2[\dot{r}\cos\vartheta - (L_1 + r)\dot{\vartheta}\sin\vartheta](\dot{q}_{21} - \dot{q}_{22}) - 2(L_1 + r)\cos\vartheta(\ddot{q}_{21} - \ddot{q}_{22}) \\
& + 4(\dot{\varphi}\sin^2\vartheta + 2\dot{\varphi}\dot{\vartheta}\cos\vartheta\sin\vartheta)(q_{11}^2 + q_{12}^2 - 2q_{11}q_{12}) + 8\dot{\varphi}\sin^2\vartheta(q_{11}\dot{q}_{11} + q_{12}\dot{q}_{12} - \dot{q}_{11}q_{12} - q_{11}\dot{q}_{12}) \\
& - 4[\dot{\varphi}\sin\vartheta\cos\vartheta(L_1 + r) + \dot{\varphi}\dot{\vartheta}\cos^2\vartheta(L_1 + r) - \dot{\varphi}\dot{\vartheta}\sin^2\vartheta(L_1 + r) + \dot{\varphi}r\sin\vartheta\cos\vartheta](q_{11} - q_{12}) \\
& \quad - 4\dot{\varphi}\sin\vartheta\cos\vartheta(L_1 + r)(\dot{q}_{11} - \dot{q}_{12}) + \ddot{\varphi}(L_1 + r)^2\cos^2\vartheta \\
& \quad + 2(L_1 + r)\dot{\varphi}r\cos^2\vartheta - 2\dot{\varphi}\dot{\vartheta}(L_1 + r)^2\cos\vartheta\sin\vartheta \Big\} = T_{c\varphi}
\end{aligned}$$

The equation of motion for $q_{11}(t)$ is,

$$\begin{aligned}
& \frac{\rho A_2}{2} \left\{ (\dot{r}^2 + r\ddot{r})(q_{11} - 1.3q_{12}) + r\dot{r}(\dot{q}_{11} - 1.3\dot{q}_{12}) + 2r\dot{q}_{11} + 2r\dot{q}_{12} + 1.56L_1(\dot{\vartheta}r + \dot{\vartheta}r) \right. \\
& + 1.14(\dot{\vartheta}r^2 + 2\dot{\vartheta}r\dot{r}) - 2(\dot{\varphi}r \sin\vartheta q_{21} + \dot{\varphi}\dot{\vartheta}r \cos\vartheta q_{21} + \dot{\varphi}r \sin\vartheta \dot{q}_{21} + \dot{\varphi}r \sin\vartheta \dot{q}_{21}) - 2\dot{\vartheta}^2 r q_{11} \\
& + 1.56r\dot{r}\dot{\vartheta} + 2\dot{\varphi}\dot{\vartheta}r \cos\vartheta q_{21} - 1.52r^2\dot{q}_{11} - 1.06r^2\dot{q}_{12} - r\dot{r}\dot{q}_{11} - 1.3r\dot{r}\dot{q}_{12} - 1.56r\dot{\vartheta}L_1 - 0.7\dot{\vartheta}r\dot{r} \\
& \left. + 2.6\dot{\varphi}r\dot{r}\sin\vartheta q_{22} - 2\dot{\varphi}r \sin\vartheta \dot{q}_{21} - 2\dot{\varphi}^2 r \sin^2\vartheta q_{11} + 1.56\dot{\varphi}^2 L_1 r \sin\vartheta \cos\vartheta + 1.14\dot{\varphi}^2 r^2 \sin\vartheta \cos\vartheta \right\} \\
& + \frac{m_p}{2} \left\{ 8(\ddot{q}_{11} - \ddot{q}_{12}) + 4\dot{\vartheta}(L_1 + r) + 4\dot{\vartheta}r - 8(\dot{\varphi}\sin\vartheta + \dot{\varphi}\dot{\vartheta}\cos\vartheta)[q_{21} - q_{22}] \right. \\
& - 8\dot{\varphi}\sin\vartheta(\dot{q}_{21} - \dot{q}_{22}) - 8\dot{\vartheta}^2(q_{11} - q_{12}) + 4r\dot{\vartheta} + 8\dot{\varphi}\dot{\vartheta}\cos\vartheta(q_{21} - q_{22}) - 8(\dot{q}_{21} - \dot{q}_{22})\dot{\varphi}\sin\vartheta \\
& \left. - 8\dot{\varphi}^2 \sin^2\vartheta(q_{11} - q_{12}) + 4\dot{\varphi}^2 \sin\vartheta \cos\vartheta(L_1 + r) \right\} = \\
& - 0.68m_p g \cos\vartheta - 2m_p g \cos\vartheta - \frac{12.362}{r^3} E I q_{11}(t) \\
& - \rho A_2 (\dot{\varphi}^2 \cos^2\vartheta + \dot{\vartheta}^2) (L_1 r + \frac{r^2}{2}) \left\{ \frac{4.65}{r} q_{11} - \frac{7.38}{r} q_{12} \right\} \\
& + \rho A_2 (\dot{\varphi}^2 \cos^2\vartheta + \dot{\vartheta}^2) [(3.08L_1 + 1.13r)q_{11} - (6.96L_1 + 3r)q_{12}] \\
& - [m_p(L_1 + r)(\dot{\varphi}^2 \cos^2\vartheta + \dot{\vartheta}^2) + (m_p + \rho A_2 r)g \sin\vartheta] \left[\frac{4.65}{r} q_{11} - \frac{7.38}{r} q_{12} \right] \\
& + \rho A_2 g \sin\vartheta [3.08q_{11} - 6.96q_{12}] + 1.14r^2 \rho A_2 \dot{\vartheta}r + \rho A_2 \dot{\varphi}^2 \cos\vartheta \sin\vartheta \left\{ 0.57r^2 L_1 + 0.225r^3 \right\}
\end{aligned}$$

The equation of motion for $q_{12}(t)$ is,

$$\begin{aligned}
& \rho A_2 \left\{ (\dot{r}^2 + r\ddot{r})(0.65q_{11} + 0.5q_{12}) + r\dot{r}(0.65\dot{q}_{11} + 0.5\dot{q}_{12}) + r\dot{q}_{12} + r\ddot{q}_{12} + 0.43L_1(\dot{\vartheta}r + \dot{\vartheta}r) \right. \\
& + 0.09(2\dot{\vartheta}r\dot{r} + \dot{\vartheta}r^2) - (\dot{\varphi}r\sin\vartheta\dot{q}_{22} + \dot{\varphi}\dot{\vartheta}r\cos\vartheta\dot{q}_{22} + \dot{\varphi}\dot{r}\sin\vartheta\dot{q}_{22} + \dot{\varphi}r\sin\vartheta\dot{q}_{22}) - \dot{\vartheta}r\dot{q}_{12} + 0.43r\dot{r}\dot{\vartheta} \\
& + r\dot{\varphi}\dot{\vartheta}\cos\vartheta\dot{q}_{22} - 0.53r^2\dot{q}_{11} - 4.34r^2\dot{q}_{12} + 0.65r\dot{r}\dot{q}_{11} - 0.5r\dot{r}\dot{q}_{12} - 0.43r\dot{\vartheta}L_1 + 0.25r\dot{r}\dot{\vartheta} \\
& \left. - 1.3\dot{\varphi}r\dot{r}\sin\vartheta\dot{q}_{21} - \dot{\varphi}r\sin\vartheta\dot{q}_{22} - r\dot{\varphi}^2\sin^2\vartheta\dot{q}_{12} + 0.43r\dot{\varphi}^2\sin\vartheta\cos\vartheta L_1 + 0.09r^2\dot{\varphi}^2\sin\vartheta\cos\vartheta \right\} \\
& + m_p \left\{ 4(\ddot{q}_{12} - \ddot{q}_{11}) - 2[\dot{\vartheta}(L_1 + r) + \dot{\vartheta}r] - 4(\dot{\varphi}\sin\vartheta + \dot{\varphi}\dot{\vartheta}\cos\vartheta)(q_{22} - q_{21}) \right. \\
& - 4\dot{\varphi}\sin\vartheta(\dot{q}_{22} - \dot{q}_{21}) - 4\dot{\vartheta}^2(q_{12} - q_{11}) - 2r\dot{\vartheta} + 4\dot{\varphi}\dot{\vartheta}\cos\vartheta(q_{22} - q_{21}) \\
& \left. - 4\dot{\varphi}\sin\vartheta(\dot{q}_{22} - \dot{q}_{21}) - 4\dot{\varphi}^2\sin^2\vartheta(q_{12} - q_{11}) - 2\dot{\varphi}^2\sin\vartheta\cos\vartheta(L_1 + r) \right\} = \\
& - 1.43m_2''g\cos\vartheta + 2m_p g\cos\vartheta - \frac{485.519}{r^3} EIq_{12} \\
& - \rho A_2(\dot{\varphi}^2\cos^2\vartheta + \dot{\vartheta}^2)(L_1r + \frac{r^2}{2}) \left[-\frac{7.38}{r}q_{11} + \frac{32.42}{r}q_{12} \right] \\
& + \rho A_2(\dot{\varphi}^2\cos^2\vartheta + \dot{\vartheta}^2) \left[-(6.96L_1 + 3r)q_{11} + (23.77L_1 + 9.73r)q_{12} \right] \\
& - [m_p(L_1 + r)(\dot{\varphi}^2\cos^2\vartheta + \dot{\vartheta}^2) + (m_p + \rho A_2r)g\sin\vartheta] \left\{ -\frac{7.38}{r}q_{11} + \frac{32.42}{r}q_{12} \right\} \\
& + \rho A_2g\sin\vartheta \left[-6.96q_{11} + 23.77q_{12} \right] + 0.182r^2\rho A_2\dot{\vartheta} + \rho A_2\dot{\varphi}^2\cos\vartheta\sin\vartheta \left[0.091L_1r^2 - 0.02r^3 \right]
\end{aligned}$$

The equation of motion for $q_{21}(t)$ is,

$$\begin{aligned}
& \rho A_2 \left\{ 0.5(\dot{r}^2 q_{21} + r\ddot{r}q_{21} + r\dot{r}\dot{q}_{21}) - 0.65(\dot{r}^2 q_{22} + r\ddot{r}q_{22} + r\dot{r}\dot{q}_{22}) + r\ddot{q}_{21} + r\dot{q}_{21} \right. \\
& \quad + \dot{\varphi}r\sin\vartheta q_{11} + \dot{\varphi}\dot{\vartheta}r\cos\vartheta q_{11} + \dot{\varphi}r\sin\vartheta\dot{q}_{11} + \dot{\varphi}r\sin\vartheta\dot{q}_{11} \\
& - 0.78[\dot{r}\dot{\varphi}L_1\cos\vartheta + r\ddot{\varphi}L_1\cos\vartheta - r\dot{\varphi}\dot{\vartheta}L_1\sin\vartheta] - 0.57[2r\dot{r}\dot{\varphi}\cos\vartheta + r^2\ddot{\varphi}\cos\vartheta - r^2\dot{\varphi}\dot{\vartheta}\sin\vartheta] \\
& - \dot{\varphi}^2 r\cos^2\vartheta q_{21} - 0.78r\dot{r}\dot{\varphi}\cos\vartheta + r\dot{\varphi}\dot{\vartheta}\cos\vartheta q_{11} + \dot{\varphi}\sin\vartheta(0.5r\dot{r}\dot{q}_{11} - 0.65r\dot{r}\dot{q}_{12} + r\dot{q}_{11}) \\
& + 0.78r\dot{\vartheta}L_1\dot{\varphi}\sin\vartheta + 0.57r^2\ddot{\varphi}\sin\vartheta - r\dot{\varphi}^2\sin^2\vartheta q_{21} - 0.76r^2\dot{q}_{21} - 0.53r^2\dot{q}_{22} - 0.5r\dot{r}\dot{q}_{21} - 0.65r\dot{r}\dot{q}_{22} \\
& - \dot{\varphi}\sin\vartheta(0.5r\dot{r}\dot{q}_{11} + 0.65r\dot{r}\dot{q}_{12}) + 0.78rL_1\dot{\varphi}\cos\vartheta + 0.35r\dot{r}\dot{\varphi}\cos\vartheta \left. \right\} + m_p \left\{ 4(\ddot{q}_{21} - \ddot{q}_{22}) \right. \\
& \quad + 4(\dot{\varphi}\sin\vartheta + \dot{\varphi}\dot{\vartheta}\cos\vartheta)[q_{11} - q_{12}] + 4\dot{\varphi}\sin\vartheta(\dot{q}_{11} - \dot{q}_{12}) \\
& - 2[\dot{r}\dot{\varphi}\cos\vartheta + (L_1 + r)\ddot{\varphi}\cos\vartheta - (L_1 + r)\dot{\varphi}\dot{\vartheta}\sin\vartheta] - 4\dot{\varphi}^2\cos\vartheta^2(q_{21} - q_{22}) - 2r\dot{\varphi}\cos\vartheta \\
& \quad + 4\dot{\varphi}\dot{\vartheta}\cos\vartheta(q_{11} - q_{12}) \\
& \quad \left. + 4\dot{\varphi}\sin\vartheta(\dot{q}_{11} - \dot{q}_{12}) + 2\dot{\vartheta}(L_1 + r)\dot{\varphi}\sin\vartheta - 4\dot{\varphi}^2\sin\vartheta^2(q_{21} - q_{22}) \right\} = \\
& \frac{-12.362}{r^3} EI q_{21}(t) - \rho A_2 (\dot{\varphi}^2 \cos^2\vartheta + \dot{\vartheta}^2) (L_1 r + \frac{r^2}{2}) \left[\frac{4.65}{r} q_{21} - \frac{7.38}{r} q_{22} \right] \\
& \quad + \rho A_2 (\dot{\varphi}^2 \cos^2\vartheta + \dot{\vartheta}^2) [(3.08L_1 + 1.13r)q_{21} - (6.96L_1 + 3r)q_{22}] \\
& - [m_p(L_1 + r)(\dot{\varphi}^2 \cos^2\vartheta + \dot{\vartheta}^2) + (m_p + \rho A_2 r)g \sin\vartheta] \left\{ \frac{4.65}{r} q_{21} - \frac{7.38}{r} q_{22} \right\} + \rho A_2 g \sin\vartheta (3.08q_{21} - 6.96q_{22})
\end{aligned}$$

The equation of motion for $q_{22}(t)$ is,

$$\begin{aligned}
& \rho A_2 \left\{ 0.65(\dot{r}^2 q_{21} + r\ddot{r}q_{21} + r\dot{r}\dot{q}_{21}) + 0.5(r\ddot{r}q_{22} + \dot{r}^2 q_{22} + r\dot{r}\dot{q}_{22}) \right. \\
& \quad + r\dot{q}_{22} + r\ddot{q}_{22} + \dot{\varphi}r \sin\vartheta q_{12} + \dot{\varphi}\dot{r} \cos\vartheta q_{12} \\
& \quad + \dot{\varphi}\dot{r} \sin\vartheta q_{12} + \dot{\varphi}r \sin\vartheta \dot{q}_{12} - 0.43L_1(\dot{r}\dot{\varphi} \cos\vartheta + r\ddot{\varphi} \cos\vartheta - r\dot{\varphi}\dot{\vartheta} \sin\vartheta) \\
& \quad - 0.09(2r\dot{r}\dot{\varphi} \cos\vartheta + r^2\ddot{\varphi} \cos\vartheta - r^2\dot{\varphi}\dot{\vartheta} \sin\vartheta) \\
& \quad - r\dot{\varphi}^2 \cos^2\vartheta q_{22} - 0.43r\dot{r}\dot{\varphi} \cos\vartheta + r\dot{\varphi}\dot{\vartheta} \cos\vartheta q_{12} + 0.43r\dot{\vartheta}L_1\dot{\varphi} \sin\vartheta + 0.09r^2\dot{\vartheta}\dot{\varphi} \sin\vartheta - r\dot{\varphi}^2 \sin^2\vartheta q_{22} \\
& \quad - 0.53r^2\dot{q}_{21} - 4.34r^2\dot{q}_{22} + 0.65r\dot{r}\dot{q}_{21} - 0.5r\dot{r}\dot{q}_{22} + \dot{\varphi} \sin\vartheta (1.3r\dot{r}\dot{q}_{11} + r\dot{q}_{12}) \\
& \quad \left. + 0.43rL_1\dot{\varphi} \cos\vartheta - 0.25r\dot{r}\dot{\varphi} \cos\vartheta \right\} \\
& + m_p \left\{ 4(\ddot{q}_{22} - \ddot{q}_{21}) + 4(\dot{\varphi} \sin\vartheta + \dot{\varphi}\dot{\vartheta} \cos\vartheta)(q_{12} - q_{11}) + 4\dot{\varphi} \sin\vartheta (\dot{q}_{12} - \dot{q}_{11}) \right. \\
& \quad + 2[\dot{r}\dot{\varphi} \cos\vartheta + (L_1 + r)\ddot{\varphi} \cos\vartheta - (L_1 + r)\dot{\varphi}\dot{\vartheta} \sin\vartheta] - 4\dot{\varphi}^2 \cos^2\vartheta (q_{22} - q_{21}) \\
& \quad + 2\dot{r}\dot{\varphi} \cos\vartheta + 4\dot{\varphi}\dot{\vartheta} \cos\vartheta (q_{12} - q_{11}) + 4\dot{\varphi} \sin\vartheta (\dot{q}_{12} - \dot{q}_{11}) - 2\dot{\vartheta}(L_1 + r)\dot{\varphi} \sin\vartheta \\
& \quad \left. - 4\dot{\varphi}^2 \sin^2\vartheta (q_{22} - q_{21}) \right\} = \\
& - \frac{485.519}{r^3} EI q_{22}(t) - \rho A_2 (\dot{\varphi}^2 \cos^2\vartheta + \dot{\vartheta}^2) \left(L_1 r + \frac{r^2}{2} \right) \left\{ -\frac{7.38}{r} q_{21} + \frac{32.42}{r} q_{22} \right\} \\
& \quad + \rho A_2 (\dot{\varphi}^2 \cos^2\vartheta + \dot{\vartheta}^2) [- (6.96L_1 + 3r) q_{21} + (23.77L_1 + 9.73r) q_{22}] \\
& - [m_p (L_1 + r) (\dot{\varphi}^2 \cos^2\vartheta + \dot{\vartheta}^2) + (m_p + \rho A_2 r) g \sin\vartheta] \left\{ -\frac{7.38}{r} q_{21} + \frac{32.42}{r} q_{22} \right\} \\
& \quad + \rho A_2 g \sin\vartheta [-6.96q_{21} + 23.77q_{22}]
\end{aligned}$$

$$T_1 = \frac{1}{2} \underline{\underline{\Omega}} \cdot \underline{\underline{H}}_0 \quad (3-8)$$

where $\underline{\underline{\Omega}}$ is the rotation vector of the $(\underline{\underline{i}}, \underline{\underline{j}}, \underline{\underline{k}})$ basis. $\underline{\underline{H}}_0$ is the angular momentum of momentum around point 0. It can be written in the following form:

$$\underline{\underline{H}}_0 = A \Omega_x \underline{\underline{i}} + B \Omega_y \underline{\underline{j}} + C \Omega_z \underline{\underline{k}} \quad (3-9)$$

Assuming properties of a thin rod (dimensions of cross section is \ll then the length of the rod), gives $A = 0$ and $B = C = \frac{m_1 L_1^2}{3}$. Substituting the values of A, B and C in (3-9) we get:

$$\underline{\underline{H}}_0 = \frac{m_1 L_1^2}{3} \cos \vartheta \dot{\varphi} \underline{\underline{j}} + \frac{m_1 L_1^2}{3} \dot{\vartheta} \underline{\underline{k}} \quad (3-10)$$

Then, the Kinetic energy of the first beam will be:

$$T_1 = \frac{m_1 L_1^2}{6} \left\{ \dot{\varphi}^2 \cos^2 \vartheta + \dot{\vartheta}^2 \right\} \quad (3-11)$$

The Kinetic energy of the second beam has rotational and translational parts:

$$T_2 = \frac{1}{2} m_2 \dot{\underline{\underline{r}}}_2^* \cdot \dot{\underline{\underline{r}}}_2^* + \frac{1}{2} \underline{\underline{\Omega}} \cdot \underline{\underline{H}}^* \quad (3-12)$$

where $\underline{\underline{H}}^*$ is the angular momentum of momentum around the mass center of the second beam, and has the following form:

$$\underline{\underline{H}}^* = A_1 \Omega_x \underline{\underline{i}} + A_2 \Omega_y \underline{\underline{j}} + A_3 \Omega_z \underline{\underline{k}} \quad (3-13)$$

where A_i 's $i = 1, 2, 3$ are the mass moment of inertia around the mass center $A_1 = 0, A_2 = A_3 = \frac{m_2 L_2^2}{12}$. Substituting (3-13) and (3-6) into (3-12) we obtain

$$T_2 = \frac{m_2}{2} \left\{ r^2 + \left[L_1 + r - \frac{L_2}{2} \right]^2 \dot{\varphi}^2 \cos^2 \vartheta + \dot{\vartheta}^2 \left[L_1 + r - \frac{L_2}{2} \right]^2 \right\} + \frac{m_2 L_2^2}{24} \left\{ \dot{\varphi}^2 \cos^2 \vartheta + \dot{\vartheta}^2 \right\} \quad (3-14)$$

The Kinetic energy of the payload, since it is considered to be a point mass, does not include rotation about its own mass center,

$$T_p = \frac{1}{2} m_p \dot{\underline{\underline{r}}}_p \cdot \dot{\underline{\underline{r}}}_p = \frac{m_p}{2} \left\{ r^2 + (L_1 + r)^2 \dot{\vartheta}^2 + (L_1 + r)^2 \dot{\varphi}^2 \cos^2 \vartheta \right\} \quad (3-15)$$

The total Kinetic energy is, $T_t = T_1 + T_2 + T_p$

$$T_t = \frac{m_1 L_1^2}{6} \left\{ \dot{\varphi}^2 \cos^2 \vartheta + \dot{\vartheta}^2 \right\} + \frac{m_2}{2} \left\{ \dot{r}^2 + \left(L_1 + r - \frac{L_2}{2} \right)^2 \dot{\varphi}^2 \cos^2 \vartheta + \dot{\vartheta}^2 \left(L_1 + r - \frac{L_2}{2} \right)^2 \right\} \\ + \frac{m_2 L_2^2}{24} \left\{ \dot{\varphi}^2 \cos^2 \vartheta + \dot{\vartheta}^2 \right\} + \frac{m_p}{2} \left\{ \dot{r}^2 + (L_1 + r)^2 \dot{\vartheta}^2 + (L_1 + r)^2 \dot{\varphi}^2 \cos^2 \vartheta \right\} \quad (3-16)$$

POTENTIAL ENERGY

The datum line is chosen to be aligned with the \underline{i} unit vector. It is horizontal and passes through point 0. Then the potential energy is:

$$V = m_1 g \frac{L_1}{2} \sin \vartheta + m_2 g \left[L_1 + r - \frac{L_2}{2} \right] \sin \vartheta + m_p g (L_1 + r) \sin \vartheta \quad (3-17)$$

which is the summation of the potential energy due to gravitational acceleration of the two beams and the payload.

VIRTUAL WORK PRINCIPLE:

The virtual work principle is implemented to obtain an expression for the generalized forces. The virtual work of the first beam is

$$\delta W_{B1} = \left(R'_1 \underline{i} + R'_2 \underline{j} \right) \cdot \delta \underline{r}_1^0 - m_1 g (\sin \vartheta \underline{i} + \cos \vartheta \underline{j}) \cdot \delta \underline{r}_1^0 \\ - F_s \underline{i} \cdot \delta \underline{r}_1|_{L_1} - (R_1 \underline{i} + R_2 \underline{j}) \cdot \delta \underline{r}_1|_{L_1} + (T'_1 + T_{c\vartheta}) \underline{k} \cdot \delta \underline{X}_1 \quad (3-18) \\ - T_1 \underline{k} \cdot \delta \underline{X}_1 + T_{c\varphi} (\sin \vartheta \underline{i} + \cos \vartheta \underline{j}) \cdot \delta \underline{X}_1$$

where R'_1 , R'_2 , F_s , R_1 , R_2 , T_1 and T'_1 are defined in APPENDIX I. After simplification we obtain

$$\delta W_{B1} = T_{c\vartheta} \delta \vartheta + T_{c\varphi} \delta \varphi + a F_s \delta \vartheta \quad (3-19)$$

where $\delta \underline{X}_1$ is the virtual rotation vector of $\underline{\Omega}$

$$\delta \underline{X}_1 = \delta \varphi \sin \vartheta \underline{i} + \delta \varphi \cos \vartheta \underline{j} + \delta \vartheta \underline{k}$$

The virtual work of the second beam is

$$\delta W_{B2} = -m_2 g (\sin \vartheta \underline{i} + \cos \vartheta \underline{j}) \cdot \delta \underline{r}_2^0 - m_p g (\sin \vartheta \underline{i} + \cos \vartheta \underline{j}) \cdot \delta \underline{r}_2|_{L_1+r} \\ + (R_1 \underline{i} + R_2 \underline{j}) \cdot \delta \underline{r}_2|_{L_1} + F_c \underline{i} \cdot \delta \underline{r}_2|_{L_1+r-\frac{L_2}{2}} + F_s \underline{i} \cdot \delta \underline{r}_2|_{L_1} + T_1 \underline{k} \cdot \delta \underline{X}_2$$

which after simplification, gives the result,

$$\delta W_{B2} = F_c \delta r - \alpha F_s \delta \vartheta \quad (3-20)$$

The total virtual work is

$$\delta W_t = \delta W_{B1} + \delta W_{B2} = T_{c\vartheta} \delta \vartheta + T_{c\varphi} \delta \varphi + F_c \delta r \quad (3-21)$$

and the generalized forces are:

$$\begin{aligned} Q_{\vartheta} &= T_{c\vartheta} \\ Q_{\varphi} &= T_{c\varphi} \\ Q_r &= F_c \end{aligned} \quad (3-22)$$

LAGRANGE'S PRINCIPLE:

Now that we have obtained the expression for the total Kinetic energy and the generalized forces, we can apply Lagrange's equation to obtain the equations of motion. Lagrange's equation can be written as:

$$\frac{d}{dt} \left(\frac{\partial T}{\partial \dot{q}_i} \right) - \left(\frac{\partial T}{\partial q_i} \right) = Q_i \quad (3-23)$$

where T is the total kinetic energy, q_i is the i^{th} generalized coordinate and Q_i is its corresponding generalized force. Making the necessary substitutions for each term in (3-23) we get the following:

$$(m_2 + m_p) \ddot{r} - \left\{ m_2 \left[L_1 + r - \frac{L_2}{2} \right] + m_p (L_1 + r) \right\} (\dot{\varphi}^2 \cos^2 \vartheta + \dot{\vartheta}^2) = F_c \quad (3-24)$$

The unconstrained equation of motion in the ϑ direction is:

$$\begin{aligned} & \left\{ \frac{m_1 L_1^2}{3} + m_2 \left[L_1 + r - \frac{L_2}{2} \right]^2 + \frac{m_2 L_2^2}{12} + m_p (L_1 + r)^2 \right\} \ddot{\vartheta} \\ & + \left\{ m_2 \left[L_1 + r - \frac{L_2}{2} \right] + m_p (L_1 + r) \right\} 2 \dot{r} \dot{\vartheta} \\ & + \dot{\varphi}^2 \cos \vartheta \sin \vartheta \left\{ \frac{m_1 L_1^2}{3} + m_2 \left[L_1 + r - \frac{L_2}{2} \right]^2 + \frac{m_2 L_2^2}{12} + m_p (L_1 + r)^2 \right\} = T_{c\vartheta} \end{aligned} \quad (3-25)$$

The unconstrained equation of motion in the φ direction is:

$$\left\{ \frac{m_1 L_1^2}{3} + m_2 \left[L_1 + r - \frac{L_2}{2} \right]^2 + \frac{m_2 L_2^2}{12} + m_p (L_1 + r)^2 \right\} (\ddot{\varphi} \cos^2 \vartheta - 2 \dot{\varphi} \dot{\vartheta} \cos \vartheta \sin \vartheta)$$

$$+ \left\{ m_2 \left[L_1 + r - \frac{L_2}{2} \right] + m_p (L_1 + r) \right\} 2\dot{r}\dot{\varphi} \cos^2\vartheta = T_{c\varphi} \quad (3-26)$$

Constraint Conditions

The motion of the robot arm is caused by the rotation of the leadscrews which connect the rigid links to the driving motors. A self-locking condition is assumed [12], that is the leadscrews cannot rotate unless the control torques are applied. The constraint equations in their direction could be stated as follows: 1. If the control force is not present (i.e. $F_c = 0$) then r will no longer change and the constraint equation will be

$$\dot{r} = 0 \quad (3-27)$$

2. If the control force is applied (i.e. $F_c \neq 0$), then the leadscrew, which causes the motion of the second beam, exerts a dynamic reaction force to cancel the inertial terms in the equation for r and the equation of motion in the r direction becomes:

$$(m_2 + m_p)\ddot{r} = F_c \quad (3-28)$$

which is an ordinary, linear second order ordinary differential equation. Similarly, the constraint equations in the ϑ direction could be written in the following way:

1. The control torque is not applied, $T_{c\vartheta} = 0$, then the constraint equation in the ϑ direction will be

$$\dot{\vartheta} = 0 \quad (3-29)$$

2. The control torque is applied, $T_{c\vartheta} \neq 0$, then due to the leadscrew constraint, the equation of motion will be completely independent of the φ coordinate. The system will behave as if it is constrained to move in a planar motion with the leadscrew constraint cancelling the centrifugal and Coriolis terms. This results in the following equation of motion,

$$\left\{ \frac{m_1 L_1^2}{3} + \frac{m_2 L_2^2}{12} + m_2 \left[L_1 + r - \frac{L_2}{2} \right]^2 + m_p (L_1 + r)^2 \right\} \ddot{\vartheta} = T_{c\vartheta} \quad (3-30)$$

There is no constraint in the φ direction.

Equations of Motion

The equations of motion are obtained by combining the constraint equations with equations (3-24) to (3-26). The resulting equations will be:

1. Equation of motion in the r direction:

$$\begin{aligned} & \left\{ (m_2 + m_p)\dot{r} - \left[m_2 \left(L_1 + r - \frac{L_2}{2} \right) + m_p(L_1 + r) \right] \left[\dot{\varphi}^2 \cos^2 \vartheta + \dot{\vartheta}^2 \right] \right\} \operatorname{sgn} |F_c| + \dot{r} \left[1 - \operatorname{sgn} |F_c| \right] \\ & = F_c - \left\{ \left[m_2 \left(L_1 + r - \frac{L_2}{2} \right) + m_p(L_1 + r) \right] \left[\dot{\varphi}^2 \cos^2 \vartheta + \dot{\vartheta}^2 \right] \right\} \operatorname{sgn} |F_c| \end{aligned} \quad (3-31a)$$

The equation of motion in the ϑ direction:

$$\begin{aligned} & \left\{ \left[\frac{m_1 L_1^3}{3} + m_2 \left(L_1 + r - \frac{L_2}{2} \right)^2 + \frac{m_2 L_2^2}{12} + m_p(L_1 + r)^2 \right] \dot{\vartheta} + \left[m_2 \left(L_1 + r - \frac{L_2}{2} \right) \right. \right. \\ & \left. \left. + m_p(L_1 + r) \right] 2\dot{r}\dot{\vartheta} + \dot{\varphi}^2 \cos \vartheta \sin \vartheta \left\{ \frac{m_1 L_1^2}{3} + m_2 \left(L_1 + r - \frac{L_2}{2} \right)^2 + \frac{m_2 L_2^2}{12} + m_p(L_1 + r)^2 \right\} \right\} \operatorname{sgn} |T_{c\vartheta}| \\ & = T_{c\vartheta} + \dot{\varphi}^2 \cos \vartheta \sin \vartheta \left\{ \frac{m_1 L_1^2}{3} + m_2 \left(L_1 + r - \frac{L_2}{2} \right)^2 + \frac{m_2 L_2^2}{12} + m_p(L_1 + r)^2 \right\} \operatorname{sgn} |T_{c\vartheta}| \\ & + \dot{\vartheta} \left[1 - \operatorname{sgn} |T_{c\vartheta}| \right] + \left\{ \left[m_2 \left(L_1 + r - \frac{L_2}{2} \right) + m_p(L_1 + r) \right] 2\dot{r}\dot{\vartheta} \right\} \operatorname{sgn} |T_{c\vartheta}| \end{aligned} \quad (3-31b)$$

The equation of motion in the φ direction is the same as equation (3-26). The results obtained in (3-26) and (3-31) show that the rigid body case can be obtained from the general case by dropping out the flexibility terms.

11. APPENDIX IV - Derivation of the Controller Design

The state variables are defined as follows:

$$\begin{aligned} y_1 &= r & y_3 &= \varphi & y_5 &= \dot{\vartheta} \\ y_2 &= \dot{\vartheta} & y_4 &= \dot{r} & y_6 &= \dot{\varphi} \end{aligned} \quad (4-1)$$

The rigid body equations of motion, written in terms of the state variables, lead to:

$$\begin{aligned} \dot{y}_1 &= y_4 \operatorname{sgn} |u_1| \\ \dot{y}_2 &= y_5 \operatorname{sgn} |u_2| \\ \dot{y}_3 &= y_6 \\ \dot{y}_4 &= \frac{u_1}{m_2 + m_p} \\ \dot{y}_5 &= \frac{u_2}{D} \\ \dot{y}_6 &= \left\{ 2Dy_6y_5\cos(y_2)\sin(y_2) - 2y_4y_6\cos^2(y_2) \left[m_2 \left(L_1 + y_1 - \frac{L_2}{2} \right) + m_p(L_1 + y_1) \right] \right. \\ &\quad \left. + u_3 \right\} (D\cos^2(y_2))^{-1} \end{aligned} \quad (4-2)$$

$$\text{where } D = \frac{m_1L_1^2}{3} + \frac{m_2L_2^2}{12} + m_2 \left(L_1 + y_1 - \frac{L_2}{2} \right)^2 + m_p(L_1 + y_1)^2$$

The sgn function is defined as follows

$$\operatorname{sgn}(x) = \begin{cases} 1 & \text{if } x > 0 \\ 0 & \text{if } x = 0 \\ -1 & \text{if } x < 0 \end{cases}$$

The sgn function is used to express the constraint conditions imposed on \dot{r} and $\dot{\vartheta}$. That is, to insure the invariance in the position of r and ϑ when the control variables u_1 and u_2 are removed. Since the sgn function is not allowed to take on negative values in the equations of motion, then the absolute value of its argument is considered. u_1 , u_2 , and u_3 are the controller torques and force. We need to linearize the state equations around the equilibrium point. The latter is determined by setting the above equations to zero. This leads to.

$$A_d = \begin{bmatrix} 0 & 0 & 0 & 1 & 0 & 0 \\ 0 & 0 & 0 & 0 & 1 & 0 \\ 0 & 0 & 0 & 0 & 0 & 1 \\ -W_{nr}^2 & 0 & 0 & -2\xi W_{nr} & 0 & 0 \\ 0 & -W_{n\vartheta}^2 & 0 & 0 & -2\xi W_{n\vartheta} & 0 \\ 0 & 0 & -W_{n\varphi}^2 & 0 & 0 & -2\xi W_{n\varphi} \end{bmatrix} \quad (4-11)$$

In order to evaluate K_s , B^{-1} has to be computed. The latter is a rectangular matrix and pseudo-inverse method is used to calculate B^{-1} [18], i.e.,

$$B^{-1} = (B^T B)^{-1} B^T = \begin{bmatrix} 0 & 0 & 0 & (m_2 + m_p) & 0 & 0 \\ 0 & 0 & 0 & 0 & \alpha & 0 \\ 0 & 0 & 0 & 0 & 0 & \alpha \end{bmatrix}$$

where B^T is the transpose of B . Substituting A , A_d and B^{-1} in (4-8) we get

$$K_s = \begin{bmatrix} (m_2 + m_p) W_{nr}^2 & 0 & 0 & 2(m_2 + m_p) \xi W_{nr} & 0 & 0 \\ 0 & \alpha W_{n\vartheta}^2 & 0 & 0 & 2\xi \alpha W_{n\vartheta} & 0 \\ 0 & 0 & \alpha W_{n\varphi}^2 & 0 & 0 & 2\xi \alpha W_{n\varphi} \end{bmatrix} \quad (4-12)$$

The block diagram of the desired system is shown in Figure 7. An integral action is added to eliminate the steady state error or any disturbances in the system. This is illustrated in Figure 8. The integral block, K^I , has the following form:

$$K^I = \begin{bmatrix} \frac{K_{11}^I}{s} & 0 & 0 \\ 0 & \frac{K_{22}^I}{s} & 0 \\ 0 & 0 & \frac{K_{33}^I}{s} \end{bmatrix} \quad (4-13)$$

where K_{ii}^I 's are determined from the root locus diagrams for r , ϑ , and φ respectively. The open loop transfer functions are obtained separately for each degree of freedom. This is done, by first writing the equations for r

$$\begin{bmatrix} \dot{y}_1 \\ \dot{y}_4 \end{bmatrix} = \begin{bmatrix} 0 & 1 \\ -W_{nr}^2 & -2\xi W_{nr} \end{bmatrix} \begin{bmatrix} y_1 \\ y_4 \end{bmatrix} + \begin{bmatrix} 0 \\ 1 \\ m_2 + m_p \end{bmatrix} u_1 \quad (4-14)$$

the output equation is:

$$Z_1 = [1 \quad 0] \begin{Bmatrix} y_1 \\ y_4 \end{Bmatrix} \quad (4-15)$$

The closed loop transfer function for the inner loop of r is

$$G_1(s) = \frac{1}{s^2 + 2\xi W_{nr}s + W_{nr}^2} \quad (4-16)$$

The corresponding block diagrams are shown in Figures 36(a) and (b). The open loop transfer function is

$$G'_1(s) = \frac{K_{11}^I}{s(s^2 + 2\xi W_{nr}s + W_{nr}^2)} \quad (4-17)$$

Using the values in Table 2 for ξ and W_{nr} , we can draw the root locus diagram for r . Similar reasoning is followed for both ϑ and φ . The resulting transfer functions are shown in Table 3. The root locus diagrams are shown in Figures 37-39. The values of the K_{ii}^I 's are chosen by trail and error from the root locus. The controller is tuned according to the nonlinear equations of motion listed in APPENDIX III. The chosen values of the K_{ii}^I 's were from the neighborhood of the breakway point.


```

0039      GO TO 34
0040      WRITE(6,11) TOUT, Y(1), Y(2), Y(3), Y(4), Y(5), Y(6)
0041      FORMAT(1X, F7.4, 2X, 5(E14.8, 2X), E14.8, 6X)
0042      I=I+1
0043      Y1(1)=Y(1)
0044      Y2(1)=Y(2)
0045      Y3(1)=Y(3)
0046      Y4(1)=Y(4)
0047      Y5(1)=Y(5)
0048      Y6(1)=Y(6)
0049      Y7(1)=Y(7)
0050      Y8(1)=Y(8)
0051      Y9(1)=Y(9)
0052      Y10(1)=Y(10)
0053      Y11(1)=Y(11)
0054      Y12(1)=Y(12)
0055      Y13(1)=Y(13)
0056      Y14(1)=Y(14)
0057      T1(1)=TOUT
0058      IF (INDEX.EQ.0) GO TO 13
0059      WRITE(6,12) INDEX
0060      FORMAT(//, 17X, 'ERROR RETURN WITH INDEX=', 17)
0061      GO TO 34
0062      TOUT=TOUT+0.05DO
0063      IF (TOUT.LE.10.0DO) GO TO 24
0064      IN=I
0065      WRITE(6,71)
0066      71 FORMAT(3X, 'TOUT', 8X, 'Y(7)', 12X, 'Y(8)', 12X, 'Y(9)', 12X, 'Y(10)', 12X,
1 12X, 'Y(12)', 8X)
0067      DO 201 I=1,200
0068      WRITE(6,202) T1(I), Y7(I), Y8(I), Y9(I), Y10(I), Y11(I), Y12(I)
0069      FORMAT(1X, F7.4, 2X, 5(E14.8, 2X), E14.8, 6X)
0070      CONTINUE
0071      WRITE(6,203)
0072      FORMAT(3X, 'TOUT', 8X, 'Y(13)', 12X, 'Y(14)')
0073      DO 205 I=1,200
0074      WRITE(6,207) T1(I), Y13(I), Y14(I)
0075      FORMAT(1X, F7.4, 2X, 2(E14.8, 2X), 2X)
0076      CONTINUE
0077      WRITE(6,16) NSTEP, NFE, NME
0078      16 FORMAT(//, 'PROBLEM COMPLETED IN', I10, 2X,
1 12X, '110, 2X, 'J EVALUATIONS', //)
1 21X, I10, 2X, 'J EVALUATIONS', //)
C
C *****
C      PLOTTER COMMANDS *****
C
0079      CALL PSCALE(6., 1., TIMIN, TIF, TI, IN, 1)
0080      CALL PSCALE(6., 1., YMIN, YIF, Y1, IN, 1)
0081      CALL PLOTS(TIMIN, TIF, YMIN, YIF, 2., 2.)
0082      CALL PLINE(TI, Y1, IN, 1, 0, 0, 1)
0083      CALL PAXIS(2., 2., 'TIME', -4, 6., 0., TIMIN, TIF, 1)
0084      CALL PAXIS(2., 2., 'Y(1)', -4, 6., 90., YMIN, YIF, 1)

```

```

547.000
548.000
549.000
550.000
551.000
552.000
553.000
554.000
555.000
556.000
557.000
558.000
559.000
560.000
561.000
562.000
563.000
564.000
565.000
566.000
567.000
568.000
569.000
570.000
571.000
571.200
572.000
573.000
574.000
575.000
576.000
577.000
578.000
579.000
580.000
581.000
582.000
583.000
584.000
585.000
586.000
587.000
588.000
590.000
591.000
592.000
593.000
594.000
595.000
596.000
597.000
598.000
599.000
600.000

```

```

0085 CALL PLEND 601.000
0086 CALL PSCALE(6.,1.,TIMIN,TIF,TI,IN,1) 603.000
0087 CALL PSCALE(6.,1.,Y2MIN,Y2F,Y2,IN,1) 604.000
0088 CALL PLTOFS(TIMIN,TIF,Y2MIN,Y2F,2.,2.) 605.000
0089 CALL PLINE(TI,Y2,IN,1.0,0,1) 606.000
0090 CALL PAXIS(2.,2.,TIME,-4.6,0.,TIMIN,TIF,1.) 607.000
0091 CALL PAXIS(2.,2.,Y(2),4.6,.90.,Y2MIN,Y2F,1.) 608.000
0092 CALL PLEND 609.000
0093 CALL PSCALE(6.,1.,TIMIN,TIF,TI,IN,1) 611.000
0094 CALL PSCALE(6.,1.,Y3MIN,Y3F,Y3,IN,1) 612.000
0095 CALL PLTOFS(TIMIN,TIF,Y3MIN,Y3F,2.,2.) 613.000
0096 CALL PLINE(TI,Y3,IN,1.0,0,1) 614.000
0097 CALL PAXIS(2.,2.,TIME,-4.6,0.,TIMIN,TIF,1.) 615.000
0098 CALL PAXIS(2.,2.,Y(3),4.6,.90.,Y3MIN,Y3F,1.) 616.000
0099 CALL PLEND 617.000
0100 CALL PSCALE(6.,1.,TIMIN,TIF,TI,IN,1) 619.000
0101 CALL PSCALE(6.,1.,Y4MIN,Y4F,Y4,IN,1) 620.000
0102 CALL PLTOFS(TIMIN,TIF,Y4MIN,Y4F,2.,2.) 621.000
0103 CALL PLINE(TI,Y4,IN,1.0,0,1) 622.000
0104 CALL PAXIS(2.,2.,TIME,-4.6,0.,TIMIN,TIF,1.) 623.000
0105 CALL PAXIS(2.,2.,Y(4),4.6,.90.,Y4MIN,Y4F,1.) 624.000
0106 CALL PLEND 625.000
0107 CALL PSCALE(6.,1.,TIMIN,TIF,TI,IN,1) 627.000
0108 CALL PSCALE(6.,1.,Y5MIN,Y5F,Y5,IN,1) 628.000
0109 CALL PLTOFS(TIMIN,TIF,Y5MIN,Y5F,2.,2.) 629.000
0110 CALL PLINE(TI,Y5,IN,1.0,0,1) 630.000
0111 CALL PAXIS(2.,2.,TIME,-4.6,0.,TIMIN,TIF,1.) 631.000
0112 CALL PAXIS(2.,2.,Y(5),4.6,.90.,Y5MIN,Y5F,1.) 632.000
0113 CALL PLEND 633.000
0114 CALL PSCALE(6.,1.,TIMIN,TIF,TI,IN,1) 635.000
0115 CALL PSCALE(6.,1.,Y6MIN,Y6F,Y6,IN,1) 636.000
0116 CALL PLTOFS(TIMIN,TIF,Y6MIN,Y6F,2.,2.) 637.000
0117 CALL PLINE(TI,Y6,IN,1.0,0,1) 638.000
0118 CALL PAXIS(2.,2.,TIME,-4.6,0.,TIMIN,TIF,1.) 639.000
0119 CALL PAXIS(2.,2.,Y(6),4.6,.90.,Y6MIN,Y6F,1.) 640.000
0120 CALL PLEND 641.000
0121 CALL PSCALE(6.,1.,TIMIN,TIF,TI,IN,1) 643.000
0122 CALL PSCALE(6.,1.,Y7MIN,Y7F,Y7,IN,1) 644.000
0123 CALL PLTOFS(TIMIN,TIF,Y7MIN,Y7F,2.,2.) 645.000
0124 CALL PLINE(TI,Y7,IN,1.0,0,1) 646.000
0125 CALL PAXIS(2.,2.,TIME,-4.6,0.,TIMIN,TIF,1.) 647.000
0126 CALL PAXIS(2.,2.,Y(7),4.6,.90.,Y7MIN,Y7F,1.) 648.000
0127 CALL PLEND 649.000
0128 CALL PSCALE(6.,1.,TIMIN,TIF,TI,IN,1) 651.000
0129 CALL PSCALE(6.,1.,Y8MIN,Y8F,Y8,IN,1) 652.000
0130 CALL PLTOFS(TIMIN,TIF,Y8MIN,Y8F,2.,2.) 653.000
0131 CALL PLINE(TI,Y8,IN,1.0,0,1) 654.000
0132 CALL PAXIS(2.,2.,TIME,-4.6,0.,TIMIN,TIF,1.) 655.000
0133 CALL PAXIS(2.,2.,Y(8),4.6,.90.,Y8MIN,Y8F,1.) 656.000
0134 CALL PLEND 657.000
0135 CALL PSCALE(6.,1.,TIMIN,TIF,TI,IN,1) 659.000
0136 CALL PSCALE(6.,1.,Y9MIN,Y9F,Y9,IN,1) 660.000
0137 CALL PLTOFS(TIMIN,TIF,Y9MIN,Y9F,2.,2.) 661.000
0138 CALL PLINE(TI,Y9,IN,1.0,0,1) 662.000
0139 CALL PAXIS(2.,2.,TIME,-4.6,0.,TIMIN,TIF,1.) 663.000

```

```

0140 CALL PAXIS(2.,2.,'Y(9)',4.6.,90.,Y9MIN,Y9F,1.)
0141 CALL PLTEND
0142 CALL PSCALE(6.,1.,TIMIN,TIF,TI,IN,1)
0143 CALL PSCALE(6.,1.,Y10MIN,Y10F,Y10,IN,1)
0144 CALL PLTDFS(TIMIN,TIF,Y10MIN,Y10F,2.,2.)
0145 CALL PLINE(TI,Y10,IN,1,O,0,1)
0146 CALL PAXIS(2.,2.,'TIME',-4.6.,0.,TIMIN,TIF,1.)
0147 CALL PAXIS(2.,2.,'Y(10)',5.6.,90.,Y10MIN,Y10F,1.)
0148 CALL PLTEND
0149 CALL PSCALE(6.,1.,TIMIN,TIF,TI,IN,1)
0150 CALL PSCALE(6.,1.,Y11MIN,Y11F,Y11,IN,1)
0151 CALL PLTDFS(TIMIN,TIF,Y11MIN,Y11F,2.,2.)
0152 CALL PLINE(TI,Y11,IN,1,O,0,1)
0153 CALL PAXIS(2.,2.,'TIME',-4.6.,0.,TIMIN,TIF,1.)
0154 CALL PAXIS(2.,2.,'Y(11)',5.6.,90.,Y11MIN,Y11F,1.)
0155 CALL PLTEND
0156 CALL PSCALE(6.,1.,TIMIN,TIF,TI,IN,1)
0157 CALL PSCALE(6.,1.,Y12MIN,Y12F,Y12,IN,1)
0158 CALL PLTDFS(TIMIN,TIF,Y12MIN,Y12F,2.,2.)
0159 CALL PLINE(TI,Y12,IN,1,O,0,1)
0160 CALL PAXIS(2.,2.,'TIME',-4.6.,0.,TIMIN,TIF,1.)
0161 CALL PAXIS(2.,2.,'Y(12)',5.6.,90.,Y12MIN,Y12F,1.)
0162 CALL PLTEND
0163 CALL PSCALE(6.,1.,TIMIN,TIF,TI,IN,1)
0164 CALL PSCALE(6.,1.,Y13MIN,Y13F,Y13,IN,1)
0165 CALL PLTDFS(TIMIN,TIF,Y13MIN,Y13F,2.,2.)
0166 CALL PLINE(TI,Y13,IN,1,O,0,1)
0167 CALL PAXIS(2.,2.,'TIME',-4.6.,0.,TIMIN,TIF,1.)
0168 CALL PAXIS(2.,2.,'Y(13)',5.6.,90.,Y13MIN,Y13F,1.)
0169 CALL PLTEND
0170 CALL PSCALE(6.,1.,TIMIN,TIF,TI,IN,1)
0171 CALL PSCALE(6.,1.,Y14MIN,Y14F,Y14,IN,1)
0172 CALL PLTDFS(TIMIN,TIF,Y14MIN,Y14F,2.,2.)
0173 CALL PLINE(TI,Y14,IN,1,O,0,1)
0174 CALL PAXIS(2.,2.,'TIME',-4.6.,0.,TIMIN,TIF,1.)
0175 CALL PAXIS(2.,2.,'Y(14)',5.6.,90.,Y14MIN,Y14F,1.)
0176 CALL PLTEND
0177 CALL EXIT
0178 STOP
0179 END
*OPTIONS IN EFFECT: ID,ERCDIC,SOURCE,NOLIST,NOCHECK,LOAD,NOMAP
*STATISTICS+ SOURCE STATEMENTS = 179,PROGRAM SIZE = 19416
*STATISTICS+ NO DIAGNOSTICS GENERATED

```

```

654.000
665.000
667.000
668.000
669.000
670.000
671.000
672.000
673.000
675.000
676.000
677.000
678.000
679.000
680.000
681.000
683.000
684.000
685.000
686.000
687.000
688.000
689.000
691.000
692.000
693.000
694.000
695.000
696.000
697.000
699.000
700.000
701.000
702.000
703.000
704.000
705.000
706.000
707.000
708.000

```

JH JH

```

C          710.000
C          711.000
C          712.000
C          713.000
C          714.000
C          715.000
C          716.000
C          717.000
C          718.000
C          719.000
C          720.000
C          721.000
C          722.000
C          723.000
C          724.000
C          725.000
C          726.000
C          727.000
C          728.000
C          729.000
C          730.000
C          731.000
C          732.000
C          733.000
C          734.000
C          735.000
C          736.000
C          737.000
C          738.000
C          739.000
C          740.000
C          741.000
C          742.000
C          743.000
C          744.000
C          745.000
C          746.000
C          746.200
C          746.400
C          747.000
C          748.000
C          749.000
C          750.000
C          751.000
C          752.000
C          753.000
C          754.000
C          755.000
C          756.000
C          757.000
C          758.000
C          759.000
C          760.000
C          761.000

0001          SUBROUTINE DIFFUN (N,TIME,Y,YDOT)
C
C          PROGRAM IDENTIFICATION *****
C
C          THIS SUBROUTINE DEFINES THE DIFFERENTIAL EQUATIONS OF MOTION
C
C *****
C
C          VARIABLE IDENTIFICATION *****
C
C M1=MASS OF THE FIRST BEAM
C M2=MASS OF THE SECOND BEAM
C MP=MASS OF THE PAYLOAD
C C1=TRANSLATIONAL CONTROLLER FORCE
C C2=ROTATIONAL CONTROLLER TORQUE AROUND K VECTOR
C C3=ROTATIONAL CONTROLLER TORQUE AROUND THE VERTICAL AXIS
C L1=LENGTH OF THE FIRST BEAM
C L2=LENGTH OF THE SECOND BEAM
C ZETA1=DAMPING RATIO IN THE R DIRECTION
C ZETA2=DAMPING RATIO IN THE TETA DIRECTION
C ZETA3=DAMPING RATIO IN THE FETA DIRECTION
C WNR=NATURAL FREQUENCY FOR R
C WNFETA=NATURAL FREQUENCY FOR FETA
C WNFETA=NATURAL FREQUENCY FOR FETA
C R1=REFERENCE INPUT IN THE R DIRECTION
C R2=REFERENCE INPUT IN THE TETA DIRECTION
C R3=REFERENCE INPUT IN THE FETA DIRECTION
C A2=CROSS SECTIONAL AREA OF THE SECOND BEAM
C ROW=DENSITY OF THE UNIFORM SECOND BEAM
C
C *****
C
C          STORAGE BLOCK *****
C
C          REAL*8 TIME,IK11,IK22,IK33,CENTAC,DIST,PALL(7)
C          INTEGER IV(7),IJ,IN,IM,IY,IUH,JIH,K
C          REAL*8 M1,M2,MP,L1,L2,R1,R2,R3,Y(N),YDOT(N),RC,DC
C          REAL*8 ALPHA,BETA,C1,C2,C3,WNR,WNFETA,WNFETA,ZETA1,PBY(7)
C          REAL*8 ZETA2,ZETA3,A2,ROW,A13,A14,A15,ROW7,ROW8
C          REAL*8 ROW1,ROW2,ROW3,ROW4,ROW5,ROW6
C          REAL*8 AL1,AL2,AL10,AL11,E1,ROW10,ROW9

```


C+++++
 C
 C
 C

805.000
 806.000
 807.000
 808.000
 808.200
 808.400
 809.000
 810.000
 811.000
 812.000
 813.000
 814.000
 815.000
 816.000
 817.000
 818.000
 819.100
 819.200
 819.300
 819.400
 820.000
 821.000
 822.000
 823.000
 824.000
 825.000
 826.000
 827.000
 828.000
 829.000
 830.000
 831.000
 832.000
 833.000
 834.000
 835.000
 836.000
 837.000
 838.000
 839.000
 840.000
 841.000
 842.000
 843.000
 844.000
 845.000
 846.000
 847.000
 848.000
 849.000
 850.000
 851.000
 852.000
 853.000
 854.000

```

0050      GENIAC=(Y(10)**2)**(DCOS(Y(2))**2)+(Y(9)**2)
0051      DIST=(L1+Y(1))+(Y(1)**2)/2.000
0052      BC=L1+Y(1)-(L2/2.000)
0053      ROW1=ROW*A2
0054      ROW2=L1-(L2/2.000)+(Y(1))/2.000
0055      ROW3=L2-Y(1)
0056      ROW4=L1+Y(1)
0057      ROW5=(L1**2)+Y(1)+L1+(Y(1)**2)+(Y(1)**3)/3.000
0058      ROW6=ROW1/2.000
0059      DC=(M1+L1**2)/3.000+M2+BC**2+(M2*L2**2)/12.000+MP+ROW4**2
0060      ALPHA=(M1+L1**2)/3.000+(M2*L2**2)/12.000+M2*(L1+1.000-
      1 (L2/2.000))**2+MP*(L1+1.000)**2
      ROW7=MP+ROW4
      ROW8=((ROW1+Y(1))+MP)+G*DSIN(Y(2))
      ROW9=ROW1+G*DSIN(Y(2))
      ROW10=ROW1+(Y(10)**2)+DSIN(Y(2))+DCOS(Y(2))
      A(1,1)=M2+MP
      A(1,2)=0.000
      A(1,3)=0.000
      A(1,4)=0.000
      A(1,5)=0.000
      A(1,6)=0.000
      A(1,7)=0.000
      A(2,1)=0.000
      A(2,2)=DC
      A(2,3)=0.000
      A(2,4)=0.000
      A(2,5)=0.000
      A(2,6)=0.000
      A(2,7)=0.000
      A(3,1)=ROW1+(Y(1)+DCOS(Y(2)))+(O.78DO*Y(6)+
      1 O.43DO*Y(7))-1.3DO*Y(1)+DSIN(Y(2))+(Y(4)+Y(7)-Y(5)+Y(6))-
      1 L1+DCOS(Y(2))+(O.78DO*Y(6)+O.43DO*Y(7))-
      1 Y(1)+DCOS(Y(2))+(O.35DO*Y(6)-O.25DO*Y(7))+MP*2.000*
      1 DCOS(Y(2))+(Y(6)-Y(7))
      A(3,2)=ROW1+(-Y(1)+DCOS(Y(2)))+(Y(4)+Y(6)+Y(5)+Y(7))
      1 -1.4*Y(1)+DSIN(Y(2))+(O.78DO*Y(6)+O.43DO*Y(7))
      1 (Y(1)**2)+DSIN(Y(2))+(O.57DO*Y(6)+O.09DO*Y(7))+MP*
      1 -4.0DO+DCOS(Y(2))+(Y(4)+Y(6)-Y(4)+Y(7)-Y(5)+Y(6)+
      1 Y(5)+Y(7))-2.0DO+L1+Y(1))+DSIN(Y(2))+(Y(6)-Y(7))
      A(3,3)=((M1+L1**2)/3.000)+(DCOS(Y(2))**2)+ROW1+ROW3
      1 + (ROW2**2)*(DCOS(Y(2))**2)+
      1 (ROW1+(ROW3**3)+(DCOS(Y(2))**2))/12.000+ROW1+(Y(1))+
      1 ((DCOS(Y(2))**2)+(Y(6)**2+Y(7)**2)+Y(1)+((DSIN(Y(2))**2)
      1 +(Y(6)**2+Y(7)**2)+Y(1))+((DSIN(Y(2))**2)+(Y(4)**2+Y(5)**2)
      1 -2.0DO+L1+DSIN(Y(2))+DCOS(Y(2)))+(Y(1)**2)+(O.57DO*
      1 Y(5))-2.0DO+DSIN(Y(2))+DCOS(Y(2)))+(Y(1)**2)+(O.57DO*
      1 Y(4)+O.09DO*Y(5))+ROW5+(DCOS(Y(2))**2)+MP*(4.0DO*
      1 ((DCOS(Y(2))**2)+(Y(6)**2+Y(7)**2)-2.0DO+Y(6)+Y(7))+
      1 4.0DO*(DSIN(Y(2))**2)+(Y(6)**2+Y(7)**2)-2.0DO*Y(6)+
      1 Y(7)+Y(4))**2+Y(5)**2-2.0DO*Y(4)+Y(5))-4.0DO*DSIN(Y(2)))*

```

00R2	1 DCOS(Y(2))*ROW4*(Y(4)-Y(5))+((ROW4**2)+(DCOS(Y(2)))**2))	855.000
00R3	1 (Y(6))-Y(7))	856.000
00B4	1 A(3,4)=-ROW1*(1)*DSIN(Y(2))+Y(6)-MP*4.0DO*DSIN(Y(2))+	857.000
00B5	1 A(3,5)=-ROW1*(1)*DSIN(Y(2))+Y(7)-MP*4.0DO*DSIN(Y(2))+Y(7)	858.000
	1 -Y(6))	859.000
	1 A(3,6)=-ROW1*(Y(1)*DSIN(Y(2))+Y(4)-1*DCOS(Y(2)))*O.78DO*	860.000
	1 Y(1)-Y(1)**2+DCOS(Y(2))*O.57DO)+MP*(4.0DO*DSIN(Y(2)))+(Y(4)	861.000
	1 -Y(5))-2.0DO*ROW4*DCOS(Y(2)))	862.000
	1 A(3,7)=ROW1*(Y(1)*DSIN(Y(2)))*Y(5)-L1*	863.000
	1 DCOS(Y(2))*O.43DO+Y(1)-(Y(1)**2)+DCOS(Y(2))	864.000
	1 +O.09DO)+MP*(4.0DO*DSIN(Y(2)))+(Y(5)-Y(4))+2.0DO	865.000
	1 +ROW4*DCOS(Y(2)))	866.000
00R6	1 A(4,1)=ROW1*(Y(1)/2.0DO)+(Y(4)-1.3DO*Y(5))	867.000
00R7	1 A(4,2)=ROWS*(1.56DO*L1+Y(1)+1.14DO*(Y(1)**2))	868.000
	1 +MP*(2.0DO*ROW4)	869.000
00R8	1 A(4,3)=-ROW1*DSIN(Y(2))+Y(1)+Y(6)-MP*4.0DO	870.000
	1 DSIN(Y(2))*(Y(6)-Y(7))	871.000
00R9	1 A(4,4)=ROW1*(1)+4.0DO*MP	872.000
009C	1 A(4,5)=-4.0DO*MP	873.000
0091	1 A(4,6)=0.0DO	874.000
0092	1 A(4,7)=0.0DO	875.000
0093	1 A(5,1)=ROW1*(1)*(O.65DO*Y(4)+O.5DO*Y(5))	876.000
0094	1 A(5,2)=ROW1*(O.43DO*L1+Y(1)+O.09DO*(Y(1)**2))	877.000
	1 -MP*2.0DO*ROW4	878.000
0095	1 A(5,3)=-ROW1*DSIN(Y(2))+Y(1)+Y(7)-4.0DO*MP*	879.000
	1 DSIN(Y(2))*(Y(7)-Y(6))	880.000
0096	1 A(5,4)=-4.0DO*MP	881.000
0097	1 A(5,5)=ROW1*(1)+4.0DO*MP	882.000
0098	1 A(5,6)=0.0DO	883.000
0099	1 A(5,7)=0.0DO	884.000
0100	1 A(6,1)=ROW1*(1)*(O.5DO*Y(6)-O.65DO*Y(7))	885.000
0101	1 A(6,2)=0.0DO	886.000
0102	1 A(6,3)=ROW1*(Y(1)*DSIN(Y(2))+Y(4)-O.78DO*Y(1))+	887.000
	1 DCOS(Y(2))*L1-O.57DO*(Y(1)**2)+DCOS(Y(2))*MP*(4.0DO*	888.000
	1 DSIN(Y(2)))+(Y(4)-Y(5))-2.0DO*ROW4*DCOS(Y(2)))	889.000
	1 A(6,4)=0.0DO	890.000
0103	1 A(6,5)=0.0DO	891.000
0104	1 A(6,6)=ROW1*(1)+4.0DO*MP	892.000
0105	1 A(6,7)=-MP*4.0DO	893.000
0106	1 A(7,1)=ROW1*(1)*(O.65DO*Y(6)+O.5DO*Y(7))	894.000
0107	1 A(7,2)=0.0DO	895.000
0108	1 A(7,3)=ROW1*(Y(1)*DSIN(Y(2))+Y(5)-O.43DO*L1+Y(1))+	896.000
0109	1 DCOS(Y(2))-O.09DO*(Y(1)**2)+DCOS(Y(2))*MP*(4.0DO*DSIN(Y(2))	897.000
	1 +Y(5)-Y(4))+2.0DO*ROW4*DCOS(Y(2)))	898.000
	1 A(7,4)=0.0DO	899.000
0110	1 A(7,5)=0.0DO	900.000
0111	1 A(7,6)=-4.0DO*MP	901.000
0112	1 A(7,7)=ROW1*(1)+4.0DO*MP	902.000
0113	1 R(1,1)=0.0DO	910.000
0114	1 B(1,2)=0.0DO	911.000
0115	1 B(1,3)=0.0DO	912.000
0116	1 B(1,4)=0.0DO	913.000
0117	1 B(1,5)=0.0DO	914.000
0118	1 B(1,6)=0.0DO	915.000
0119	1 B(1,7)=0.0DO	916.000
0120		

```

0121          R(2.1)=0.000          917.000
0122          R(2.2)=0.000          918.000
0123          R(2.3)=0.000          919.000
0124          R(2.4)=0.000          920.000
0125          R(2.5)=0.000          921.000
0126          R(2.6)=0.000          922.000
0127          R(2.7)=0.000          923.000
0128          PART1=-ROW1*(Y(10)+*(ROW2**2)+((DCOS(Y(2))))**2)
          +ROW1*(ROW3+Y(10)+*ROW2*((DCOS(Y(2))))**2)-((ROW1+
          (ROW3**2))/4.000)*Y(10)+((DCOS(Y(2))))**2)+ROW1*
          (Y(10)+((DCOS(Y(2))))**2)*Y(6)**2
          (Y(7)**2)+*(Y(8)+DCOS(Y(2)))-Y(1)+*Y(9)*DSIN(Y(2)))
          +*O.7800*Y(6)+O.4300*Y(7))+Y(1)+*DCOS(Y(2)))+
          (O.7800*Y(13)+O.4300*Y(14))-Y(9)*DCOS(Y(2)))+(Y(14)+Y(6)+
          Y(5)+Y(7))-DSIN(Y(2))+Y(11)+*(O.5000*(Y(11)+Y(6)+
          Y(4)+Y(13))+O.6500*(Y(11)+Y(7)+Y(4)+Y(14))
          -O.6500*(Y(12)+Y(6)+Y(5)+Y(13))+O.500*(Y(12)+Y(7))+
          Y(5)+Y(14)))
          PART2=ROW1*(-DSIN(Y(2)))+(Y(11)+Y(6)+Y(12)+Y(7))
          -L1*Y(9)+DSIN(Y(2)))+(O.7800*Y(6)+O.4300*Y(7))
          -2.000*Y(1)+Y(9)+*DSIN(Y(2)))+(O.5700*Y(6)+O.0900*Y(7))
          +Y(10)+*(DSIN(Y(2))))**2)+*(Y(6)**2+Y(7)**2)+
          (Y(8)+DSIN(Y(2)))+Y(1)+Y(9)+*DCOS(Y(2)))+
          (1+.300*Y(6)+Y(5)-1.300*Y(7)+Y(4)))
          PART3=ROW1*(DSIN(Y(2)))+Y(11)+*(O.500*(Y(13)+Y(4)+
          Y(6)+Y(11))+O.6500*(Y(13)+Y(5)+Y(6)+Y(12)))-
          O.6500*(Y(14)+Y(4)+Y(7)+Y(11))+O.500*(Y(14)+Y(5)
          +Y(7))+Y(12))+*DSIN(Y(2)))+(Y(13)+Y(4))+
          Y(14)+Y(5))+L1*Y(9)+*DSIN(Y(2)))+(O.7800*Y(6)+
          O.4300*Y(7))-L1*DCOS(Y(2)))+(1.5600*Y(13))+
          (O.8600*Y(14)))
          PART4=ROW1*(-(Y(8)+*DCOS(Y(2)))-Y(11)+Y(9)+*DSIN(Y(2)))+(O.3500*
          Y(6)-O.2500*Y(7))-DCOS(Y(2)))+Y(11)+*(O.3500*
          Y(13)-O.2500*Y(14))-2.000*Y(1)+*DCOS(Y(2)))+
          (O.5700*Y(13)+O.0900*Y(14))+Y(10)+*(DSIN(Y(2))))
          **2)+*(Y(4)**2+Y(5)**2)-2.000*Y(1)+*(O.5700*Y(2))
          +*DCOS(Y(2)))+(O.7800*Y(4)+O.4300*Y(5))-4.000*Y(1)+Y(10)
          +*DSIN(Y(2))+*DCOS(Y(2)))+(O.5700*Y(4)+O.0900*Y(5)))
          PART5=ROW1*(Y(10)+*(DCOS(Y(2))))**2)+((L1**2)+
          2.000*Y(1)+Y(1)+*(Y(1)**2)))+*MP+(-4.000*Y(9)+*DSIN(Y(2)))+
          (Y(6)-Y(7))-4.000*Y(10)+*DCOS(Y(2))+*DSIN(Y(2)))+
          (Y(4)-Y(5))+2.000*Y(10)+*(DCOS(Y(2))))**2))
          B(3.1)=PART1+PART2+PART3+PART4+PART5
          PART6=-O.666700*M1*(L1**2)+Y(10)+*DCOS(Y(2)))+
          DSIN(Y(2))-2.000*ROW1*(ROW3+Y(10))+*(ROW2**2)+
          DSIN(Y(2))+*DCOS(Y(2)))-((ROW1*(ROW3**3)+Y(10)+*DSIN(Y(2))
          +*DCOS(Y(2))))/6.000+ROW1*(-2.000*Y(10)+Y(1)+*DCOS(Y(2)))+
          DSIN(Y(2)))+(Y(6)**2+Y(7)**2)+Y(9)+Y(1)+*DSIN(Y(2)))+
          (Y(4)+Y(6)+Y(5)+Y(7))-Y(1)+*DCOS(Y(2)))+(Y(11)+Y(6)+
          Y(4)+Y(13)+Y(12)+Y(7)+Y(5)+Y(14))-Y(1)+*DCOS(Y(2)))+
          (Y(11)+Y(6)+Y(12)+Y(7)))
          PART7=ROW1*(-L1*Y(1)+Y(9)+*DCOS(Y(2)))+
          (O.7800*Y(6)+O.4300*Y(7))-L1*Y(1)+*DSIN(Y(2)))+
          (O.7800*Y(13)+O.4300*Y(14))-Y(11)+*Y(9)+*DCOS(Y(2)))+
          (O.5700*Y(6)+O.0900*Y(7))-DSIN(Y(2)))+(Y(11)**2)+

```

```

0136      1 (0.57DO*Y(13)+0.09DO*Y(14))+2.0DO*Y(10)*Y(11)+
          1 D SIN(Y(2))+DCOS(Y(2))*Y(6)**2+Y(7)**2
          1 +Y(1)*DCOS(Y(2))*Y(13)+Y(4)+Y(14)+Y(5)))
          1 PART8=ROW1*(L1+D SIN(Y(2)))+(0.78DO*Y(1)+Y(13)+
          1 0.43DO*Y(1)+Y(14))+Y(11)**2)*D SIN(Y(2))+(0.57DO*Y(13)+
          1 0.09DO*Y(14))+2.0DO*Y(2))*DCOS(Y(2))*Y(10)*
          1 Y(1)+Y(4)**2+Y(5)**2)
          1 -2.0DO*Y(1)*Y(10)*((DCOS(Y(2))**2)*Y(11)
          1 -Y(10)+D SIN(Y(2))**2)*Y(11)+(0.78DO*
          1 Y(4)+0.43DO*Y(5))-2.0DO*Y(10)*Y(1)**2)*
          1 ((DCOS(Y(2))**2)-(D SIN(Y(2))**2))+(0.57DO*Y(4)
          1 +0.09DO*Y(5)))
          1 PART9=ROW1*(-2.0DO*Y(10)*D SIN(Y(2))+DCOS(Y(2))
          1 +ROW5)+MP*(Y(10)*DCOS(Y(2))+D SIN(Y(2)))+(8.0DO*
          1 (Y(4))+2*Y(5))+2-2.0DO*Y(4)+Y(5))-2.0DO*(ROW4**2))
          1 +4.0DO*Y(9)+D SIN(Y(2))*Y(4)+Y(6)-Y(4)+Y(7)-
          1 Y(5)+Y(6)+Y(5)+Y(7))-4.0DO*DCOS(Y(2))+(2.0DO*Y(11)+
          1 Y(6)+Y(4)+Y(13)-2.0DO*Y(11)+Y(7)-Y(4)*Y(14)
          1 -2.0DO*Y(12)+Y(6)-Y(5)+Y(13)+2.0DO*Y(12)+Y(7))+
          1 Y(5)+Y(14))-2.0DO*Y(9)+ROW4+DCOS(Y(2))*Y(6)-Y(7))+
          1 4.0DO+DCOS(Y(2))*Y(13)+Y(4)-Y(13)+Y(5)-Y(14)+Y(4)+
          1 Y(14)+Y(5))-(Y(10)*((DCOS(Y(2))**2)+ROW4-Y(10)*
          1 (D SIN(Y(2))**2)+ROW4)*Y(4)-Y(5))+4.0DO)
          1 B(3.2)=PART6+PART7+PART8+PART9
          1 B(3.3)=ROW1*(Y(1)+2.0DO*Y(6)+Y(13)+Y(7)+Y(14))+
          1 Y(1)+((D SIN(Y(2))**2)+2.0DO*Y(4)+Y(11)+Y(5))+
          1 Y(12))-2.0DO*Y(1)*D SIN(Y(2))+DCOS(Y(2))+(0.78DO*
          1 L1+Y(11)+0.43DO*Y(1)+Y(12))+0.57DO*Y(1)+Y(11)+0.09DO*
          1 Y(1)+Y(12))+MP*(8.0DO*Y(6)+Y(13)+Y(7)+Y(14)-Y(13)
          1 +Y(7)-Y(6)+Y(14))+8.0DO*(D SIN(Y(2))**2)+Y(4)*Y(11)+
          1 Y(5)+Y(12)-Y(11)*Y(5)-Y(4)+Y(12))-4.0DO*D SIN(Y(2))+
          1 DCOS(Y(2))+ROW4*(Y(11)-Y(12)))
          1 B(3.4)=0.0DO
          1 B(3.5)=0.0DO
          1 B(3.6)=0.0DO
          1 B(3.7)=0.0DO
          1 B(4.1)=ROW6*(Y(8)+Y(4)-1.3DO*Y(5))+Y(9)*Y(1)+
          1 3.14DO-2.0DO*Y(10)+D SIN(Y(2))*Y(6)-2.0DO*Y(8)*
          1 (A13+Y(4)+A14*Y(5))+2.6DO*Y(10)*D SIN(Y(2))+
          1 Y(1)+Y(7))+MP*4.0DO*Y(9)
          1 B(4.2)=-ROW1*Y(9)+Y(1)+Y(4)-4.0DO*MP*Y(9)*Y(4)
          1 -Y(5))
          1 B(4.3)=ROW6*(-2.0DO*Y(10)*((D SIN(Y(2))**2)*Y(11)
          1 +Y(4)+Y(10)+D SIN(Y(2)))+DCOS(Y(2))*Y(1)+4.56DO*
          1 L1+1.14DO*Y(1))+MP*(-4.0DO*Y(10)*((D SIN(Y(2))**2)
          1 +Y(4)-Y(5))+2.0DO*Y(10)*D SIN(Y(2))+DCOS(Y(2))
          1 +ROW4)
          1 B(4.4)=ROW6+2.0DO*Y(8)
          1 B(4.5)=-ROW6+2.6DO*Y(1)+Y(8)
          1 B(4.6)=-ROW6+Y(10)+4.0DO*D SIN(Y(2))+Y(1)-8.0DO
          1 +MP*Y(10)*D SIN(Y(2))
          1 B(4.7)=8.0DO*MP*Y(10)*D SIN(Y(2))
          1 B(5.1)=ROW1*(Y(8)+(0.65DO*Y(4)+0.5DO*Y(5))
          1 +0.86DO*Y(9)+Y(1)+Y(10)+D SIN(Y(2))*Y(7)-
          1 Y(8)+(A14+Y(4)+A15+Y(5))-1.30DO*Y(10)+

```

```

972.000
973.000
974.000
975.000
976.000
977.000
978.000
979.000
980.000
981.000
982.000
983.000
984.000
985.000
986.000
987.000
988.000
989.000
990.000
991.000
992.000
993.000
994.000
995.000
996.000
997.000
998.000
999.000
1000.000
1001.000
1002.000
1003.000
1004.000
1005.000
1006.000
1007.000
1008.000
1009.000
1010.000
1011.000
1012.000
1013.000
1014.000
1015.000
1016.000
1017.000
1018.000
1019.000
1020.000
1021.000
1022.000
1023.000
1024.000
1025.000
1026.000

```

```

0152      1 DSIN(Y(2))+Y(1)+Y(6))-MP+4.ODO*Y(9)
          B(5.2)=ROW1+(-Y(9)+Y(1)+Y(5))-4.ODO*MP
          +Y(9)+Y(5)-Y(4))
0153      B(5.3)=ROW1+(-Y(1)+Y(10)+(DSIN(Y(2))))+2)
          +Y(5)+Y(10)*DSIN(Y(2))+DCOS(Y(2))+Y(1)+
          +O.43DO*Y(1)+O.09DO*Y(11))+MP+(-4.ODO*
          +Y(10)+(-DSIN(Y(2))))+2)+Y(5)-Y(4))-2.ODO*
          +Y(10)*DSIN(Y(2))+DCOS(Y(2))+ROW4)
          B(5.4)=ROW1+1.3DO*Y(1)+Y(8)
          B(5.5)=ROW1+Y(8)
          B(5.6)=MP+8.ODO*Y(10)+DSIN(Y(2))
          B(5.7)=-ROW1+2.ODO*Y(10)+DSIN(Y(2))+Y(1)
          -8.ODO*MP+Y(10)+DSIN(Y(2))
          B(6.1)=ROW1+Y(8)+10.5DO*Y(6)-O.55DO*Y(7))
          +Y(10)+DSIN(Y(2))+Y(4)+Y(10)+DCOS(Y(2))
          +(-1.57DO*Y(1))+Y(10)+DSIN(Y(2))+Y(1)+
          +(-1.3DO*Y(5))-Y(8)+(A13+Y(6)+A14+Y(7)))
          +MP+(-4.ODO*Y(10)+DCOS(Y(2)))
          B(6.2)=ROW1+(2.ODO*Y(1)+Y(10)+DCOS(Y(2))+Y(4)+
          +1.56DO*Y(1)+1*DSIN(Y(2))+Y(10)+1.14DO*(Y(1)+2)
          +Y(10)+DSIN(Y(2)))+MP+(8.ODO*Y(10)+DCOS(Y(2))
          +Y(4)-Y(5))+ROW4+4.ODO*Y(10)+DSIN(Y(2)))
          B(6.3)=-ROW1+Y(1)+Y(10)+Y(6)-4.ODO*MP+Y(10)
          +Y(6)-Y(7))
          B(6.4)=2.ODO*ROW1+Y(10)+DSIN(Y(2))+Y(1)+8.ODO
          +MP+Y(10)+DSIN(Y(2))
          B(6.5)=-8.ODO*MP+Y(10)+DSIN(Y(2))
          B(6.6)=ROW1+Y(8)
          B(6.7)=-ROW1+1.3DO*Y(1)+Y(8)
          R(7.1)=ROW1+Y(8)+10.65DO*Y(6)+O.5DO*Y(7))+Y(10)
          +DSIN(Y(2))+Y(5)-O.86DO*Y(1)+*Y(10)+DCOS(Y(2))
          -Y(8)+(A14+Y(6)+A15+Y(7))+1.3DO*Y(10)+DSIN(Y(2))
          +Y(1)+Y(4))
          +MP+4.ODO*Y(10)+DCOS(Y(2))
          B(7.2)=ROW1+(2.ODO*Y(1)+Y(10)+DCOS(Y(2))+Y(5)+
          +O.18DO*(Y(1)+2)+Y(10)+DSIN(Y(2))+O.86DO*Y(1)+Y(1)
          +Y(10)+DSIN(Y(2)))+MP+(8.ODO*Y(10)+DCOS(Y(2)))+
          +Y(5)-Y(4))-4.ODO*ROW4+Y(10)+DSIN(Y(2))
          R(7.3)=-ROW1+Y(1)+Y(10)+Y(7)-4.ODO*MP+Y(10)+
          +Y(7)-Y(6))
          B(7.4)=-MP+8.ODO*Y(10)+DSIN(Y(2))
          R(7.5)=ROW1+2.ODO*Y(10)+DSIN(Y(2))+Y(1)+8.ODO
          +MP+Y(10)+DSIN(Y(2))
          B(7.6)=ROW1+1.3DO*Y(1)+Y(8)
          B(7.7)=-ROW1+Y(8)
          C1=-((M2+MP)*WNR+2*(Y(1)-R1)+2.ODO*ZETA1+WNR
          +(M2+MP)+Y(8))+IK11+Y(15)
          C2=-((WNETETA+2)*ALPHA+Y(2)
          +2.ODO*ZETA2+WNETETA*ALPHA+Y(9))+IK22+Y(16)
          C3=-((WNFETA+2)*ALPHA+Y(3)+
          +2.ODO*ZETA3+WNFETA*ALPHA+Y(10))+IK33+Y(17)
          F(1)=C1
          F(2)=C2
          F(3)=C3
          F(4)=O.ODO
    
```

```

0179 F(5)=-O.ODO 1080.000
0180 F(6)=-O.OPN 1081.000
0181 F(7)=-O.ODO 1082.000
0182 D(1)=-O.ODO 1083.000
0183 D(2)=-O.ODO 1084.000
0184 D(3)=-O.ODO 1085.000
0185 D(4)=-R0W1+Y(1)+G*DC05(Y(2))*AL1-2.0DO*MP+G 1086.000
+DC05(Y(2))-(E1+Y(4)*AL10)/(Y(1)**3) 1087.000
+((R0W1+CEN1AC+DIST*(4.65DO*Y(4))-7.38DO*Y(5)))/Y(1)+ 1087.200
R0W1+CEN1AC*(3.08DO*L1+1.13DO*Y(1))*Y(4)-(6.96DO*L1 1087.300
+3.0DO*Y(1))*Y(5)-((R0W7+CEN1AC+R0W8)*(4.65DO*Y(4))- 1087.400
7.38DO*Y(5)))/Y(1)+R0W9*(3.08DO*Y(4))-6.96DO*Y(5) 1087.500
+1.14DO*(Y(1)**2)+R0W1*Y(8)*Y(9)+R0W10*(O.57DO* 1087.600
(Y(1)**2)+L1+O.225DO*(Y(1)**3)) 1087.600
D(5)=-R0W1+Y(1)+G*DC05(Y(2))*AL2+2.0DO*MP 1088.000
+G*DC05(Y(2))-(E1+Y(5)*AL11)/(Y(1)**3) 1089.000
+((R0W1+CEN1AC+DIST*(4.65DO*Y(4))+3.2.42DO*Y(5)))/Y(1)+ 1089.100
R0W1+CEN1AC*(4.65DO*L1+3.0DO*Y(1))*Y(4)+(23.77DO*L1 1089.200
+9.73DO*Y(1))*Y(5)-((R0W7+CEN1AC+R0W8)*(-7.38DO*Y(4)+ 1089.300
32.42DO*Y(5)))/Y(1)+R0W9*(-6.96DO*Y(4))+23.77DO*Y(5))+ 1089.400
+O.182DO*(Y(1)**2)+R0W1*Y(8)*Y(9)+R0W10*(O.091DO*L1+ 1089.500
(Y(1)**2)-O.02DO*(Y(1)**3)) 1089.600
D(6)=-((AL10*E1+Y(6)))/(Y(1)**3)-((R0W1+CEN1AC+DIST*(4.65DO*Y(6) 1090.000
-7.38DO*Y(7)))/Y(1)+R0W1+CEN1AC*(3.08DO*L1+1.13DO*Y(1)) 1090.100
+Y(6))-6.96DO*L1+3.0DO*Y(1))*Y(7)-((R0W7+CEN1AC 1090.200
+R0W8)*(4.65DO*Y(6))-7.38DO*Y(7)))/Y(1)+R0W9*( 1090.300
3.08DO*Y(6))-6.96DO*Y(7)) 1090.400
D(7)=-((AL11*E1+Y(7)))/(Y(1)**3)-((R0W1+CEN1AC+DIST*(4.65DO*Y(7) 1091.000
+Y(6))+3.2.42DO*Y(7)))/Y(1)+R0W1+CEN1AC*(3.08DO*L1+1.13DO*Y(1)) 1091.100
+3.0DO*Y(1))*Y(6)+(23.77DO*L1+9.73DO*Y(1))*Y(7)) 1091.200
-((R0W7+CEN1AC+R0W8)*(-7.38DO*Y(6))+32.42DO*Y(7))) 1091.300
/Y(1)+R0W9*(-6.96DO*Y(6))+23.77DO*Y(7)) 1091.400
/Y(1)+Y(8) 1092.000
Y(8) 1092.000
Y(9) 1093.000
Y(10) 1094.000
Y(11) 1095.000
Y(12) 1096.000
Y(13) 1097.000
Y(14) 1098.000
DO 60 IN=1.M 1098.050
PBV(IN)=O.ODO 1098.100
DO GO IM=1.M 1098.150
PBV(IN)=PBV(IN)+(-R(IN,IM))*Y(ECT(IM)) 1098.200
CONTINUE 1098.250
DO 61 IV=1.M 1098.300
PALL(IV)=O.ODO 1098.350
PALL(IV)=PBV(IV)+F(IV)+D(IV) 1098.400
CONTINUE 1098.450
CALL DLUD(M,7,A,7,T,IV) 1098.500
IF(IV(M).EQ.O) GO TO 90 1098.550
GO TO 91 1098.600
DO 61 91 1098.600
S=O.ODO 1098.650
GO TO 14 1098.700
S=1.ODO 1098.750
CALL DBS(M,7,T,IV,PALL) 1098.800

```

0212	YDOT(1)=Y(8)+SGN(C1)	1143.000
0213	YDOT(2)=Y(9)+SGN(C2)	1144.000
0214	YDOT(3)=Y(10)	1145.000
0215	YDOT(4)=Y(11)	1146.000
0216	YDOT(5)=Y(12)	1147.000
0217	YDOT(6)=Y(13)	1148.000
0218	YDOT(7)=Y(14)	1149.000
0219	YDOT(8)=(PALL(1))*SGN(C1)	1149.800
0220	YDOT(9)=(PALL(2))*SGN(C2)	1150.600
0221	YDOT(10)=PALL(3)	1151.400
0222	YDOT(11)=PALL(4)	1152.200
0223	YDOT(12)=PALL(5)	1153.000
0224	YDOT(13)=PALL(6)	1153.800
0225	YDOT(14)=PALL(7)	1154.600
0226	YDOT(15)=R1-Y(1)	1155.400
0227	YDOT(16)=R2-Y(2)	1156.200
0228	YDOT(17)=R3-Y(3)	1157.000
0229	14 RETURN	1159.000
0230	END	1160.000

*OPTIONS IN EFFECT+ ID,EBDCIC,SOURCE,NOLLST,NODECK,LOAD,NOMAP
 *OPTIONS IN EFFECT+ NAME = DIFFUN . LINECNT = 57
 *STATISTICS+ SOURCE STATEMENTS = 230,PROGRAM SIZE = 27560
 *STATISTICS+ NO DIAGNOSTICS GENERATED

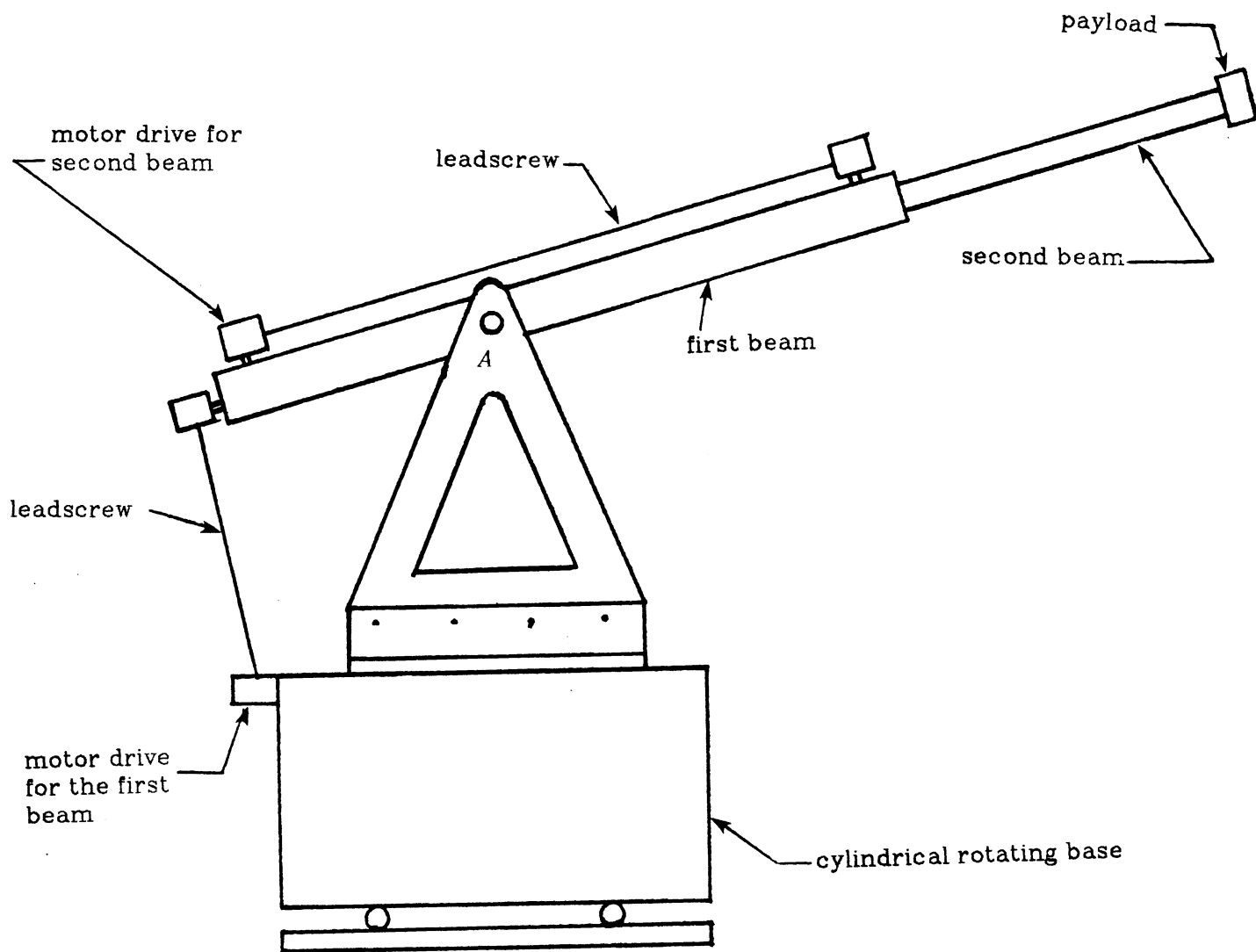
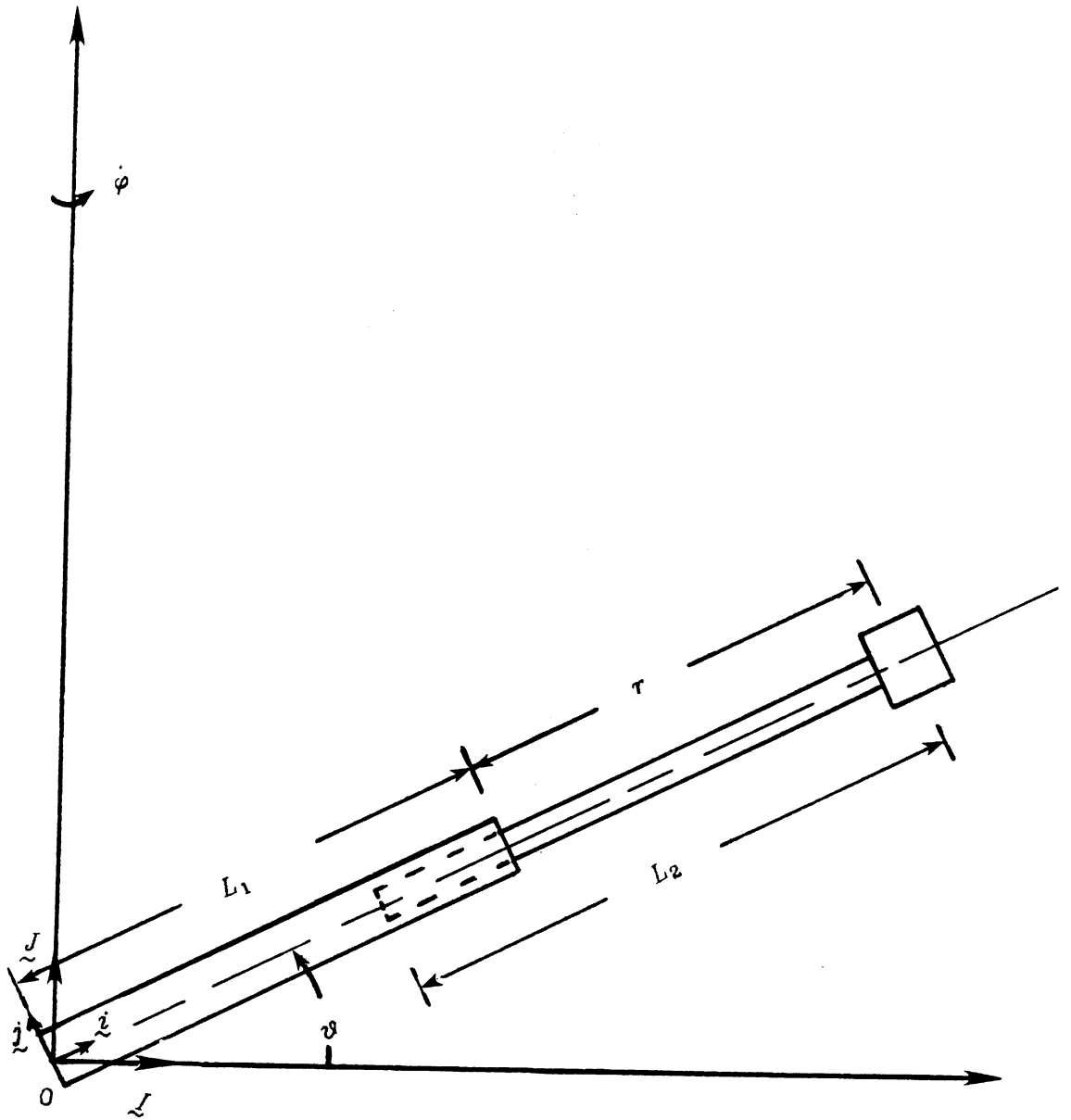


Figure 1. A schematic of the physical system



$\odot \vec{k}$

Figure 2. Illustration of the model

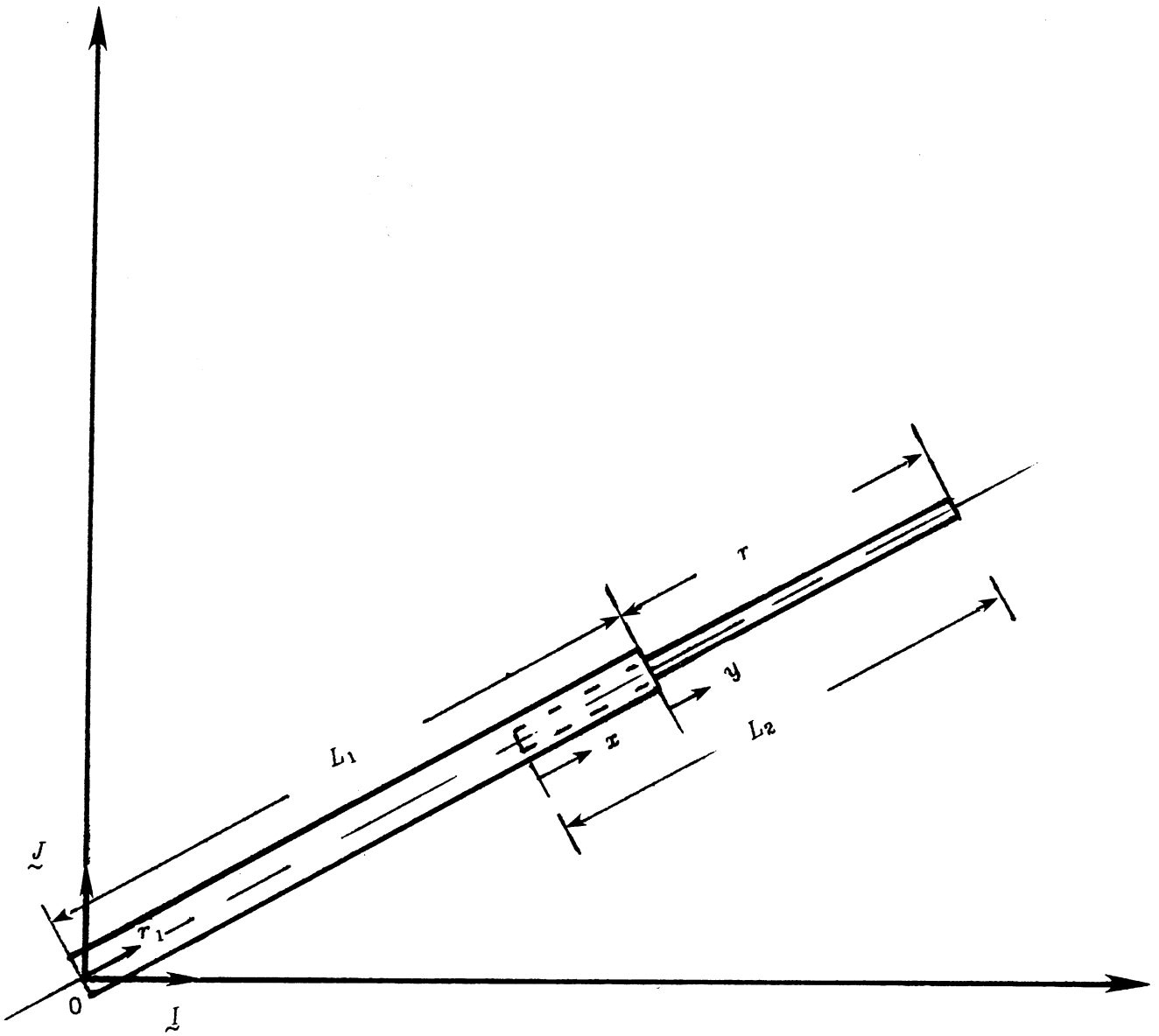


Figure 3. Illustration of the parameter used in the dynamic model

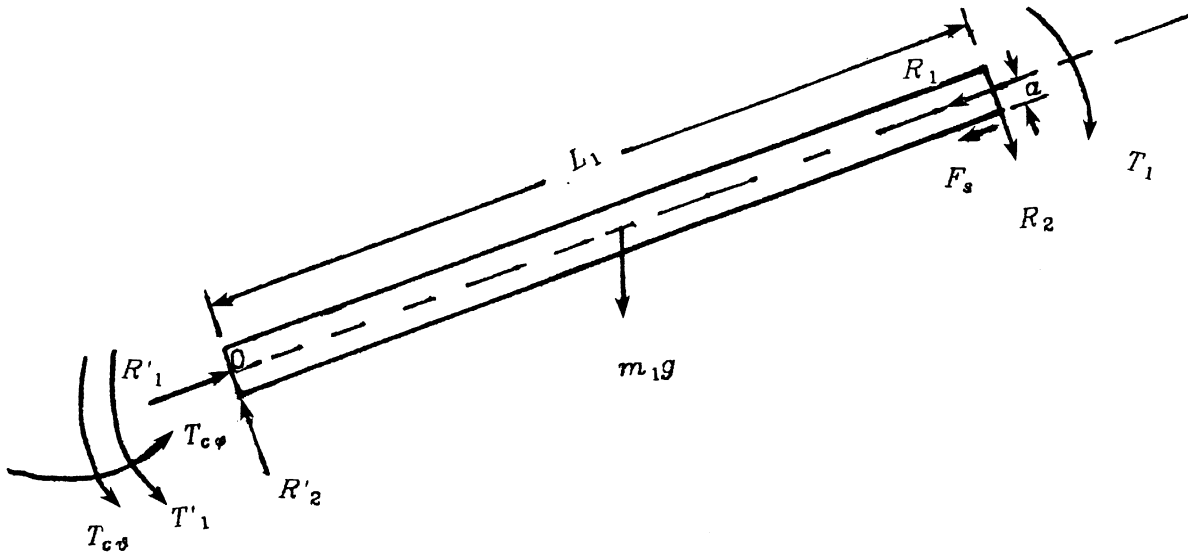


Figure 4. Free body diagram of the first beam

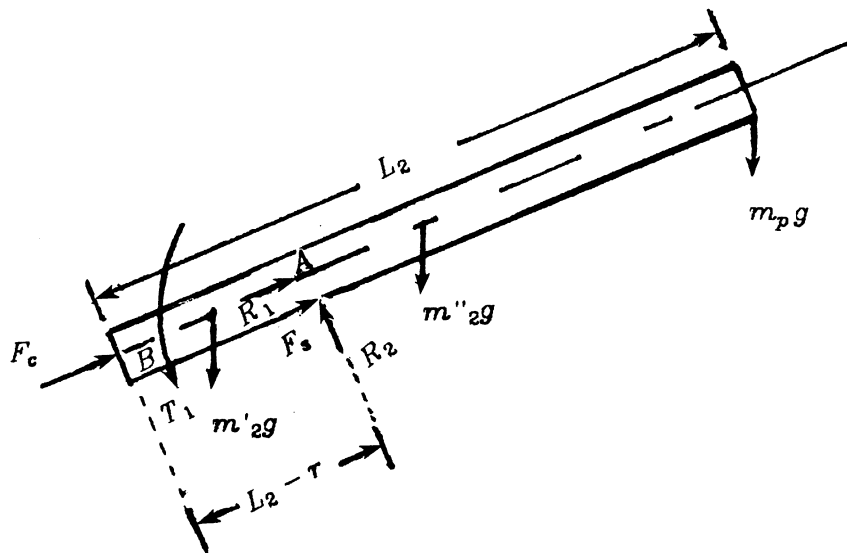


Figure 5. Free body diagram of the second beam

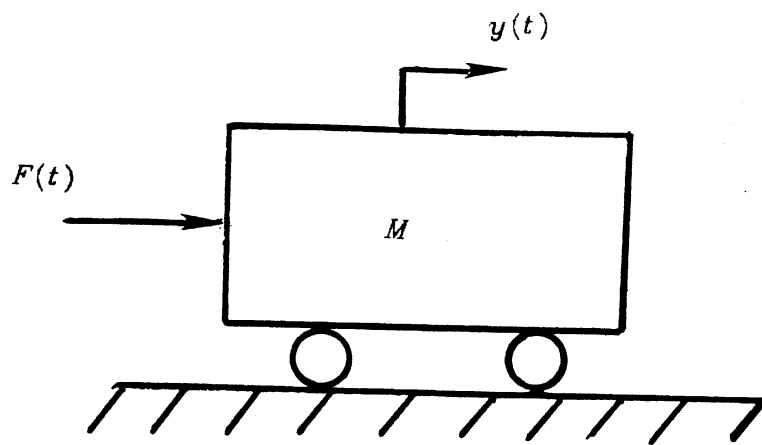


Figure 6 Simple rigid body translational degree of freedom model

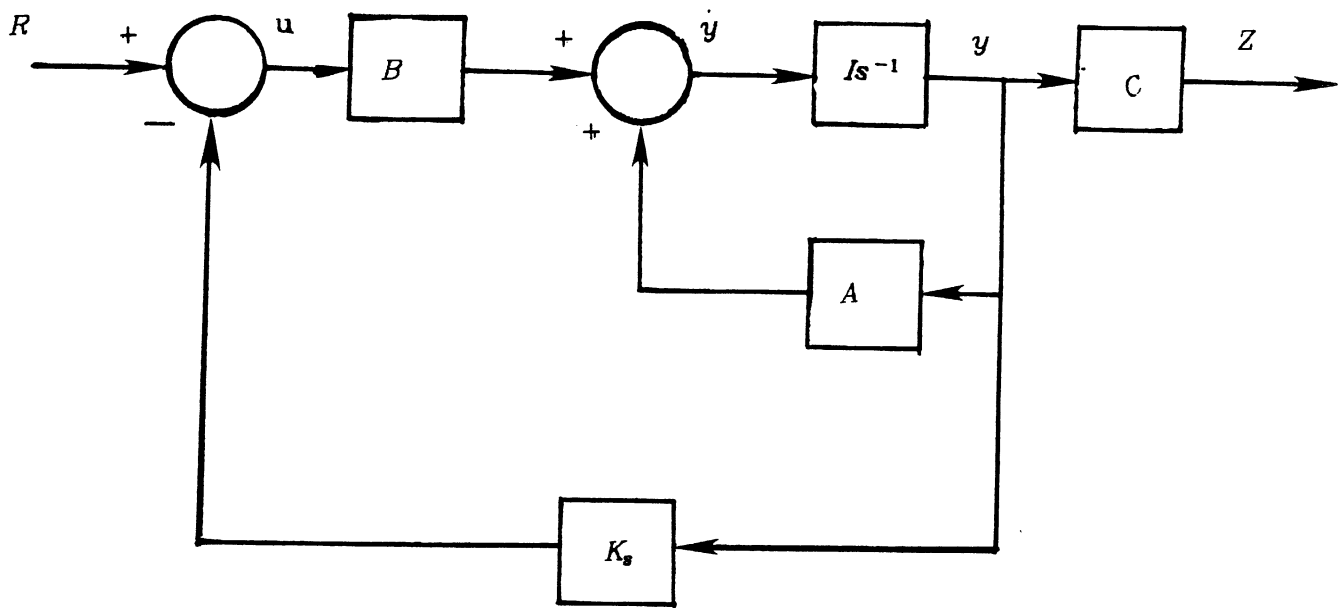


Figure 7. Block diagram of the state feedback controller applied to the linear system

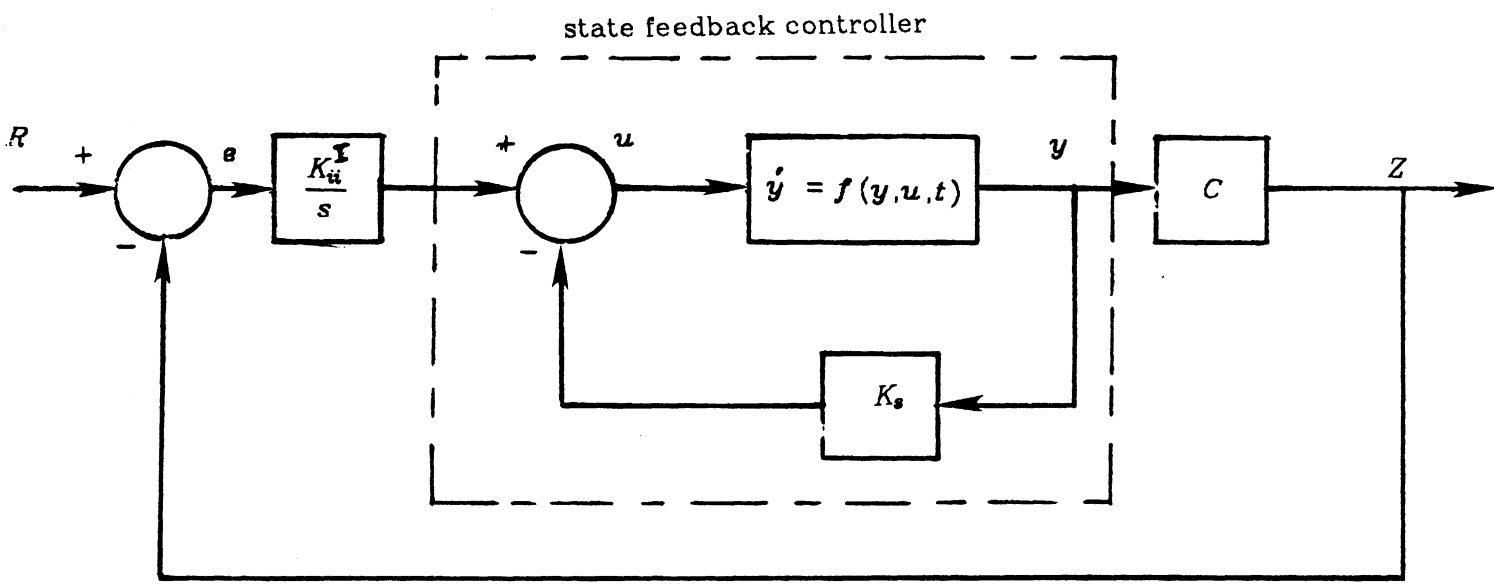


Figure 8. Block Diagram of the integral plus state feedback controller applied to the nonlinear system

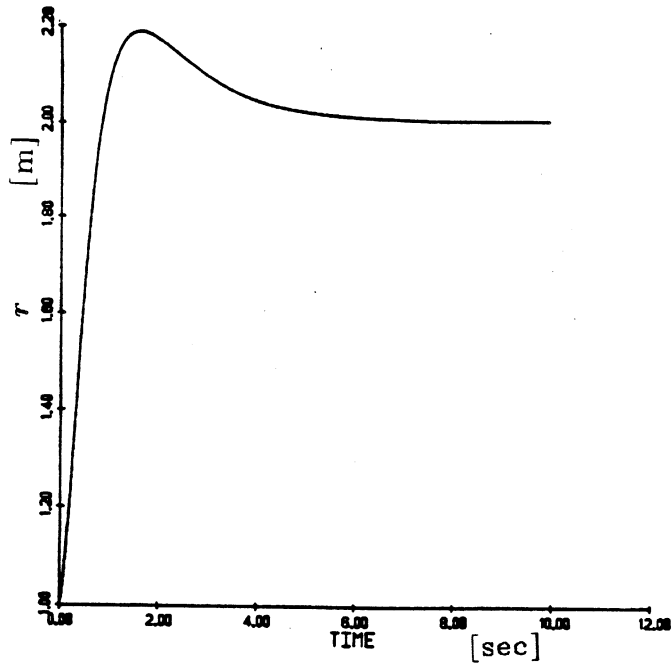


Figure 9. r displacement, obtained from the equations representing the rigid body motion only

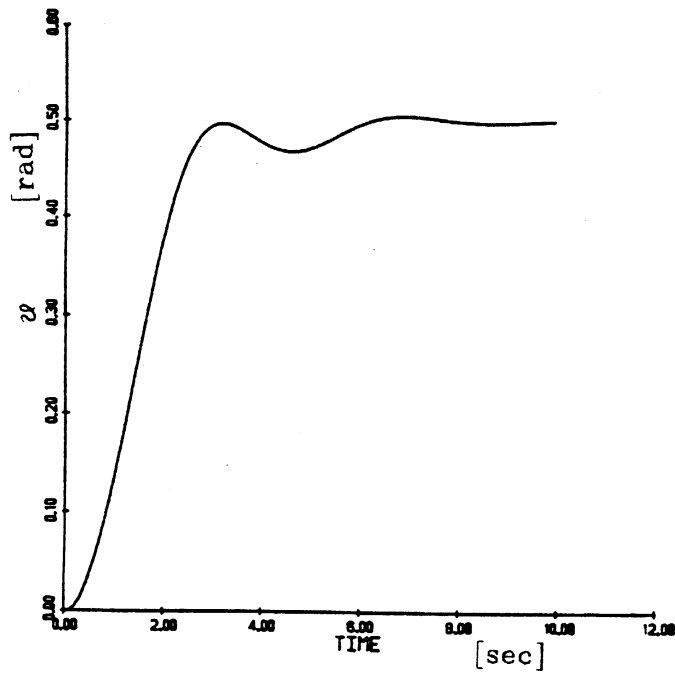


Figure 10. φ displacement, obtained from the equations representing the rigid body of motion only

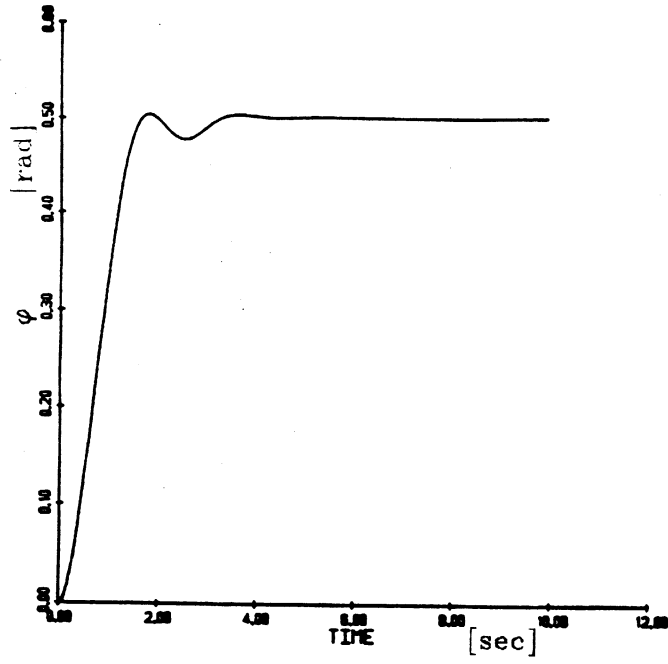


Figure 11. ϕ displacement, obtained from the equation describing rigid body motion only

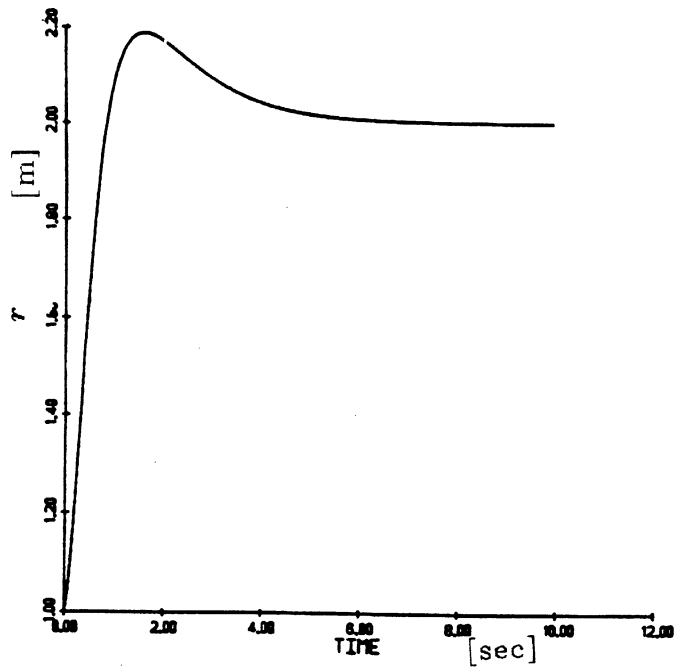


Figure 12. r displacement, obtained from the base run

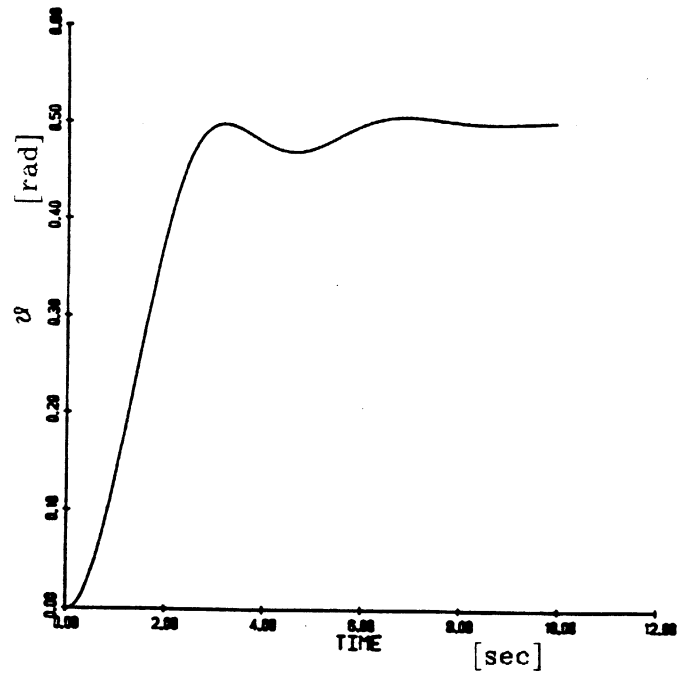


Figure 13. ϑ displacement, obtained from the base run

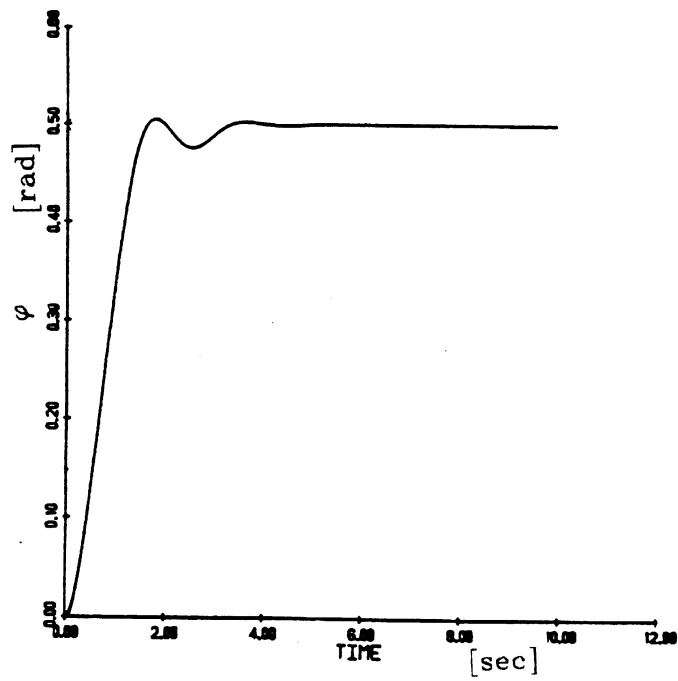


Figure 14. φ displacement, obtained from the base run

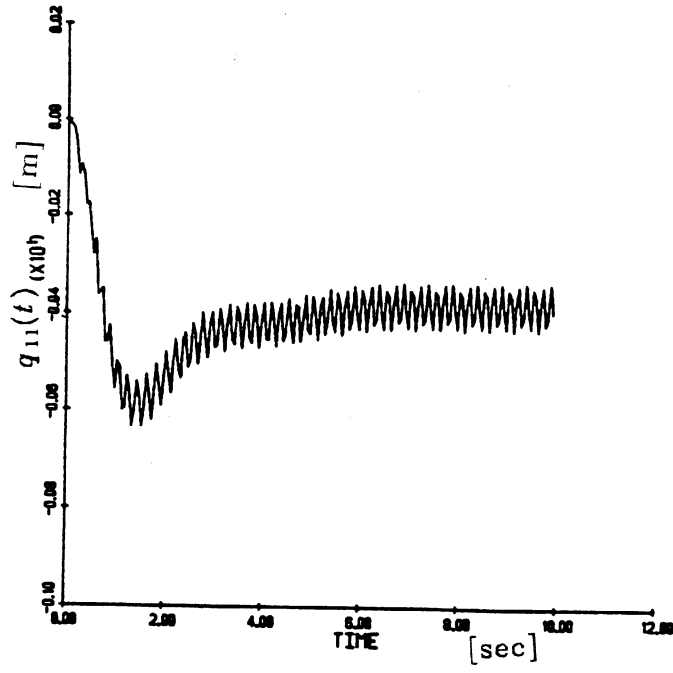


Figure 15. $q_{11}(t)$ displacement, obtained from the base run

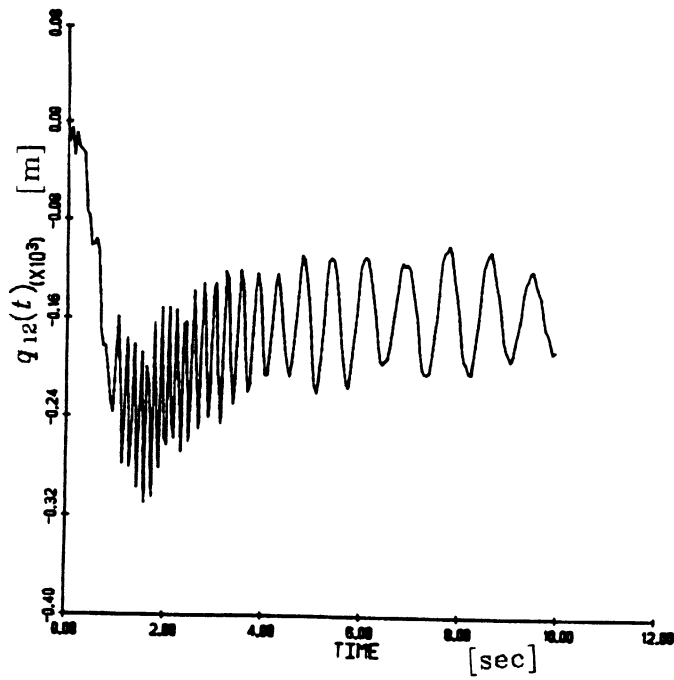


Figure 16. $q_{12}(t)$ displacement, obtained from the base run

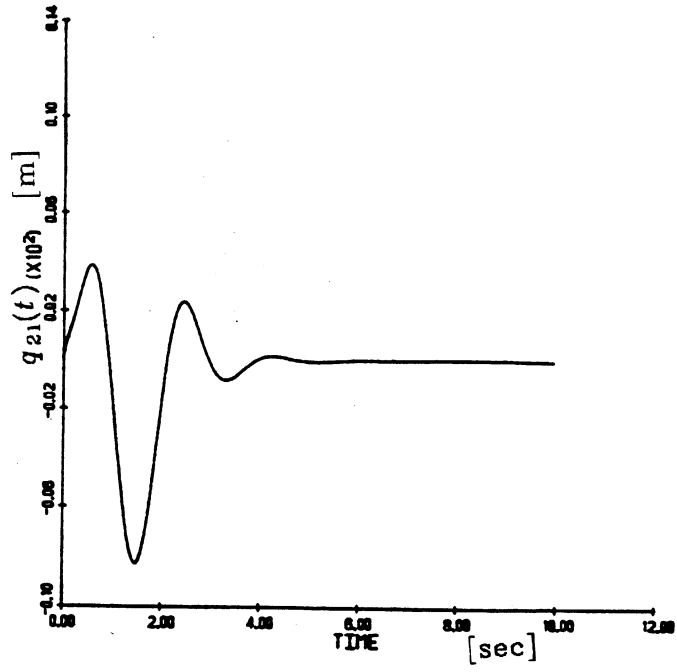


Figure 17. $q_{21}(t)$ displacement, obtained from the base run

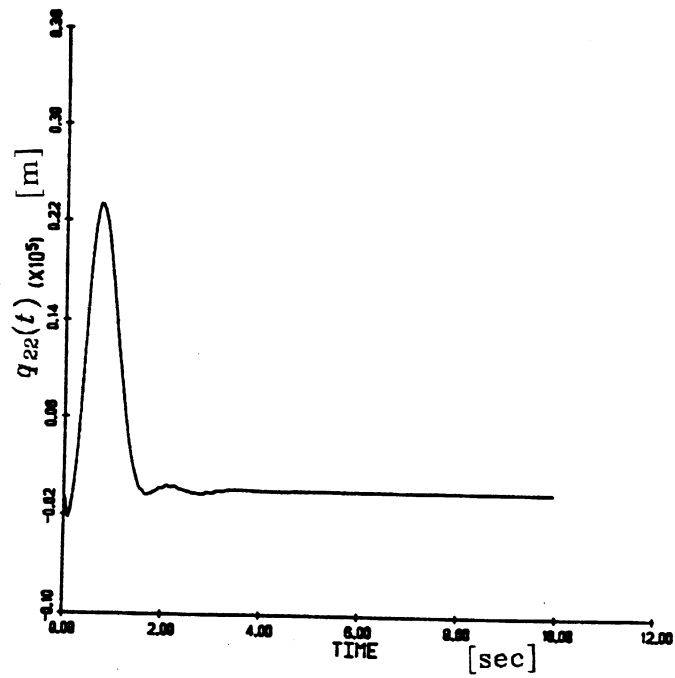


Figure 18. $q_{22}(t)$ displacement, obtained from the base run

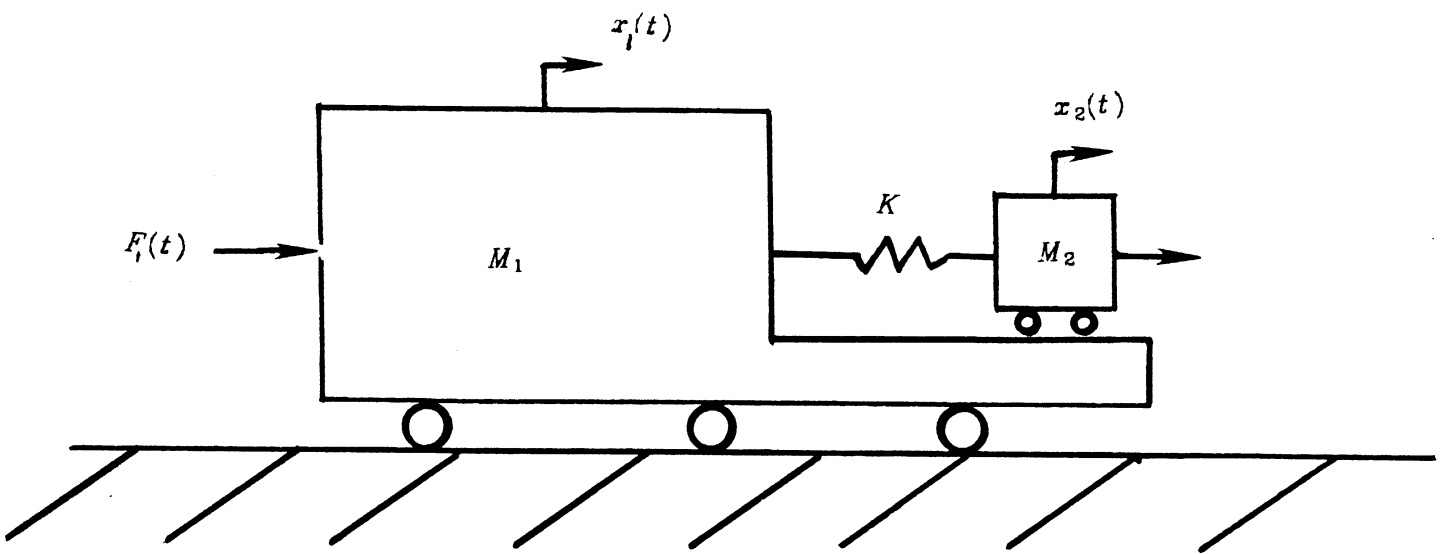


Figure 19. Model of the rigid body motion with one flexible mode.

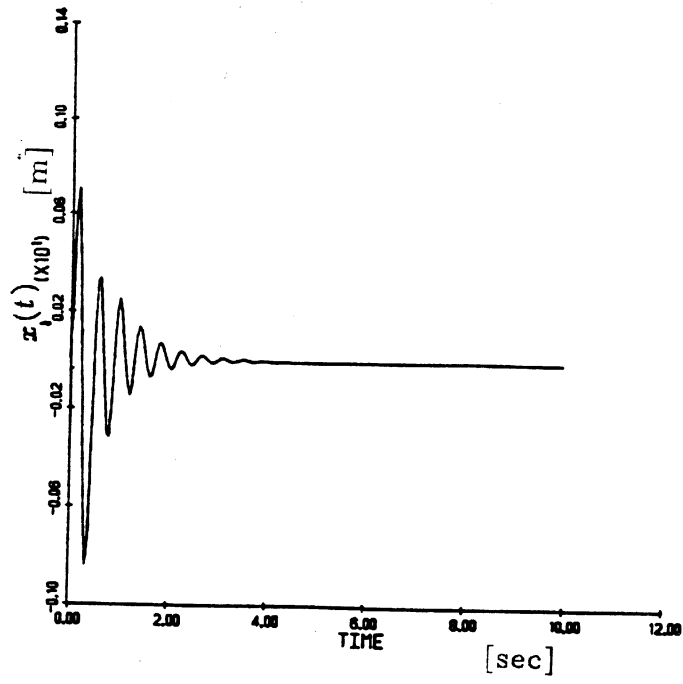


Figure 20. Rigid body displacement, $x_1(t)$

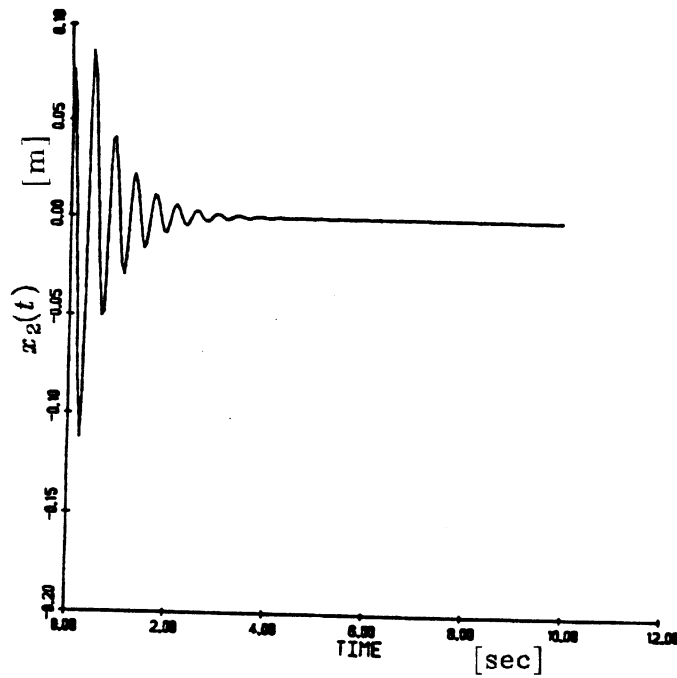


Figure 21. Flexible motion, $x_2(t)$

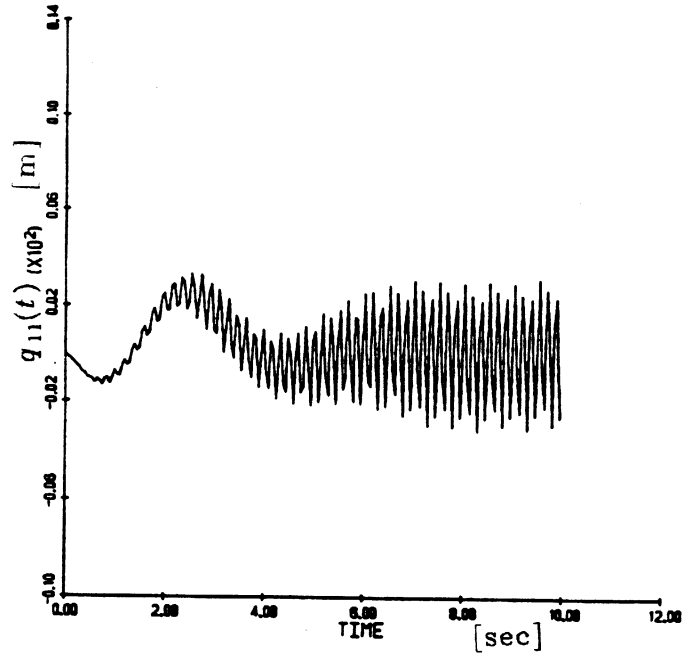


Figure 22. $q_{11}(t)$ displacement, obtained from the base run with $g=0$

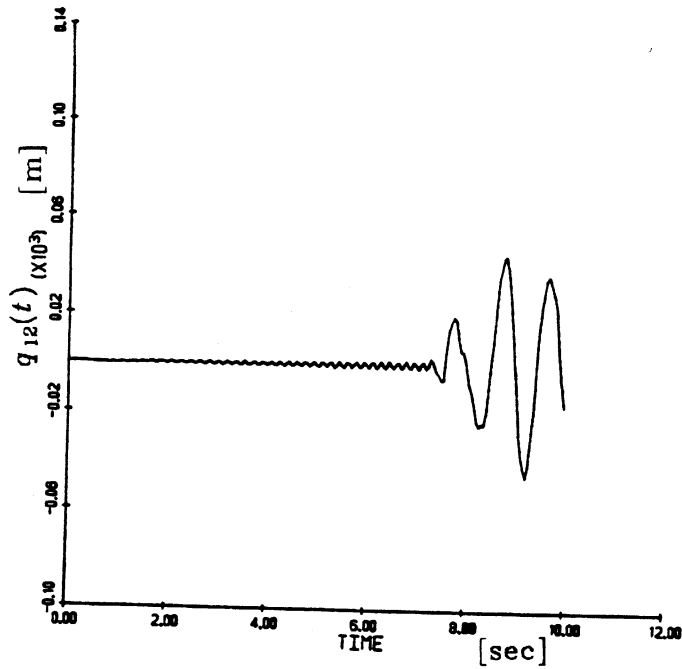


Figure 23. $q_{12}(t)$ displacement, obtained from the base run with $g=0$

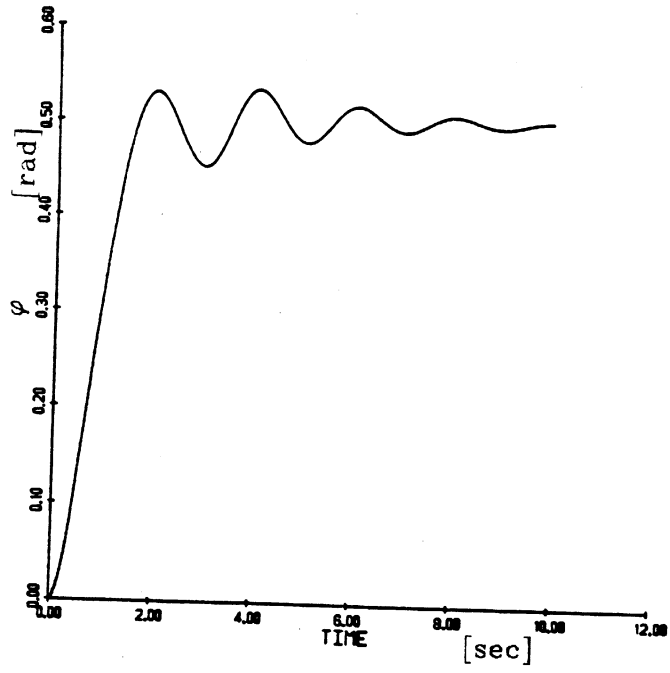


Figure 24. φ displacement, obtained from base run with $g=0$ and $EI = 17.04P_a$

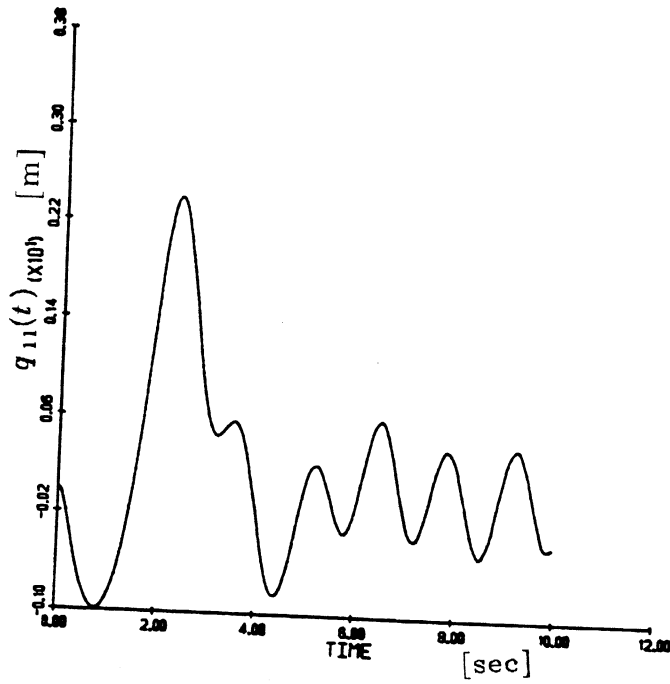


Figure 25. $q_{11}(t)$ displacement, obtained from the base run with $g=0$ and $EI = 17.04P_a$

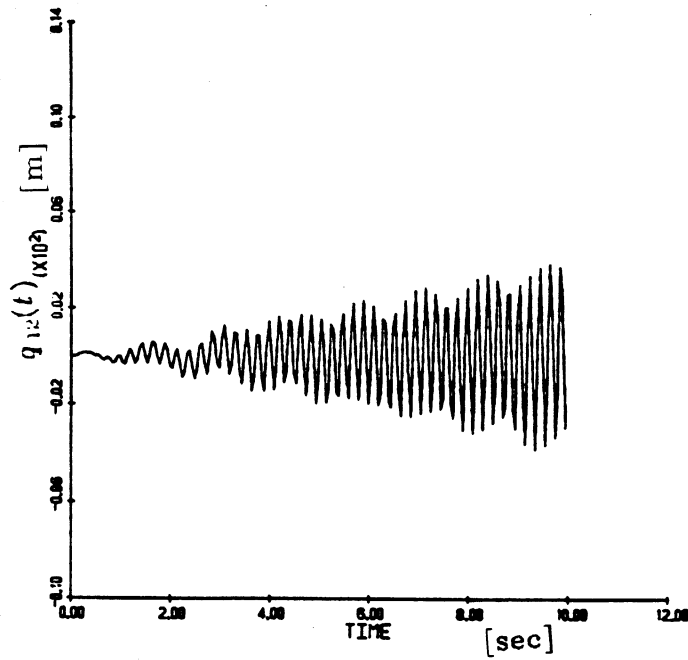


Figure 26. $q_{12}(t)$ displacement, obtained from the base run with $g = 0$ and $EI = 17.04P_a$

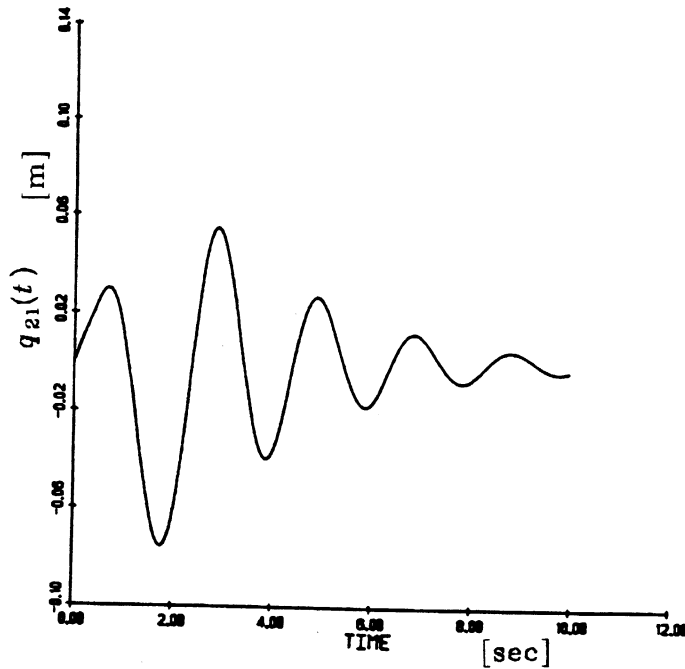


Figure 27. $q_{21}(t)$ displacement, obtained from the base run with $g = 0$ and $EI = 17.04P_a$

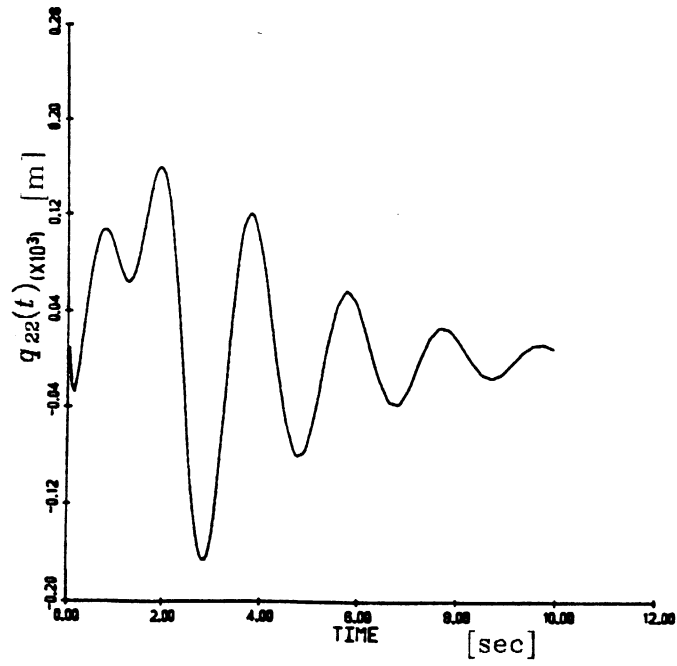


Figure 28. $q_{22}(t)$ displacement, obtained from the base run with $g = 0$

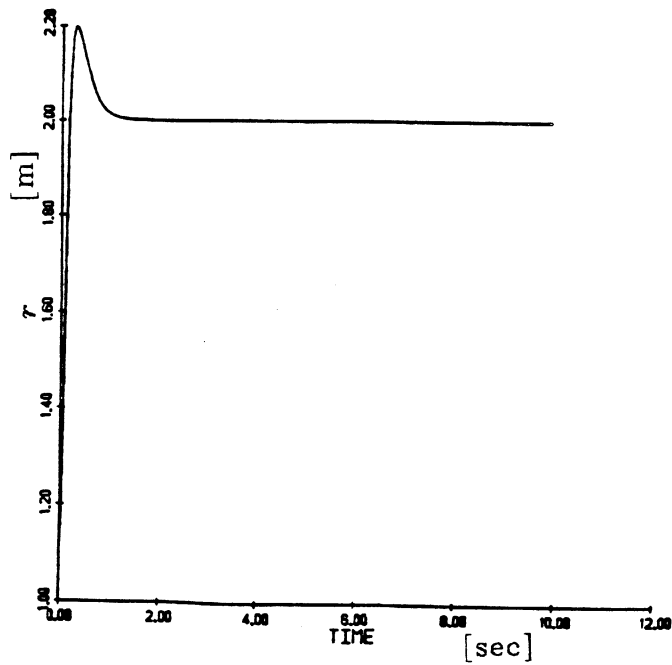


Figure 29. r displacement, obtained from the base run with $g = 0$ and high servo loop frequencies

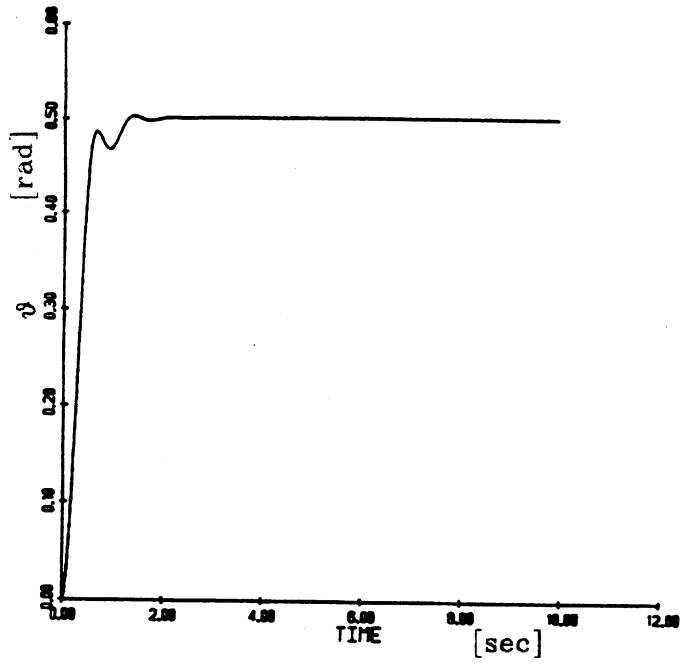


Figure 30. ϕ displacement, obtained from the base run with $g=0$ and high servo loop frequencies

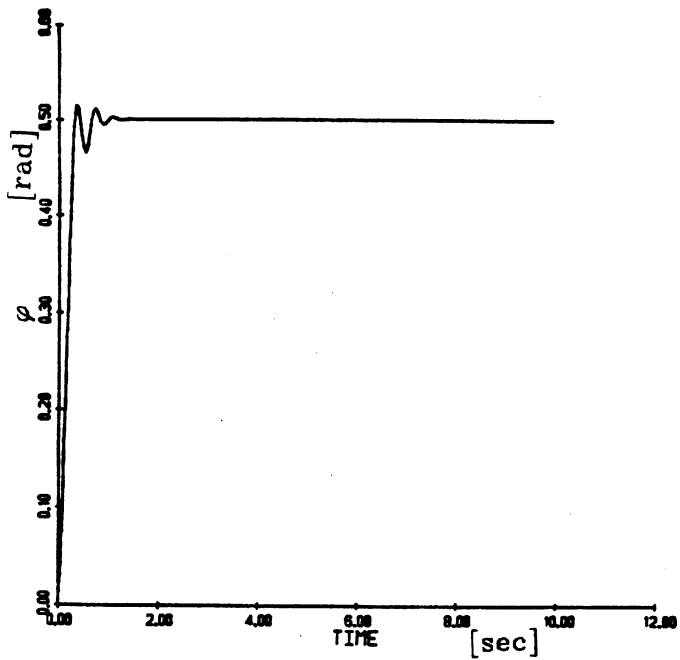


Figure 31. ϕ displacement, obtained from the base run with $g=0$ and high servo loop frequencies

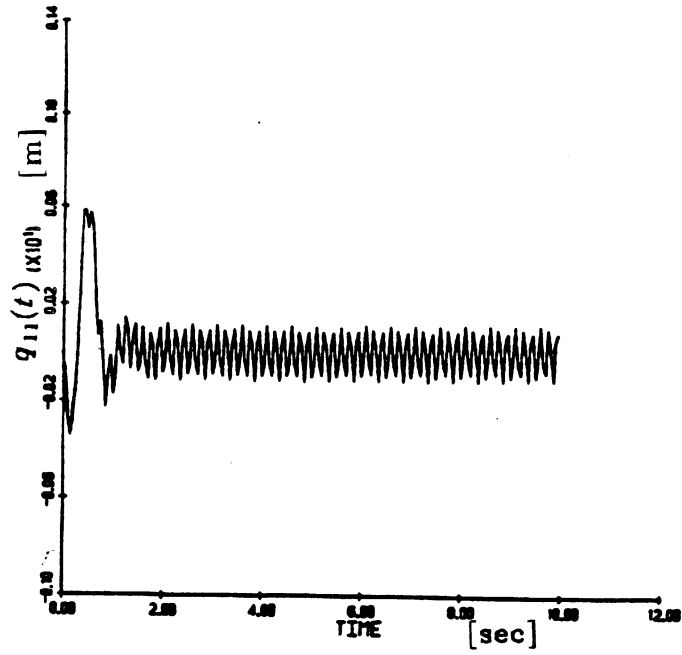


Figure 32. $q_{11}(t)$ displacement, obtained from the base run with $g=0$ and high servo loop frequencies

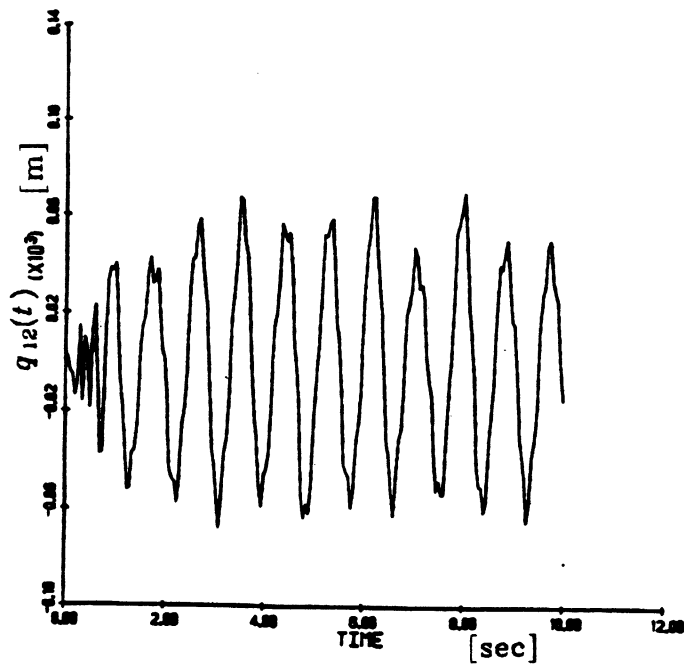


Figure 33. $q_{12}(t)$ displacement, obtained from the base run with $g=0$ and high servo loop frequencies

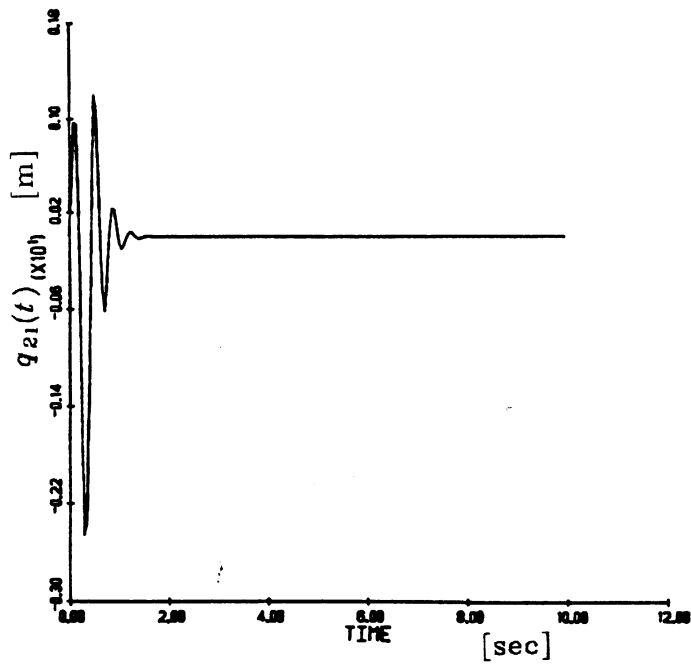


Figure 34. $q_{21}(t)$ displacement, obtained from the base run with $g = 0$ and high servo loop frequencies.

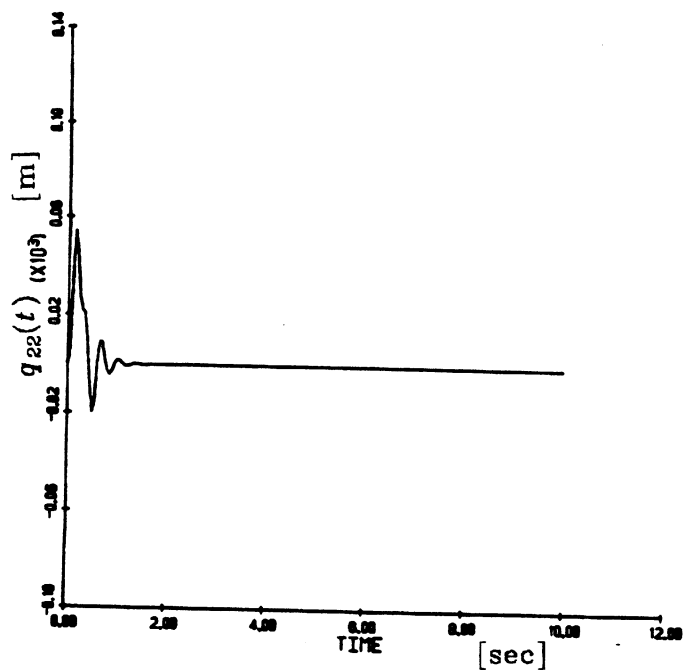


Figure 35. $q_{22}(t)$ displacement, obtained from the base run with $g = 0$ and high servo loop frequencies.

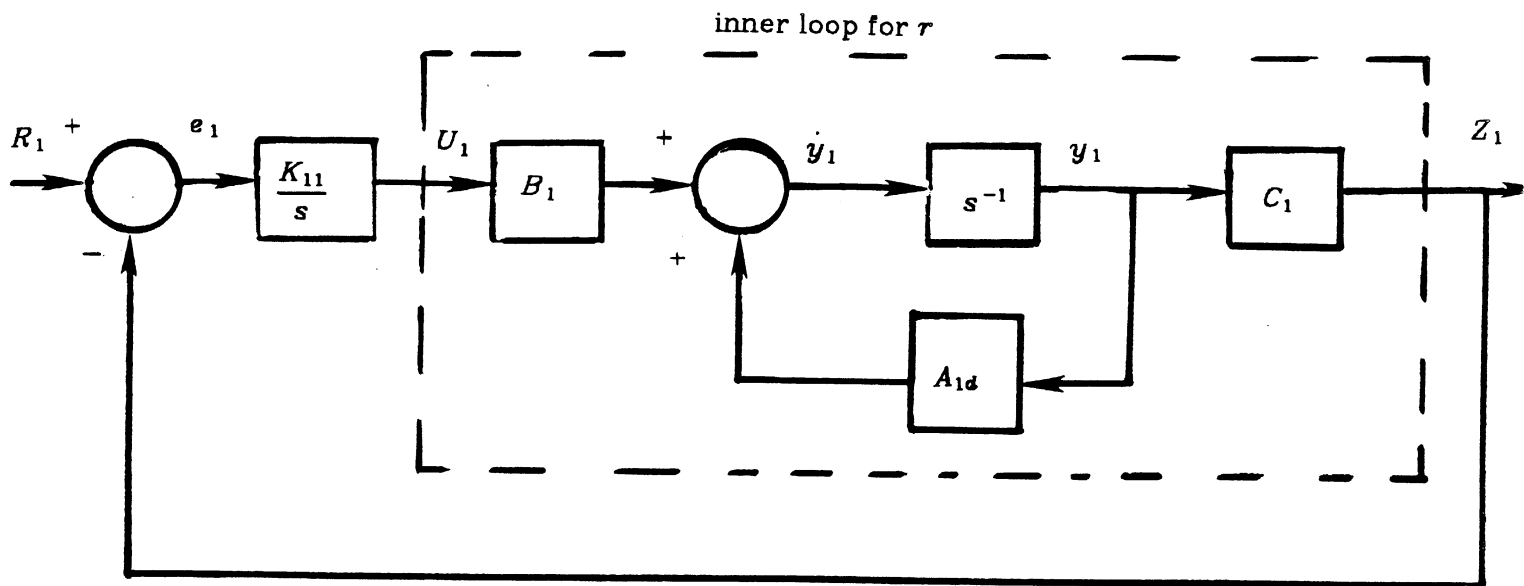


Figure 36(a). BLOCK DIAGRAM for τ only

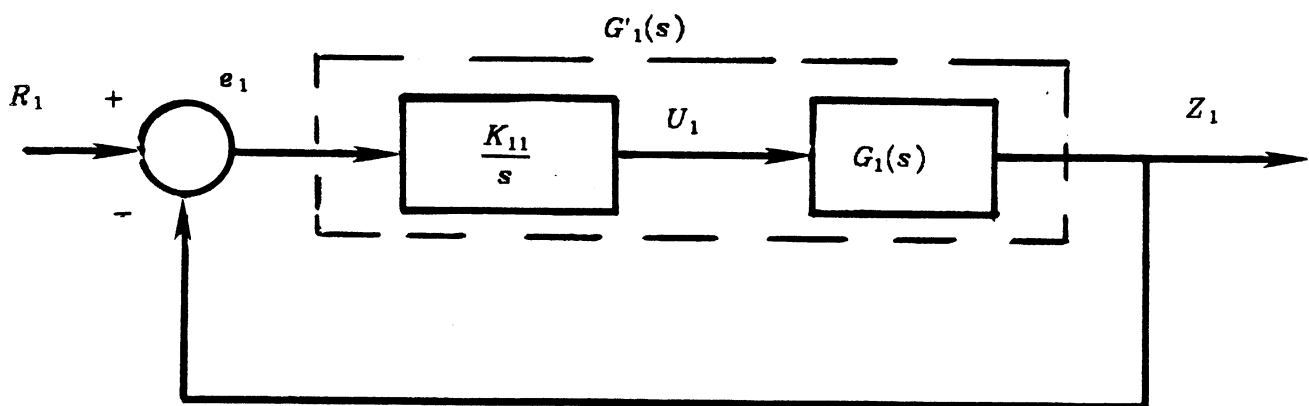


Figure 36(b). Simplified form of the block diagram for τ

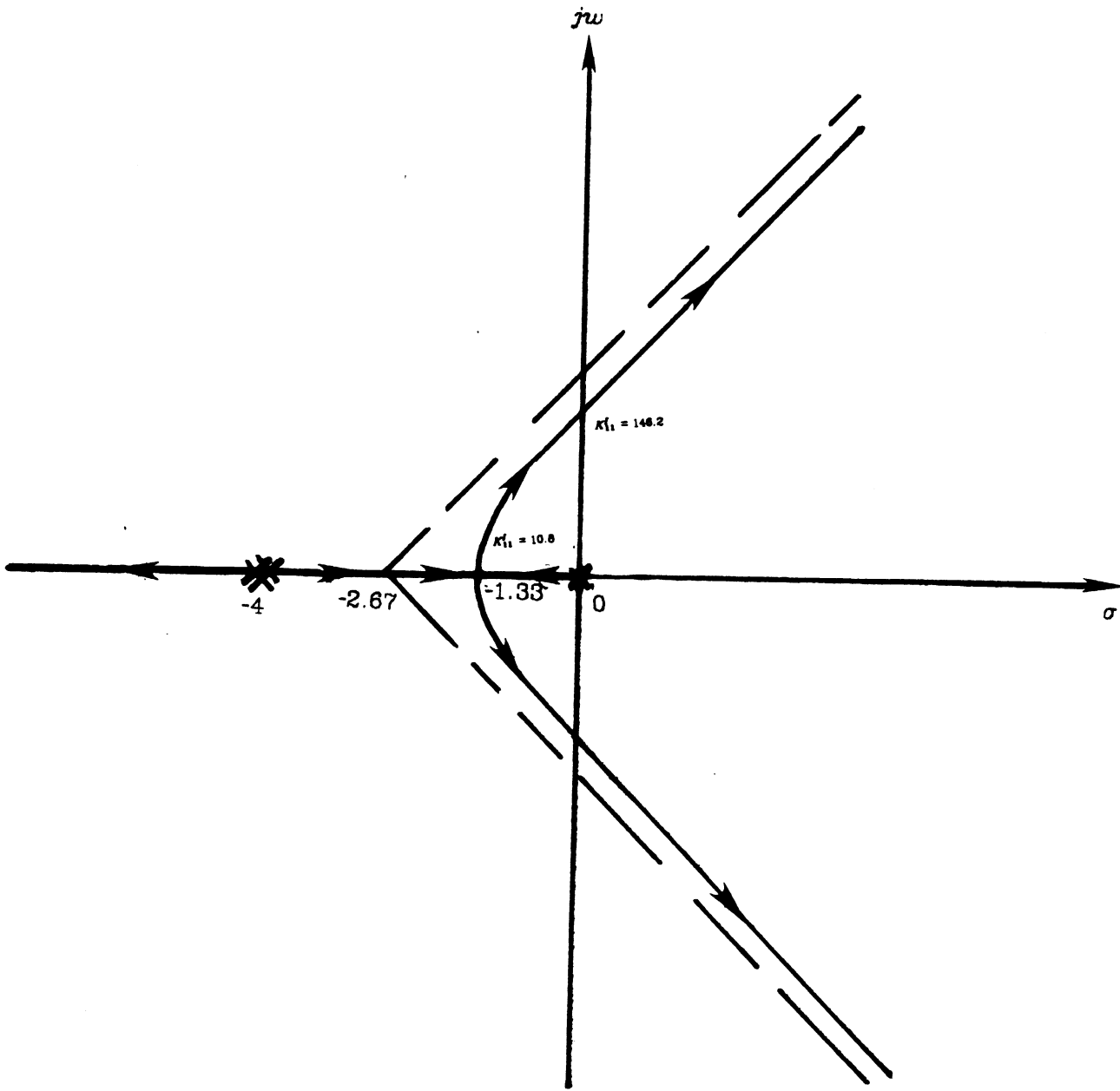


Figure 37. Root locus for τ

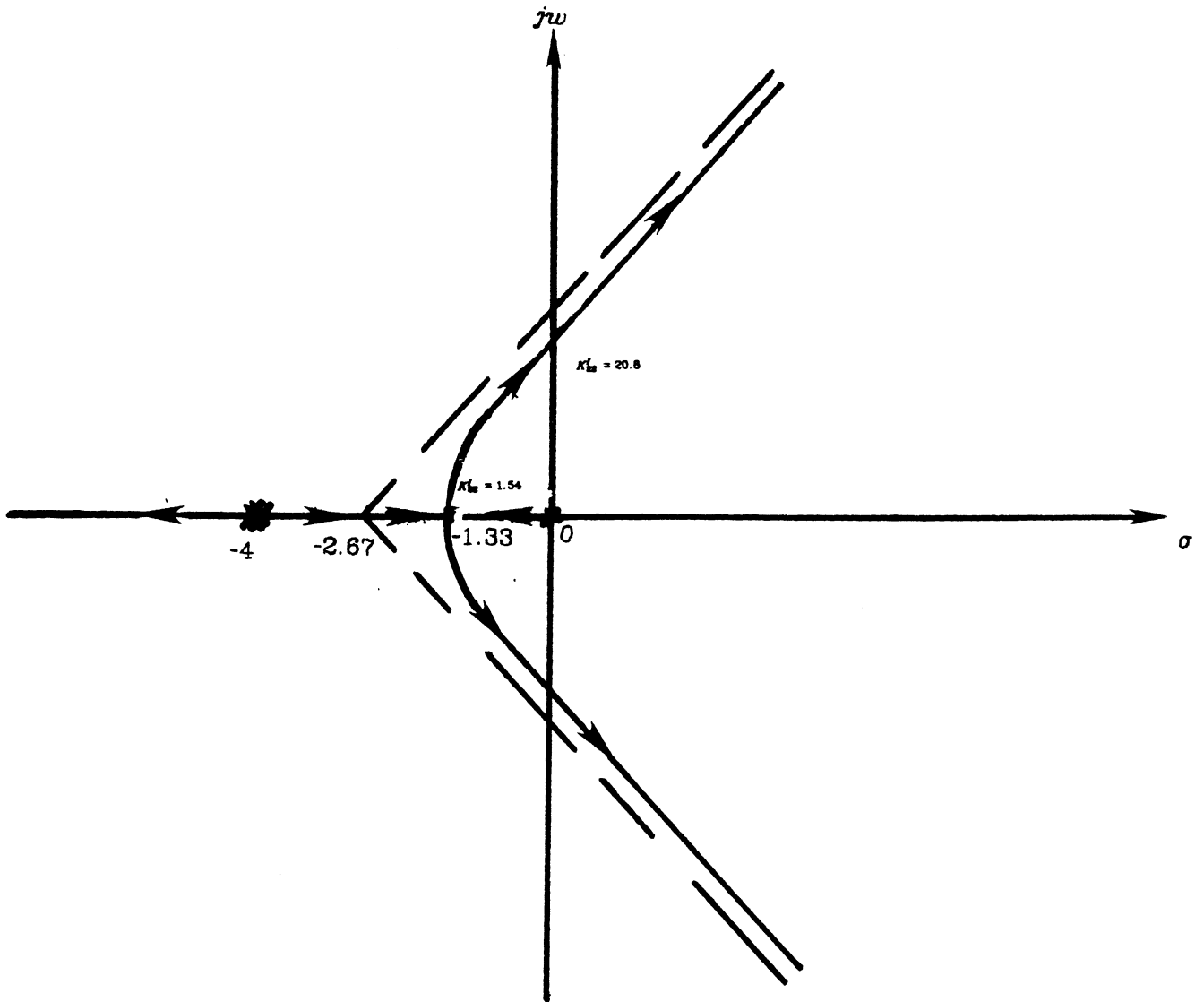


Figure 38. Root locus for ϕ

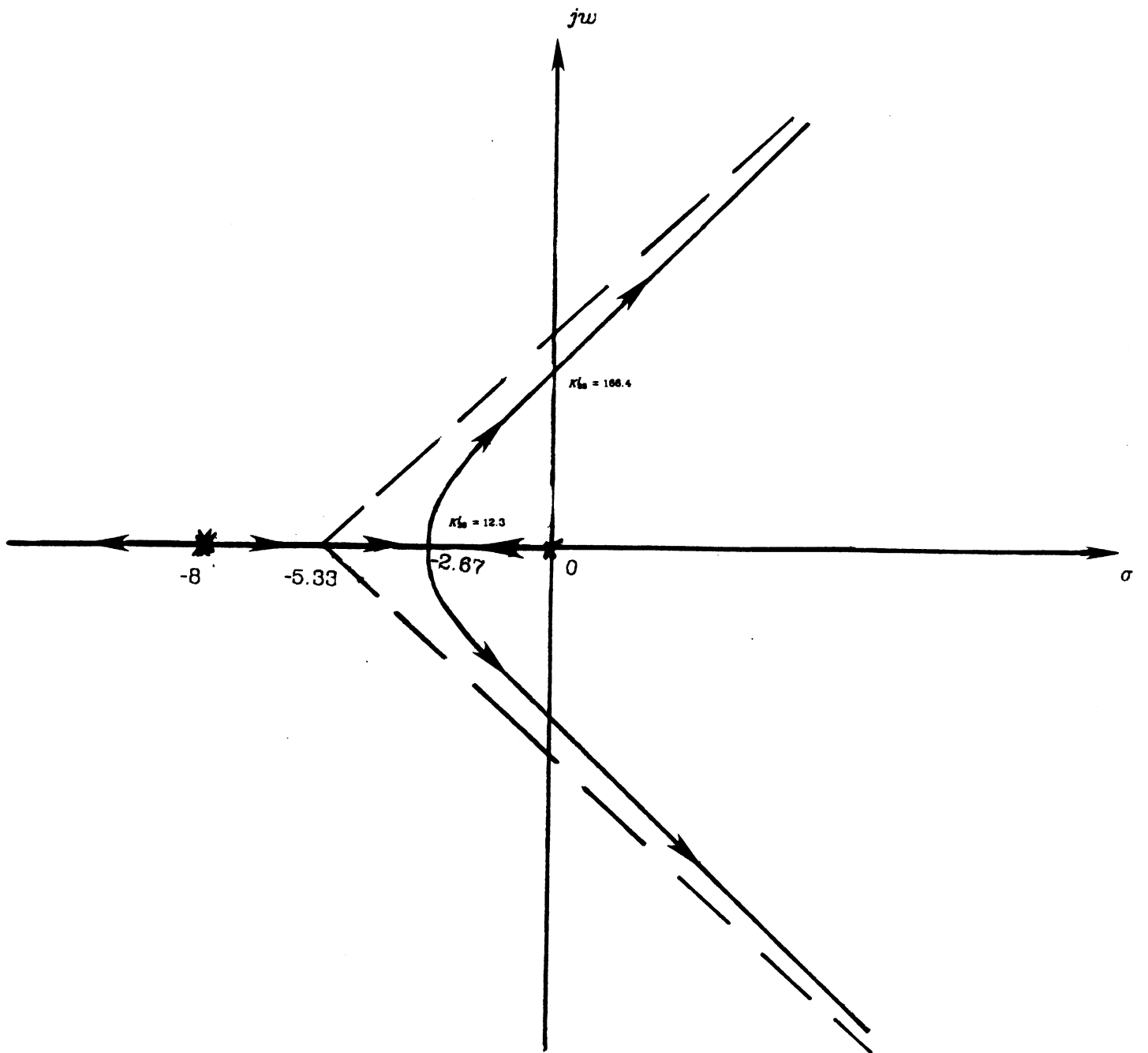


Figure39. Root locus for ϕ

	First Mode	Second Mode
ε_i	1.8751041	4.640911
α_i	0.7340955	1.01846644

TABLE 1 Values of α_i and ε_i for a Clamped Free Beam

	Settling Time (2% error)	Damping ratio ξ	Number of Time Constant	Natural frequency W_n (rad/s)
r	1.0	1.0	4	4
ϑ	1.0	1.0	4	4
φ	0.5	1.0	4	8

TABLE 2 Desired System Parameters.

	Closed-loop Transfer Function for the inner loop	Open-loop Transfer Function for the inner loop
r	$G_1(s) = \frac{1}{(m_2 + m_p) s^2 + 2\xi W_{nr} s + W_{nr}^2}$	$G'_1(s) = \frac{K_{11}^I}{s(s^2 + 2\xi W_{nr} s + W_{nr}^2)}$
ϑ	$G_2(s) = \frac{(\frac{1}{\alpha})}{s^2 + 2\xi W_{n\vartheta} s + W_{n\vartheta}^2}$	$G'_2(s) = \frac{K_{22}^I}{s(s^2 + 2\xi W_{n\vartheta} s + W_{n\vartheta}^2)}$
φ	$G_3(s) = \frac{(\frac{1}{\alpha})}{s^2 + 2\xi W_{n\varphi} s + W_{n\varphi}^2}$	$G'_3(s) = \frac{K_{33}^I}{s(s^2 + 2\xi W_{n\varphi} s + W_{n\varphi}^2)}$

TABLE 3 The Required Transfer Functions for Drawing the
Root Locus.

UNIVERSITY OF MICHIGAN



3 9015 02651 8327